Investigating the photosynthetic and hydraulic trade-off during drought recovery in eucalypts

by

Alta Saunders

Dissertation presented for the degree of

Doctor of Philosophy (Agricultural Sciences)

at

Stellenbosch University

Department of Forest and Wood Science, Faculty of AgriSciences

Supervisor: Prof Dave Drew

April 2022

Declaration

By submitting this dissertation electronically, I declare that the entirety of the work contained therein is my own, original work, that I am the sole author thereof (save to the extent explicitly otherwise stated) that reproduction and publication thereof by Stellenbosch University will not infringe any third-party rights and that I have not previously in its entirety or in part submitted it for obtaining any qualification.

Date: April 2022

Abstract

Stomatal regulation plays a vital role in maintaining the water status of a plant by minimising water loss, however, decreases in stomatal conductance can lead to reductions in carbon uptake. The stomata balance a trade-off between water loss and carbon gain. The hydraulic system and stomatal conductance are closely linked but play opposing roles within a plant. The hydraulic system ensures that there is a sufficient water supply to leaves, while stomatal conductance regulates the loss of water from the leaves. During periods of drought, reductions in hydraulic conductance due to embolism formation can be seen, however stomatal regulation can help reduce embolism formation or prevent runaway cavitation during drought. Understanding how plant hydraulics and stomatal regulation influence production rates is becoming more important to model stomatal responses in a changing climate, especially for Eucalyptus species which is often grown in drought prone environments. Plants use a wide range of strategies to reduce or mitigate the negative impact of embolism formation, with this study focusing on the strategies utilised by commercially significant *Eucalyptus* hybrids. Two *Eucalyptus* hybrids, *E. grandis X camaldulensis* (*GC*) and *E. urophylla X grandis* (*UG*), where subjected to a drought-recovery treatment where they were periodically droughted. During the experimental period the stomatal responses, together with transpiration rates, photosynthetic capacity and biomass allocation was measured. Hydraulic measurements together with CT-scan imaging was also utilised to determine whether these plants can recover lost hydraulic pathways post-drought, and what the underlying mechanism for this might be. During the study two distinct hydraulic strategies were observed. *GC* was more resistant to embolism formation compared to *UG*, however *GC* showed lower levels of hydraulic recovery after rewatering. The drought responses could also be split into a resilient v. a resistant response, with the more resilient hybrid, UG, maintaining stomatal conductance throughout drought periods running the risk of hydraulic failure, however with the ability to recover lost hydraulic pathways through refilling post-drought. This is in comparison with the resistant strategy seen in *GC*, where water loss during drought was minimised, however this also reduced carbon uptake and production. From this study the stomatal responses could also be accurately modelled using a gain-risk model that assumes stomata optimise the trade-off between water loss and carbon gain. It was however clear, that the strategy used by plants need to be considered when using a gain-risk model, with the gain-risk model performing better for the *Eucalyptus* hybrid that utilised a resistant strategy, since plants that uses a resilient strategy will maintain stomatal conductance during drought, regardless of the hydraulic risk. The use of alternative models was also investigated during this study, with Machine Learning models being able to accurately predict stomatal responses on a global scale. Major increases in tree mortality are predicted due to changes in climate. To properly predict these changes, accurate models of plant responses to water limitations and other environmental changes

are therefore becoming increasingly important for effective forest management. Understanding how hydraulic traits and stomatal regulation covary, can help model drought-induced tree mortality in a changing climate.

Opsomming

Die regulasie van gaswisseling deur die huidmondjies is belangrik aangesien dit nie net die verlies van water deur transpirasie reguleer nie, maar ook die opname van CO_2 wat nodig is vir fotosintese en produksie. Die hidroulise sisteem van ‘n plant en huidmondjies is gekoppel, maar speel teenoorgestelde rolle. Die hidrouliese sisteem beheer hoeveel water beskikbaar is vir die plant, terwyl die huidmondjies water verlies deur transpirasie beheer. Tydens droogtes, word die hidrouliese geleiding van water deur die plant bellemer deur die vorming van embolisme/lugborrels. Die huidmondjies kan wel die verspreiding van hierdie lugborrels verminder of verhoed deur water verlies te beheer. Dit is dus belangrik om te verstaan wat die interaksie tussen die huidmondjies en die hidrouliese sisteem van ‘n plant is om akurate modelle van gaswisseling te bou, veral vir *Eucalyptus* spesies, aangesien hulle gereeld in droogte geteisterde areas geplant word. Plante geskik van ‘n verskeidenheid van strategieë om die negatiewe impak van embolisme te vermider. Die studie het dus gefokus op die strategieë wat *Eucalyptus* kruise gebruik. Die gaswisseling en groei was gemeet van twee *Eucalyptus* kruise, *E. grands X camaldulensis* (*GC*) en *E. urophulla X grandis* (*UG*), tydens ‘n droogte eksperiment waar die plante vir sekere periodes nie water ontvang het nie. Meetings van die hidroulise geleiding en hidroulise einskappe was ook gemeet deur gebruik te maak van beide traditionele metodes, sowel as rekenaartomografie-skanderings, om te bepaal of die plante van die embolisme/lugborrels in die hidrouliese sisteem kan vul na ‘n droogte. Tydens die studie was dit duidelik dat die twee *Eucalyptus* kruise twee verskillend hidrouliese strategieë benut. *GC* was meer bestand teen droogte en die vorming van embolisme in vergelyking met *UG*, maar *GC* kon nie die embolisme in die hidroulises sisteem weer vul met water na die droogte nie. Die strategieë wat benut was kon ook beskryf word as ‘n weerstandbiedige strategie teenoor ‘n veerkragtige strategie. *UG* het ‘n veerkragtige strategie benut, waar gaswisseling gehandhaaf was tydens droogte, maar het ‘n hoër risiko gehad dat die hidrouliese sisteem misluk, terwyl *GC* ‘n weerstandbiedige strategie gehandhaaf het, waar gaswissinling and water verlies deur transpirasie verminder was, maar so ook CO_2 opname. Tydens die study kon ons ook die gaswisseling voorspel deur ‘n wins-risiko model te gebruik wat aaneem dat die huidmondjies ‘n balans vind tusen water verlies en CO_2 opname. Dit was egter duidelik dat die hidrouliese strategieeë in ag geneem moet word, aangesien die model meer akuraat was vir plante wat ‘n weerstandbiedige strategie benut. Dit is aangesien ‘n plant wat ‘n veerkragtige strategie benut gaswisseling sal handhaaf tydens droogte, ongeag die hidrouliese risiko. Ondersoek was ook ingestel om alternatiewe modelle te gebruik om gaswisseling te modelleer en dit was gevind dat masjienleermodelle ook gebruik kan word. Grootskaalse sterftes van bome word verwag asgevolg van klimaats verandering. Om die impak van dit te voorspel, is dit dus belangrik om akkurate modelle van gaswisseling in reaksie tot klimaats

verandering te ontwikkel. As ons verstaan hoe die hidrouliese en gaswisseling sisteme van plante reageer, kan ons beter modelle bou om boom streftes te voorspel.

Acknowledgements

I would like to acknowledge the following people and organisations for their contributions:

- Dr Leandra Moller and Dr Kim Martin for technical support throughout the project.
- Prof Dave Drew for supervising the project and guiding me throughout the study.
- My mom, sister and husband for support and encouragement throughout the study period.
- The entire EucXylo team for support and comradery throughout the study period.

Table of Contents

Chapter 1: Introduction **1**
Aims and Objectives 2

Chapter 2: Literature Review **3**
Plant water relations 4
Hydraulic conductance 4
Embolism and xylem cavitation 4
Drought stress 6
Embolism Recovery 6
Photosynthesis 7
Modelling photosynthesis and stomatal conductance 7
The link between photosynthesis and hydraulic conductance 9
Eucalyptus and South Africa 10

Chapter 3: Measurements done on excised stems indicate that hydraulic recovery can be an important strategy used by Eucalyptus hybrids in response to drought **12**

This chapter was published in **Treas: Structure and Function** on 4 August 2021

Chapter 4: Stomatal responses of Eucalyptus spp. under drought can be predicted with a gain-risk optimisation model **26**
Abstract 27
Introduction 27
Methods 30
Model description 30
Model adaptation 32
Plant material 33
Dry-down and re-watering treatments 34
Model inputs 34
Plant variables 36
Statistical analysis 36
Results 37
Plant characteristics 37
Treatments 38
Model Accuracy 38
Complete v. reduced or delayed hydraulic recovery 45
Environmental physiological drivers 47
Discussion 48
Conclusion 53
Supplement material 54

Chapter 5: The co-ordination of stomatal regulation, hydraulic properties, and biomass allocation influence drought strategies in two Eucalyptus hybrids 58
Abstract 59
Introduction 59
Materials and Methods 62
Plant material 62
Experimental design and treatments 62
Hydraulic and Photosynthetic traits 63
Statistical analysis 64
Results 64
Experimental treatments 64
Plant Characteristics 65
Stomatal responses to drought 66
Production and photosynthetic response to drought 68
Discussion 69
Water-use strategies during drought 69
Drought resistance, embolism resistance and stomatal regulation 71
Embolism resistance and hydraulic properties 73
Drought resistance and biomass partitioning 73
Conclusion 74

Chapter 6: Machine learning models perform better than traditional empirical models for stomatal conductance when applied to multiple tree species across different forest biomes 76

This Chapter was published in **Trees: Forest & People** on 10 September 2021

Chapter 7: General Conclusion 89
Recovery of lost hydraulic capacity in eucalypt hybrids 90
Modelling the balance between risk and gain 91
Machine learning methods for predicting stomatal conductance 92
Modelling plant responses in a changing climate 92

References 94

List of Tables

Table 4.1 Physiological parameters used in gain-risk model of all *E. grandis X camaldulens* (*GC*) and *E. urophylla X grandis* (*UG*) plants 36

Table 4.2 Environmental variables used in the gain risk model 36

Table 4.3 Performance of model predictions of transpiration rate (E) and stomatal conductance (Gw) for both *E.urophylla X grandis* (*UG*) and *E. grandis X camaldulensis* (*GC*). RMSE (root mean square error) and MAE (mean absolute error) are given in model output units. R2 and slope of linear regression between measured and predicted variables are also presente 39

List of Figures

Figure 4.1 Measured vs modelled stomatal conductance (Gw) and transpiration (E) for *E. grandis X camaldulensis* (*GC*). Solid black line indicates 1:1 relationship. Linear regression results for plants in the control treatment were significant for models with complete hydraulic recovery (E: $p < 0.001$, R2 = 66 %; Gw: $p < 0.001$, R2 = 51 %) and with partial hydraulic recovery (E: $p < 0.001$, R2 = 64 %; Gw: $p < 0.001$, R2 = 49 %). Linear regression results for plants in the dry-down treatment were significant for models with complete hydraulic recovery (E: $p < 0.001$, R2 = 54 %; Gw: $p < 0.001$, R2 = 65 %) and with partial hydraulic recovery (E: $p < 0.001$, R2 = 52 %; Gw: $p < 0.001$, R2 = 62 %) 40

Figure 4.2 Measured vs modelled stomatal conductance (Gw) and transpiration (E) for *E. urophylla X grandis* (*UG*). Solid black line indicates 1:1 relationship. Linear regression results for plants in the control treatment were significant for models with complete hydraulic recovery (E: $p < 0.001$, R2 = 60 %; Gw: $p < 0.001$, R2 = 57 %) and with partial hydraulic recovery (E: $p < 0.001$, R2 = 62 %; Gw: $p < 0.001$, R2 = 58 %). Linear regression results for plants in the dry-down treatment were significant for models with complete hydraulic recovery (E: $p < 0.001$, R2 = 54 %; Gw: $p < 0.001$, R2 = 44 %) and with partial hydraulic recovery (E: $p < 0.001$, R2 = 54 %; Gw: $p < 0.001$, R2 = 34 %) 41

Figure 4.3 The gain-risk model performance of stomatal conductance (Gw) and transpiration rate (E) of *E. grandis X camaldulensis* (*GC*) plants over the experimental period. Measured variables are plotted in black. Predicted variables that is modelled with complete and partial hydraulic recovery is plotted in blue and red respectfully. Mean values with 95 % confidence intervals are plotted. 42

Figure 4.4 The gain-risk model performance of stomatal conductance (Gw) and transpiration rate (E) of *E. urophylla X grandis* (*GC*) plants over the experimental period. Measured variables are plotted in black. Predicted variables that is modelled with complete and partial hydraulic recovery is plotted in blue and red respectfully. Mean values with 95 % confidence intervals are plotted 43

Figure 4.5 Measured soil water potentials vs. modelled leaf water potentials for models with complete hydraulic recovery (blue) and partial/delayed hydraulic recovery (red). Modelled water potentials are given for *E. grandis X camaldulensis* at the top (A) and *E. urophylla X grandis* at the bottom (B) 44

Figure 4.6 The modelled leaf water potentials over time for *E. grandis X camaldulensis* (A) and *E. urophylla X grandis* (B). Modelled values from the model that allows for full hydraulic recovery is given in blue. Modelled values for the model that allows for partial/ delayed hydraulic recovery is given in red. The P50, which indicates pressure/potential at which 50% loss of conductance is seen, is indicated with a dashed line for both hybrids 46

Figure 4.7 Total effects of the Sobol sensitivity analysis testing the gain-risk model that includes the hydraulic limitation. The total effects are plotted for transpiration rates (E) and photosynthesis (An). Physiological parameters on the x-axis include vulnerability curve parameters (b and c), Maximum carboxylation rate (Vmax25) and electron transport rate (Jmax25) at 25°C, maximum hydraulic conductance (Kmax), leaf area to basal area ratio and the xylem recovery index (XRI). The total effects are plotted for transpiration rates (E) and photosynthesis (An)..... 47

Figure 4.8 Biplot for principal component 1 and 2 yielded by the PCA of the environmental variables measured, and absolute error of predicted transpiration rates and stomatal conductance. Variables include relative humidity (RH), soil water pressure (Psoil), air temperature (Temp), soil irradiance (Solar) and absolute error of model v. measured stomatal conductance (AE.Gw) and transpiration rates (AE.E) 48

Figure 4.9 Experimental design layout of drought-recovery experiment 55

Figure 4.10 Soil volumetric water content and soil water pressure curve as calculated by the van Genuchten model..... 56

Figure 4.11 Soil water pressure of control and drought-recovery treatment over the experimental period..... 56

Figure 5.1 Vessel size distribution (left) and hydraulic conductance (right) of *E. urophylla X grandis* and *E.grandis X camaldulensis* as calculated based on cross-sections of the stem 65

Figure 5.2 Stomatal conductance measurements for *E. urophylla X grandis* (top) and *E. grandis X camaldulensis* (bottom) of plants in the control group that received continuous watering (Control) and plants that were subjected to a cyclic-drought treatment (Drought). The volumetric soil moisture content for the experimental period is also given (bottom). The dashed grey lines indicate the periods of a droughting events. Means with 95% confidence intervals are given..... 67

Figure 5.3 Cumulative growth for *E. urophylla X grandis* (top) and *E. grandis X camaldulensis* (bottom) of plants in the control group that received continuous watering (Control) and plants that were subjected to a cyclic-drought treatment (Drought). Means and standard deviation are given..... 68

Figure 5.4 The dried root-stem ratio and the dried leaf-weight ratio for *E. urophylla X grandis* (top row) and *E. grandis X camaldulensis* (bottom row) plants of the control treatment (Control) and cyclic drought-recovery treatment (Drought). Mean and standard errors given 69

Figure 5.5 Schematic representation of the two distinct responses to drought observed between two *Eucalyptus* hybrids: *E. grandis X camaldulensis* and *E. urophylla X grandis*. *reductions in leaf biomass was seen, however it was not significant 70

Abbreviations

The list of abbreviations is given in alphabetical order and not the order of appearance within the manuscript.

∂A/∂E	Marginal water use efficiency
ΔΨ	Water potential/pressure gradient
A	Photosynthetic rate
A(Ψ)	Photosynthetic uptake at a specific water potential
ABA	Abscisic acid
A_c	Assimilation Rate
AE.E	Absolute error of transpiration
AE.gsw	Absolute error of stomatal conductance
AIC	Akaike's information criterion
A_j	Electron transport rate
A_{max}	Instantaneous photosynthetic uptake
A_{net}	Net photosynthesis
ANN	Artificial neural network
As	Sapwood area
BWB	Ball-Berry stomatal conductance model
C_i	Intercellular CO_2 concentration
CO_2	Carbon Dioxide
d	Radius of vessel
DT	Decision Trees
E	Transpiration rate
F_m'	Maximum fluorescence of a light adapted leaf
F_s	Minimum fluorescence of a light adapted leaf
GC	*E. grandis X camaldulensis*
G_c	CO_2 diffuse conductance
GLM	Generalised linear model
gsw/ Gw	Stomatal conductance
gsw_{BWB}	Stomatal conductance calculated with the Ball-Berry model
J	Electron transport rate
J_{max25}/J_{max}	Maximum electron transport rate at 25 degrees Celsius
K (Ψ)	Hydraulic conductance at a specific water potential

K_c	Michaelis coefficient for CO_2
KCl	Potassium Chloride
K_{cmax}	Instantaneous maximum hydraulic conductance
K_{crit}	Critical hydraulic conductance
K_h/K_h	Hydraulic conductance
k_{int}	Measured/initial hydraulic conductance
K_{max}/K_{max}	Maximum hydraulic conductance
K_o	Michaelis coefficient for O_2
k_s	Specific hydraulic conductance
LA:BA	Leaf area to Basel area ratio
LWP	Leaf water potential
MAE	Mean Absolute error
MAPE	Percentage mean absolute error
ML	Machine Learning
MLR	Multiple linear regression
MSE	Mean squared error
NSCs	Non-structural carbohydrates
O_2	Oxygen
O_a	Intercellular O_2 concentration
P50	Pressure/potential water gradient at which 50% of hydraulic conductance is lost
PAR	Photosynthetically active radiation
P_{atm}	Atmospheric pressure
PCA	Principal component analysis
PDF	Probability density function
PLC	Percentage loss of conductance
PLC_D/$PLC_{drought}$	Percentage loss of hydraulic conductance after drought
PLC_r	Percentage loss of hydraulic conductance recovered
PLC_{RW}/$PLC_{rewatered}$	Percentage loss of hydraulic conductance after rewatering
$PLC_t(\Psi_x)$	Vulnerability curve at any point in time
PLC_W/$PLC_{watered}$	Percentage loss of hydraulic conductance before drought
P_{soil}/Ψ_{soil}	Soil water pressure/potential
Q	Sap flow
R_d	Dark respiration rate
RF	Random Forest

RMSE	Root mean square error
SLA	Specific leaf area
Solar	Solar irradiance
SPAC	Soil-plant-space continuum
Temp/T_{air}	Air temperature
T_{leaf}	Leaf temperature
UG	*E. urophylla X grandis*
V_{max25}/V_{max}	Maximum carboxylation rate at 25 degrees Celsius
VPD	Vapor pressure deficit
XRI	Xylem Recovery Index
Γ	CO_2 compensation point
η	Viscosity of water
Θ	Hydraulic cost
Θ (Ψ)	Normalised cost at a specific water potential
ΦPSII	Efficiency of photosystem II
Ψl	Leaf water potential/pressure
Ψx	Xylem water potential/pressure
***β*(Ψ)**	Normalised gain at a specific water potential

Chapter 1

Introduction

Chapter 1: Introduction

Plants are constantly balancing a trade-off between water loss and carbon gain. Stomatal regulation plays an important role in this by controlling the rate of water loss and carbon gain through CO_2 uptake (Xiong and Nadal 2020). There isincreasing evidence that stomatal morphology and behaviour have evolved to optimise this trade-off (Sperry et al. 2017).

Stomatal conductance is closely linked to rates of transpiration and carbon uptake within plants. It has been shown that regulation of stomatal conductance in leaves are affected by hydraulic changes within a plant (Tardieu and Davies 1993). The hydraulic system and stomatal conductance are therefore closely linked but play opposing roles within a plant. The hydraulic system ensures that there is a sufficient water supply to leaves, while stomatal conductance regulates the loss of water from the leaves. This interaction between the hydraulic system and stomatal conductance has an influence on the water potential and directly influence the carbon assimilation of a plant (Ding et al. 2020).

Plant water supply, a major factor in understanding plant-level carbon sequestration, is not only regulated by stomatal conductance, but also limited by a decrease in hydraulic conductance due mainly to embolism formation (Tyree and Sperry 1988, Sperry et al. 1993). This reduction of xylem conductance cannot be directly regulated by the plant, but it is generally understood that plants can use stomatal regulation to help prevent runaway cavitation (Sperry et al. 1993).

Plants incur an opportunity cost during drought when soil water becomes limiting to conductance and growth (Lu et al. 2020). The historic reduction in soil water experienced by a plant during drought will control the hydraulic limitation for as long as embolism persists and will influence subsequent photosynthesis (Xiong and Nadal 2020). This is particularly important in *Eucalyptus*, which are often grown in drought-prone environments and are highly responsive to water availability following drought (Saadaoui et al. 2017, Binkley et al. 2020).

A wide range of water use strategies have been observed within *Eucalyptus* (Saadaoui et al. 2017), however there is uncertainty as to how hydraulic and stomatal responses of *Eucalyptus* species are coordinated, especially under drought conditions (Zhang et al. 2016). Trees use a variety of strategies to mitigate or reduce drought induced hydraulic failure (Choat et al. 2012) and recovery of hydraulic conductance after drought stress can also be an important mechanism used to avoid

drought induced mortality (Klein et al. 2018, Saunders and Drew 2021). The underlying mechanism of hydraulic recovery is, however, still poorly understood (Klein et al. 2018).

Stomata play an important part in regulating not only water loss within a plant, but they also regulate carbon uptake (Schulze and Hall 1982, Morrison 1987, Xiong and Nadal 2020). By understanding stomatal and hydraulic responses within a plant, predictions of plant productivity can be improved (Menezes-Silva et al. 2019). Although plants can regulate water loss through both hydraulic properties as well as through stomatal responses, stomatal responses are dynamic and can change over short time periods (Aloni 2015, Tng et al. 2018). By understanding how hydraulic traits and stomatal responses covary, plant scientists can get a better insight into how trees respond during drought and post-drought (McDowell et al. 2008).

Aims and Objectives

Multiple models have been proposed to explain combined processes of photosynthesis, transpiration and carbon transport within a plant, but few focus on the response of stomata to both carbon assimilation and water loss during drought and post-drought recovery (Whitehead et al. 1996, Damour et al. 2010, Nikinmaa et al. 2014, Coussement et al. 2018).

This knowledge gap is even wider in the eucalypts, very likely the world's most widely planted hardwoods (Myburg et al. 2014). A wide variability of drought responses exist among *Eucalyptus* (Bourne et al. 2017, Saadaoui et al. 2017). In the studies reported in this thesis, attention is paid to the basis of these differences by elucidating the underlying physiology, particularly in terms of how embolism recovery influences photosynthesis and what role stomatal regulation plays in observed drought responses.

The aims of the research in the PhD study reported in this thesis were therefore to:

- Better understand the mechanism for drought recovery through embolism refilling
- Determine if the strategy of drought recovery or resistance is related to specific physiological or anatomical variables
- Determine if stomata regulation optimises between carbon gain and water loss and how this is affected by drought and drought recovery
- Investigate if delayed/partial hydraulic recovery response affects stomatal conductance via a modelling approach
- Understand how hydraulic and stomatal traits influence drought strategies and determine how this affects production
- Investigate the use of machine learning as a method for predicting stomatal responses

Chapter 2

Literature Review

Chapter 2: Literature Review

This chapter will give a brief overview of plant hydraulics and photosynthesis. A more comprehensive literature review, pertaining to each topic, can be found within each specific chapter.

Plant water relations

Hydraulic conductance

The hydraulic conductance of plants refers to the flow rate of water through the xylem due to a change in the water potential gradients seen within a plant (Sperry et al. 1993, Sperry and Love 2015).

$$k_h = \frac{Q}{\Delta\Psi}$$

where k_h is hydraulic conductance (kg s^{-1} Mpa^{-1} m^{-1}), Q is sap flow (kg m^{-2} h^{-1}) and $\Delta\Psi$ is the water potential gradient.

The hydraulic conductance can also be calculated as a function of the measured sapwood area.

$$k_s = \frac{k_h}{\mathrm{As}}$$

where k_s is the specific hydraulic conductance (kg s^{-1} m^{-1} MPa^{-1}) and As is the sapwood area (m^2). The resistance of xylem can be calculated as the inverse of hydraulic conductance (Zimmerman 1983).

Embolism and xylem cavitation

Transpiration drives water through the soil-plant-atmosphere continuum (SPAC). Loss of water through transpiration is unavoidable since stomata need to open in order to absorb carbon dioxide for photosynthesis (Xiong and Nadal 2020). Transpiration increases the water pressure gradients between the soil and plant canopies, with the water pressure of plant canopies becoming more negative with an increase in transpiration (Tyree and Sperry 1988).

If the gradients become too negative, the continuous water column within the plant can be disturbed by dissolved gasses filling the xylem conduit (Tyree and Sperry 1988). If the water gradients become more negative, the air bubble can increase in size until the xylem conduit is filled

preventing the movement of water. This process is known as xylem cavitation with the blocking of the xylem conduit known as embolism (Tyree and Sperry 1988).

The hydraulic structure of plants influences the movement of water through the SPAC, but also determine how vulnerable plants are to xylem cavitation (Xiong and Nadal 2020). It has been suggested that there is a trade-off between xylem structure that is efficient, which will result in higher productivity, and xylem structure that is less vulnerable to cavitation (Gleason et al. 2016). Various studies suggest that this trade-off can be seen since larger xylem conduits, which allow for higher water transport efficiency, are more vulnerable to cavitation than their smaller counter parts (Wheeler et al. 2005, Hacke et al. 2006, Gleason et al. 2016).

Although there is a correlation between xylem conduit size and vulnerability to cavitation, it has been suggested that it is due to the area of pits observed on the xylem (Wheeler et al. 2005). The "rare pit" hypothesis proposes that the pit area increases with xylem conduit size. The likelihood of finding larger pits is therefore higher, which will allow for embolism to spread more easily (Wheeler et al. 2005). The anatomical differences in pits seen between species also result in differences in vulnerability of xylem to cavitation (Tyree et al. 1995).

Xylem cavitation and embolism formation can be caused by drought (Sperry and Pockman 1993) with embolism formation even seen in plants that are only slightly water stressed. Embolism restricts the movement through the SPAC and influence water pressure gradients seen in the plant. Increased negative water pressure gradients can lead to stomatal closure (Becker et al. 2000). Stomatal closure helps prevent water loss through transpiration, but also affects CO_2 uptake needed for photosynthesis (Kramer and Boyer 1995, Becker et al. 2000). Xylem cavitation is unavoidable and has a significant effect on plant productivity and growth (Lo Gullo and Salleo 1992).

The extent of embolism formation is often measured as the percentage loss of hydraulic conductance (PLC). PLC is calculated as the ratio of measured hydraulic conductance over maximum hydraulic conductance (Choat et al. 2010).

$$PLC = 100(k_{max} - k_{int})/k_{max}$$

where k_{max} is the maximum hydraulic conductance and k_{int} is the measured hydraulic conductance. Vulnerability curves are used to describe the loss of hydraulic conductance due to embolism formation. Vulnerability curves show the percentage loss of hydraulic conductance as a function of xylem water potential/pressure (Choat et al. 2010)

Drought stress

The hydraulic conductance of a plant has a significant effect on the plant water balance and fluctuates in response to environmental changes (Maurel and Chrispeels 2001). Differences in physiological and morphological characteristics can explain differences in drought tolerance seen between various species.

Plants cannot regulate the reduction in hydraulic conductance due to embolism formation but can however regulate other mechanism like stomatal conductance to help and manage the spread of embolism (Sperry et al. 2002). Changes in stomatal conductance or reduction in leaf area helps to decrease the demand on the water supply (Silva et al. 2004). Difference in hydraulic conductance and the vulnerability of xylem to cavitation can also be seen in species with different tolerances to drought stress, with drought resistant species being able to tolerate more negative water pressure gradients (Tyree and Ewers 1991).

In species with high resistance to xylem cavitation, it has been found that the xylem cell wall is reinforced (Hacke et al. 2001, Jacobsen et al. 2005). Fernandez et al (2019) found that *Eucalyptus* species that are resistant to cavitation, have an increased 'halo –area', that consist out of tracheid and parenchyma cells, surrounding xylem vessels (Barotto et al. 2016, Fernández et al. 2019). The 'halo-area' helps to reinforce xylem conduits to withstand higher pressure gradients. An increase in the 'halo-area' also positively correlates with higher P50 (pressure gradient at which 50 % of hydraulic conductance is lost) (Fernández et al. 2019).

A decrease in plant hydraulic conductance due to a reduction to water availability has been documented in various species (Maherali et al. 2004, Silva et al. 2004). The effect of drought stress on production is highly linked to changes in hydraulic conductance. It is important to understand the different mechanisms that govern the responses of plant species to drought stress to understand how plant production will be affected by changes in climate.

Embolism Recovery

Embolism formation restricts the water movement within a plant and reduces hydraulic conductance (Becker et al. 2000), which is one of the main causes of drought-induced tree mortality (Anderegg, Plavcová, et al. 2013) . Plants have developed a range of strategies to deal with this ranging from regrowth of new xylem vessels, avoiding embolism formation through stomatal closure and refilling of embolised vessels (Ogasa et al. 2013, Sperry and Love 2015, Klein et al. 2018). Many studies

have focussed on how plants avoid embolism formation (Gleason et al. 2016, Barotto et al. 2018), with less focus given to other strategies like embolism recovery (Klein et al. 2018).

It has been found that many species operate with xylem tensions close to the point of critical runaway cavitation, but that these species can recover when soil water pressure is increased again (Choat et al. 2012, Ogasa et al. 2013). This might suggest that these species use a hydraulic strategy of hydraulic recovery after drought, where embolism refilling takes place (Klein et al. 2018), rather than a strategy of embolism avoidance (Trifilò et al. 2014, 2015).

There is, however, still a debate surrounding the possibility of embolism refilling, with many researchers still speculating on whether refilling can take place over short time periods (Cochard et al. 2001, Nardini et al. 2011, Klein et al. 2018). There is also still uncertainty regarding what the underlying mechanism are for embolism refilling (Nardini et al. 2011).

It has been well established that embolism refilling can take place when water pressure in the soil increases (Brodersen and McElrone 2013), with evidence of embolism refilling overnight even found in a few *Eucalyptus* species (Ogasa et al. 2013, Zeppel et al. 2019). It has been proposed that the availability of carbohydrates also play a role in embolism recovery by changing osmotic gradients within the plant (Nardini et al. 2011, Tomasella, Casolo, et al. 2019, Tomasella, Petrussa, et al. 2019). It has also been proposed that embolism refilling is energy dependent and that the availability of sugars in the apoplast can aid hydraulic recovery (Secchi et al. 2021). Evidence in support of this has been found with the upregulation of genes relating to carbohydrate metabolism seen in parenchyma during drought (Secchi and Zwieniecki 2010).

The phenomenon of embolism reversal can be an important strategy used by plants, however it is clear that more information regarding what the underlying mechanisms for embolism refilling is or which species rely on embolism refilling is needed (Nardini et al. 2011, Klein et al. 2018). A better understanding of hydraulic recovery strategies used by plants will also help us to get a better understanding of how plants will respond to future changes in climate.

Photosynthesis

Modelling photosynthesis and stomatal conductance

The physiological model of Farquhar, van Caemmer and Berry (1980) has been widely used to model photosynthesis at leaf scale. The model simplifies photosynthesis by simulating CO_2 assimilation in response to key variables (Bernacchi et al. 2013). Because of its simplicity, the

model has performed well in various studies (Farquhar et al. 1980). A variety of biochemical parameters are required to use the model, with the most important parameters being the maximum electron transport rate, the maximum Rubisco capacity and the quantum use efficiency (Farquhar et al 1980). Due to the performance of the model, there has been an increase in availability of these parameters for various species seen in literature (Bernacchi et al. 2002, Yin and Struik 2009).

The use of the biochemical model however requires the value of the interior CO_2. The model has therefore been linked with a stomatal conductance model to calculate the intercellular CO_2 concentration. The Farquhar model has also been adapted to include the mesophyll conductance to calculate the CO_2 partial pressure at the chloroplast, increasing the robustness of the model (Wang and Leuning 1998, Yin and Struik 2009, Fatichi et al. 2019). These changes link stomatal conductance to CO_2 assimilation (Farquhar et al. 1980, Fatichi et al. 2019).

The robustness of this biochemical model has been proven in various studies, however the type of stomatal conductance model used has been criticised, since these models are mainly empirical (Buckley 2017, Fatichi et al. 2019). Empirical models are wildly used for plant modelling; however the underlying controls are not considered in empirical models (Buckley 2017). Process-based models for stomatal conductance do exist (Buckley and Mott 2013, Buckley 2017), with most of them focusing on stomatal response to changes in water relations within the leaf and cells (Vialet-Chabrand et al. 2017).

One of the most widely used stomatal conductance model, the Ball-berry model for stomatal conductance, requires a sensitivity parameter to calculate the interior CO_2 concentration. The sensitivity parameter varies with changes in water potential and is difficult to capture for all leaves in a canopy (Tenhunen et al. 1977). Various models have been proposed to couple photosynthesis to leaf water potential. Stomatal conductance regulates both photosynthesis and water loss and is often used as the key coupling variable in photosynthetic models (Kim and Lieth 2003, Tuzet et al. 2003, Dewar et al. 2018).

Tuzet et al (2003) proposed a model that couples, water movement in the plant, stomatal conductance, the leaf energy balance and photosynthesis. The model uses the Farquhar, von Caemmer and Berry model to calculate photosynthesis (Farquhar et al. 1980, Tuzet et al. 2003). The model developed by Dewar (2002) combined the stomatal-conductance models of Tardieu-Davies and Ball-Berry-Leuning (Ball et al. 1987, Tardieu and Davies 1993, Leuning 1995, Dewar 2002). In the Tardieu-Davies model, stomatal conductance was calculated from changes in abscisic acid

(ABA) concentration and leaf water potential, while the Ball-Berry-Leuning model calculated stomatal conductance from VPD, CO_2 partial pressure and net photosynthetic rates without taking the change in leaf water status into account (Ball et al. 1987). Buckley et al (2003) developed a hydro-mechanical model that incorporates feedback loops where guard cell pressure is regulated by a portion of the turgor pressure in the leaf.

Optimisation models have also been proposed as an alternative to empirical stomatal models (Cowan and Farquhar 1977, Sperry et al. 2017). Optimisation models propose that plants will allow water loss to increase productivity and CO_2 uptake when water is abundant, however plants will sacrifice productivity during drought to minimise water loss (Schulze and Hall 1982, Morrison 1987). Although optimisation models have successfully explained some empirical models for stomatal conductance (Manzoni et al. 2011, Lin et al. 2015), these models are still not often used since it is not clear how to interpret certain water use efficiency parameters within the model (Buckley et al. 2017). Although optimisation models show promise in modelling stomatal conductance, there is still not a lot of research focussing on the use and testing of these models for different plant species. In a review done by Damour et al. (2010) on stomatal conductance models, optimisation models were not even covered, highlighting the need for further investigation into the use of these models (Damour et al. 2010).

The link between photosynthesis and hydraulic conductance

Stomatal regulation plays an important role in the overall carbon and water balance of plants by controlling the rate of water loss and carbon gain through CO_2 uptake. Plants are constantly balancing a trade-off between water loss and carbon gain (Xiong and Nadal 2020). If the loss of water through transpiration exceeds the water supplied from the soil and roots, the relative water content of the plant decreases (Lambers et al. 1998). When stomata close in response to drought, a reduction in CO_2 uptake is seen, which in effect reduces the photosynthetic capacity of plants.

Drought stress has both direct and indirect effects on photosynthesis. Not only is CO_2 uptake reduced, but reductions in the efficiency of carboxylation have also been seen as a response to drought stress (Ramanjulu et al. 1998). Reductions in leaf area (through the shedding of leaves) have also been noted in plants experiencing drought stress (Rouhi et al. 2007). This helps decrease the net assimilation rate and reduces the demand on the water supply. Reductions in stomatal conductance and assimilation rate per leaf area have been noted in species that are more resistant to drought (Rouhi et al. 2007). Franks (2005) showed that stomatal conductance and assimilation rates

are connected, with assimilation rates decreasing with a decrease in stomatal conductance (Franks 2006).

Stomatal conductance and the hydraulic system of a plant operate in somewhat opposing roles. The hydraulic system ensures the water supply, while stomatal conductance regulates the water loss through transpiration. This interaction seen between the hydraulic system and stomatal conductance has an influence on the water pressure gradient and directly influence the carbon assimilation of a plant (Ding et al. 2020). As previously mentioned, the hydraulic conductance of a plant is affected by changes in environmental variables, which constrains assimilation rates of plants (Franks 2006). Photosynthesis and hydraulic conductance are indirectly connected, through stomatal conductance (Brodribb and Jordan 2008).

Various studies have focused on how changes in hydraulic conductance affect photosynthesis. Increased hydraulic conductance has been positively correlated with photosynthetic rates and stomatal conductance in *Phaseolus vulgaris* (Sober 1998) and in various angiosperms (Brodribb and Feild 2000). Irvine *et al*. (1998) showed that a decrease in hydraulic conductance was associated with stomatal closure and reduced production rates in mature Scots pine (Irvine et al. 1998).

Eucalyptus and South Africa

Eucalyptus, an important genus consisting of large number of species, is a member of the Myrtaceae family. *Eucalyptus* species grow in a wide range of habitats, and many are popular for commercial hardwood production (Turnbull 2000). Due to their fast-growing nature, rotation periods for eucalypt pulp are short (8 – 10years), and they are grown for a wide variety of products including for solid wood production, oil and pulp (Morris 2008). In South Africa, commercial forestry accounts for more than 1.5 million of agricultural land, with *Eucalyptus* plantations accounting for almost 40 % of the afforested land (Morris 2008, Boreham and Pallett 2009).

The short rotation periods of *Eucalyptus* also means that *Eucalyptus* are more sensitive to changes in the environment. The high growth rates of *Eucalyptus* are dependent on high photosynthetic rates, which are affected by fluctuations in environmental variables. Although the potential production rates of *Eucalyptus* are high, these rates are not always seen due to suboptimal environmental conditions (Whitehead and Beadle 2004).

One of the main environmental variables that limit growth rates in South Africa is the availability of water. *Eucalyptus* plantations in South Africa are therefore mainly located in higher rainfall areas (DWAF 2005). Dye (1996) showed that the availability of water has a significant effect on tree growth, especially in South Africa, where temperatures and soil types are optimal for forestry (Dye 1996, 2000). Understanding the relationship between water transport and photosynthesis and how this relationship is affected by changes in climate, is important to understand growth and production rates of *Eucalyptus*.

In South Africa, and other drought-prone countries like Australia (Li et al. 2005), shifts in precipitation and temperature are predicted due to climate change. Areas with optimal environmental conditions for forestry are likely to shift (Warburton and Schulze 2008). Understanding how *Eucalyptus* species respond to changes in water availability, will give valuable insight into the management of *Eucalyptus* plantations in a changing environment.

Chapter 3

Measurements done on excised stems indicate that hydraulic recovery can be an important strategy used by *Eucalyptus* hybrids in response to drought

Published in *Trees: Structure and Function* on 04 August 2021
(doi.org/10.1007/s00468-021-02188-7)

Trees
https://doi.org/10.1007/s00468-021-02188-7

ORIGINAL ARTICLE

Measurements done on excised stems indicate that hydraulic recovery can be an important strategy used by *Eucalyptus* hybrids in response to drought

Alta Saunders[1] · **David M. Drew**[1]

Received: 16 February 2021 / Accepted: 22 July 2021

Abstract

Key message ***A high-risk hydraulic strategy might be linked to embolism recovery in Eucalyptus hybrids, allowing plants to have high hydraulic conductivity regardless of safety.***

Abstract Plants use a variety of strategies to mitigate or reduce drought-induced hydraulic failure. Recovery of hydraulic conductivity after drought stress can be an important mechanism used to avoid drought-induced mortality; however, the underlying mechanism of hydraulic recovery is still poorly understood. We examined the hydraulic recovery response between *E. grandis* × *camaldulensis* (*GC*) and *E. urophylla* × *grandis* (*GU*) after drought. We aimed to determine if there is a trade-off between xylem safety and hydraulic recovery and what the underlying mechanism might be. Destructive measurements together with X-ray microtomography measurements were used to determine the extent of hydraulic recovery at various time intervals. We found two distinct hydraulic strategies used by plants. *GC* was more resistant to embolism formation as compared to *UG*; however, *GC* showed lower levels of hydraulic recovery after rewatering. Larger vessel sizes were related to increases in drought vulnerability. Hydraulic recovery was also related to functional traits of cells surrounding vessels, highlighting the possible role that these cells play to increase hydraulic conductance in the xylem and increasing connectivity between vessels. Our study suggest that hydraulic recovery can be an important hydraulic strategy used by *Eucalyptus* hybrids in response to drought. A high-risk hydraulic strategy might be linked to embolism recovery, allowing plants to have high hydraulic resistance regardless of safety.

Keywords Embolism · Recovery · Refilling · Drought stress

Introduction

An increase in drought-induced tree mortality (Hammond et al. 2019), which can be expected to have a significant impact on plant survival in a changing climate, has been found in several studies in the last few years (Anderegg et al. 2013; Allen et al. 2015; McDowell et al. 2018). Major increases in tree mortality are likely to have an impact on global carbon and hydrological cycles (Bonan 2008). It is, therefore, important to understand the strategies that trees use to avoid drought-driven mortality to improve production and vegetation models (Fatichi et al. 2019; Hammond et al. 2019).

During drought stress the continuous water column in the xylem can be disrupted by the formation of air bubbles or embolism which can reduce hydraulic conductivity leading to hydraulic failure (Tyree and Sperry 1988; Sperry et al. 2017; Xiong and Nadal 2020). Embolism formation restricts the water movement through the soil–plant–atmosphere-continuum (SPAC) and can lead to stomatal closure which helps prevent further water loss (Becker et al. 2000). However, this leads to a reduction in CO_2 uptake which is needed for photosynthesis (Kramer and Boyer 1995; Becker et al. 2000). The restriction of water movement through the SPAC also affects the transport of carbohydrates, ultimately limiting metabolism and growth (McDowell et al. 2008; Anderegg et al. 2015; Trugman et al. 2018).

Communicated by Andrea Nardini.

✉ Alta Saunders

David M. Drew
drew@sun.ac.za

[1] Department of Forest and Wood Science, Stellenbosch University, Private Bag X1, Stellenbosch, South Africa

Published online: 04 August 2021

A wide range of strategies are used by plants to mitigate or reduce hydraulic failure, ranging from avoiding embolism formation, refilling embolism or repairing damaged hydraulic pathways through regrowth (Ogasa et al. 2013; Sperry and Love 2015; Klein et al. 2018). Many previous studies have focussed on how plants avoid hydraulic failure (Pittermann et al. 2006; Gleason et al. 2016; Venturas et al. 2017; Barotto et al. 2018), with focus not always given to recovery strategies deployed by plants (Klein et al. 2018). While it has been suggested by several researchers that plants can recover lost hydraulic conductance, there is still a debate about the underlying mechanisms and whether or not recovery can take place over short time periods (Cochard et al. 2001; Nardini et al. 2011; Klein et al. 2018).

It is well established that embolism refilling can take place when soil water potential increases (Brodersen and McElrone 2013; Niu et al. 2017), with evidence showing that some species refill embolism at night following increases in soil water potential (Ogasa et al. 2013; Brodersen and McElrone 2013; Klein et al. 2018; Zeppel et al. 2019). The use of nonstructural carbohydrates (NSC's) have also been suggested to play a role in aiding hydraulic recovery (Nardini et al. 2011; Tomasella et al. 2019a, b). Liu et al. (2019) found that corticular photosynthesis promoted accumulation of NSC's in the bark and was correlated with water uptake assisting in hydraulic recovery, while Secchi et al. (2021) showed that recovery is energy dependant and that the accumulation of sugars within the apoplast assisted in recovery. The physiological characteristics of plants related to embolism refilling and whether the strategies used by plants depend on their resistance to cavitation is, however, still largely unknown (Ogasa et al. 2013; Fernández et al. 2019).

Understanding these phenomena is of particular relevance to the genus *Eucalyptus*, a planted hardwood with a wide distribution (Myburg et al. 2014) and of great commercial significance. It has been shown that there is a wide variation in hydraulic responses to drought within the *Eucalyptus* genus (Bourne et al. 2017). Recent work by Choat et al. (2018) using CT imaging found that embolised vessels in various *Eucalyptus* spp. were not completely refilled even 72 h after rewatering, however evidence of possible partial refilling was seen. Complete recovery was however not seen in the experiment, with air bubbles persisting in all vessels to some degree (Choat et al. 2018). Work done by Zeppel et al. (2019), however, showed evidence of hydraulic recovery within *Eucalyptus* spp. after 12 h rewatering.

Measurements of hydraulic recovery using percentage loss of hydraulic conductance (Ogasa et al. 2013; Zeppel et al. 2019) have, however, been criticised for possible measurement artefacts caused by cutting xylem under tension, which allows the entry of air into vessels even when xylem is excised under water (Wheeler et al. 2013; Torres-Ruiz et al. 2015). The significance of these artefacts has, however, also been questioned (Trifilò et al. 2014; Ogasa et al. 2016), with some authors arguing that rehydration to relax xylem tension might be the cause of discrepancies seen in measurements and should be accompanied by in vivo measurements as well (Nardini et al. 2011, 2017; Ogasa et al. 2016; Savi et al. 2016; Nolf et al. 2017).

Despite concerns regarding measurement artifacts leading to overestimating xylem vulnerability to embolism (Wheeler et al. 2013; Torres-Ruiz et al. 2015; Charrier et al. 2016; Lamarque et al. 2018), the number of studies showing recovery when there is a reduction in drought stress has been growing (Brodersen and McElrone 2013; Nardini et al. 2017; Brodersen et al. 2018; Liu et al. 2019; Tomasella et al. 2019a; Secchi et al. 2021). Studies combining in vivo measurements, such as X-ray microtomography (Kim and Lee 2010; Torres-Ruiz et al. 2015; Choat et al. 2015; Knipfer et al. 2016) and magnetic resonance imaging (Zwieniecki et al. 2013; Ogasa et al. 2016) with traditional measurements of embolism formation and recovery, can help validate recovery responses seen in the xylem (Nardini et al. 2017).The use of CT scans has created the opportunity to study embolism recovery in conjunction with traditional hydraulic measurement methods to avoid possible controversies regarding refilling. More studies are also needed where plants are not rewatered, to exclude refilling through increased root pressure.

In response to these questions, we looked at a variety of physiological variables related to the hydraulics of a plant to understand the drought recovery response, focussing on two physiologically contrasting commercial *Eucalyptus* hybrids. We focussed on using both hydraulic measurements and imaging methods (micro-CT) of hydraulic recovery. We aimed to (1) determine if the strategy of xylem embolism recovery and xylem embolism resistance is related to specific physiological or anatomical variables and (2) determine if there is a trade-off between xylem safety and a plants ability to recover from embolism after drought.

Methods

Plant material

All work was done using 42 potted rooted cuttings of two *Eucalyptus* hybrids. A 2-year-old *E. grandis X camaldulensis* (*GC*) ($n=21$) and *E. urophylla* × *grandis* (*UG*) ($n=21$) plants were grown under the same conditions under shade netting and were watered to field capacity twice a day prior to experimental work. Plants were grown in 2 L pots in a soil mixture with a ratio of 1:2 fine sand and composted pine bark. When plants were initially planted in pots, plants were fertilised once with a composted chicken manure.

Plants were then periodically fertilised with the controlled release Haifo Multicote 8 (N:15%, P:3%, K:12%, S:7%) fertiliser until the start of sampling. The height of plants varied between 0.7 and 1.2 m, with the canopy starting roughly halfway up the stem. No significant difference in height was seen between the two hybrids. The average stem diameter of all plants was 6.47 ± 0.94 mm as measured at 20 cm above the base of the stem. All measurements were done during May–December 2020.

Vulnerability curves

Vulnerability curves were constructed using the bench dehydration method and plotting the changes of hydraulic conductivity over xylem water potential (Ψx) (Tyree and Sperry 1988). The xylem tension at which stems lose 50% of their hydraulic conductance (P50) is used as a measure of how resistant plants are to embolism formation caused by drought (Martin-StPaul et al. 2017).

Plants were cut at the base of the stem before dawn, placed in water and covered with a black plastic bag before being transported to the laboratory where they were dried to different Ψx. Bench dehydration was used as it relies on desiccation and the introduction of artefactual embolism can be minimised as compared to methods like the centrifuge technique (López et al. 2018). Xylem water potential was measured from excised leaves using a pressure chamber (SKYE plant moisture system, SKPM 1400 series). Cut plants were placed in a sealed bag with a damp paper towel and allowed to equilibrate water potential between leaves and stem for 30 min before any measurements were made.

After Ψx measurements were made, hydraulic conductivity (K_h) was measured to obtain Ψx and K_h pairs. Stems were recut roughly 2–5 cm above the base of the plant while being submerged in water. Stem segments of 15–20 cm, which is more than half the stem length, were then cut while submerged and ends were shaved with a razer blade before being connected to tubes. Using gravity to create a hydraulic pressure head, samples were first perfused with distilled water and measurements were only made when the flow rate became stable after a few minutes (Torres-Ruiz et al. 2012). It is important to note that although steps have been taken to minimise cutting artifacts, possible cutting artifacts could however have occurred during sample preparation.

The K_h was calculated as the flowrate (kg s^{-1}) over the water potential difference (MPa^{-1}) along the stem segment. The hydraulic pressure head never exceeded 5.5 kPa to ensure that emboli were not artificially flushed during measurements. Flowrate was measured on an analytical balance, which can make measurements up to 3 decimal points, as change in water mass over time. Flowrate was measured at three different hydraulic pressure heads, including flow rate at no hydraulic pressure head to improve the accuracy of K_h measurements of each stem segment (Torres-Ruiz et al. 2012).

Xylem recovery index

The Xylem Recovery Index (XRI) is based on the ratio of hydraulic conductivity under rewatered conditions and wet conditions (Ogasa et al. 2013). Zeppel et al. (2019) adjusted the XRI to account for the extent of drought experienced. The hydraulic method similar to the method used to construct vulnerability curves was used to make hydraulic measurements. Plants were dehydrated until more than 65% of hydraulic conductivity was lost based on Ψx (*UG*: mean $= -2.86 \pm -0.9$ MPa; *GC*: mean $= -3.26 \pm -0.23$ MPa). Cut stems with intact canopies that were dehydrated during the construction of vulnerability curves were rehydrated overnight (at least 15 h) by placing the cut base of stems in water before measuring the hydraulic conductivity of each species after rewatering. Hydraulic measurements were made in three stems of plants before dehydration, on three stems of plants that were dehydrated and then three stems of plants that were rehydrated over night after dehydration.

The hydraulic conductivity of cut stems of plants were measured before drought, during drought and after rewatering using the method described above. XRI can be calculated as:

$$\mathrm{XRI} = \frac{K_{hD} - K_{hRW}}{K_{hD} - K_{hw}}$$

where K_{hD} is the K_h measured during drought, K_{hRW} is the K_h measured after rewatering and K_{hW} is the K_h measured before drought is induced.

Micro-CT scans and Image analysis

Plants were cut at the base of the stem late afternoon before scanning and allowed to dehydrate over night until > 65% loss of hydraulic conductivity was achieved based on leaf water potential (Ψl) measurements. Dehydrated cut stems with plant canopies intact were scanned the following morning and then placed in water to allow rehydration after scanning for two hours. Cut plants with intact canopies were rehydrated for 2 h by placing cut base of stems in water. A single replication was also done on plants that were rehydrated for 24 h. Leaf water potential measurements were done on rehydrated plants to ensure that recovery took place. The rehydrated plants were then rescanned. The scanned area on the stem was marked to ensure that the same area was rescanned over time. Scans were taken in the central part of the stem below leaf formation, which was more than 16 cm away from the cut base. The scanned distance from the cut also minimised any recovery

artefacts seen as a result of capillary action. It is important to note that although steps were taken to minimise the introduction of artefactual embolism, it could not have been fully excluded from the study. The duration of scans was 30 min and to ensure that plants lost minimal amount of water during scans, the leaves of plants were wrapped in clingwrap and the cut stem was sealed with parafilm for the duration of the scan.

All scans were done at the CT facility situated at Stellenbosch University (du Plessis et al. 2016). To generate an image with 15 µm voxel size, 1800 projections were taken during a 360° rotation with 140 kV and 80 µA. Cross-sectional (2D) images were extracted from the middle of the 3D scan volume using Volume Graphics VGStudioMax 3.1. An adaptive Gauss filter was used to reduce noise in the image.

All cross-sectional images were further analysed using the image analysis software ImageJ (Schneider et al. 2012). A threshold was applied to all images to extract only black pixels. This ensured that only air-filled vessels were captured, since air appeared as black on images due to density differences. To determine which vessels refilled, an overlay was created with images taken at dehydration and after rewatering. Images were aligned based on feature selection and visually inspected to ensure alignment (Fig. 1). Within ImageJ, the *analyse particles* function was used to measure vessel dimensions and co-ordinates. Vessel co-ordinates were used to calculate the distance to the nearest vessel neighbour as well as the distance of vessels from the perimeter of the stem.

To determine which vessels were embolised during dehydration, cross sectional slices of stems were made after the CT scanning and stained with an alcian blue and safranin solution. Images of the cross sections and 2D images generated from the CT scans were aligned based on feature selection (Figs. 10 and 11 in supplementary material). To determine the accuracy of vessel area extraction during image processing, the percentage extracted vessel area was compared with the black/white pixel ratio of the original cross-sectional CT images.

In between scans, plants were removed from the CT scanner and placed in water. The plants had to be placed back in the CT scanner after rewatering. Even though the area that was scanned was marked on each stem, there was a small margin of error due to alignment differences.

The theoretical hydraulic conductivity (kg MPa^{-1} s^{-1} m) was calculated for all embolised and refilled vessels (Tombesi et al. 2010). The K_h of embolised and refilled vessels were calculated based on the Hagen–Poiseuille's law (Tyree and Ewers 1991) modified by Tombesi et al. (2010):

$$K_h = \left(\frac{\pi\rho}{128\eta}\right)\sum_{i=1}^{n} d_i^4$$

where η is viscosity of water set at 1×10^{-9} MPs·s; ρ is fluid density of water set at 1000 kg m^{-3} and d is the radius of a vessel (m) (Tombesi et al. 2010).

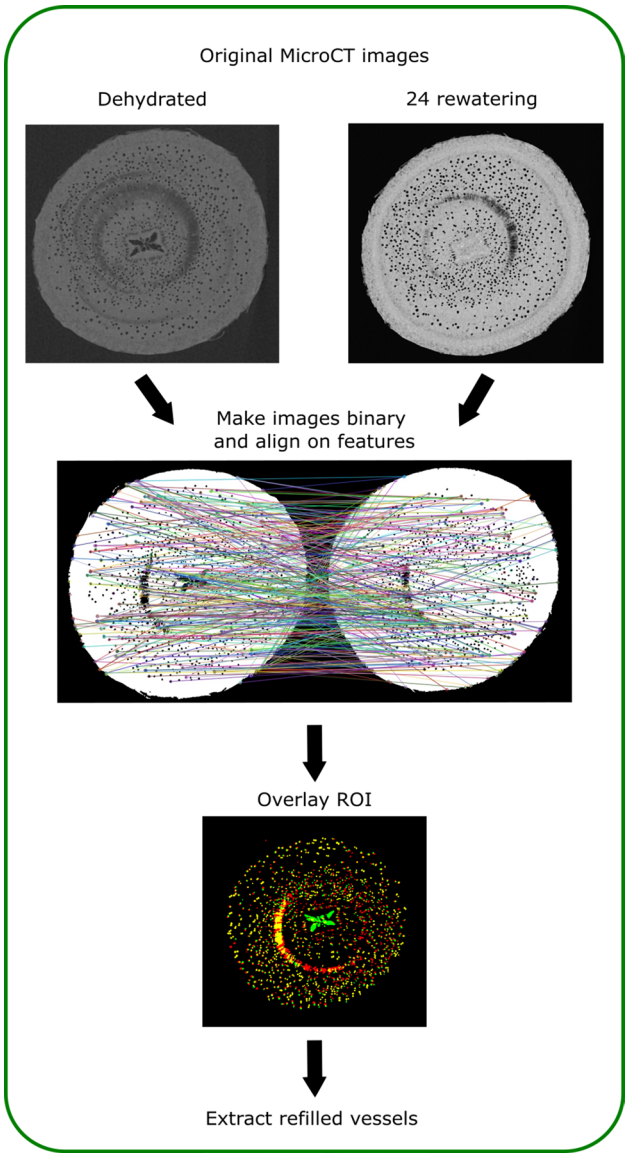

Fig. 1 Image processing pipeline to extract refilled vessels as captured from cross-sectional images from CT scans

Anatomical variables

In order to visually determine the extent to which water exits vessels and moves into adjacent tissue, a 1% safranin solution was allowed to flow through a 15 cm stem segment using a similar set-up as described in the vulnerability curve methods. This was done for three plants before dehydration for both hybrids. The hydraulic pressure head ranged between 5–7 kPa. The solution flowed through the stem segment until the safranin solution was seen at the distal end of the stem. Cross sections of the stem segments were manually made in the middle of each 15 cm stem segment.

The following measurements were made from photos of the cross sections using ImageJ software (Schneider et al.

2012): vessel area (mm^2), the stained areas (mm^2) (area that was stained by the safranin dye outside of the vessel), bridge length (µm) (the distance between two vessels if there is a continuous stained area between them) and number of connecting vessels (vessels that are connected by the stained area) (Fig. 2).

Cross-sections of stems after CT scanning was also taken and stained with an Alcian blue and safranin solution. This allowed for the pattern detection of nonlignified cells surrounding vessels (which can include parenchyma and vasicentric tracheids) (Vazquez-Cooz and Meyer 2002).

All images used for processing were obtained using a Motic BA310Pol polarizing microscope with the 40× objective.

Statistical analysis

All data was tested for normality before analysis. Homogeneity of variances was also tested before analysis. A single sample t-test was used to test for difference in the recovery strategies, which included the vulnerability curves and xylem recovery index, used between the two hybrids.

A Spearman's correlation matrix was used (since data did not show normality) to determine whether there was any significant relationship between anatomical features and functional hydraulic traits. The relationship between the following variables were tested: vessel area (mm^2), the stained area (mm^2), bridge length (µm) and number of connecting vessels. A non-parametric Kruskal–Wallis test was used to determine if there was a significant difference in anatomical features and hydraulic traits between hybrids. Distribution curves were used to compare vessel size distribution between the two hybrids.

From the CT-scanned images the percentage difference in vessel area and vessel k_h was used to determine if vessels refilled. Distribution curves were used to compare vessel size and the distance of the nearest vessel neighbour distribution between the refilled and embolised vessels for both hybrids.

Results

Functional hydraulic traits

The two hybrids exhibited different xylem morphological characteristics (Table 1). There was a significant difference seen in the distribution of vessel sizes between the two hybrids ($H = 14.139$, $p < 0.05$), with larger vessels found in *UG* but a higher count of vessels in *GC* (Table 1) (Fig. 3). *GC* showed high counts of smaller vessels with the highest frequency of vessels close to its mean. *UG* had the largest vessels with a maximum vessel area of 0.015 mm^2 as compared to the maximum vessel size of 0.008 mm^2 seen in *GC*.

Importantly, there was also a distinct difference seen in the hydraulic strategies used by the two hybrids. The vulnerability curves of the two hybrids were different, with *GC* losing halve of its hydraulic conductivity at a Ψx (P50) of − 2.72 MPa as compared to *UG* which had a P50 value of − 2.33 MPa ($t = -2.65$, $p = 0.008$) (Fig. 4). The hydraulic recovery response was also different between

Table 1 Kruskal–Wallis *H* value and significance levels of hydraulic characteristics between *E. urophylla* × *grandis* (*UG*) and *E. grandis* × *camaldulensis* (*GC*)

	Kruskal–Wallis test	*UG*	*GC*
Bridge length (µm)	$H = 5.109$	51.38 ± 38.17	34.933 ± 25.34
Vessel area (µm²)	$H = 14.139$***	2290 ± 1116	1933.8 ± 3000
Stained area (µm²)	$H = 52.423$***	9766 ± 5924	5333 ± 4553
Connecting vessels	$H = 3.837$*	0.957 ± 1.141	1.385 ± 1.624

Mean and standard deviation of hydraulic characteristic of each hybrid ($n = 3$)

Significant values are indicated as follows: * indicates significance of $0.05 < p < 0.06$, ** indicates significance of $0.001 < p < 0.05$, *** indicates significance of $p < 0.001$

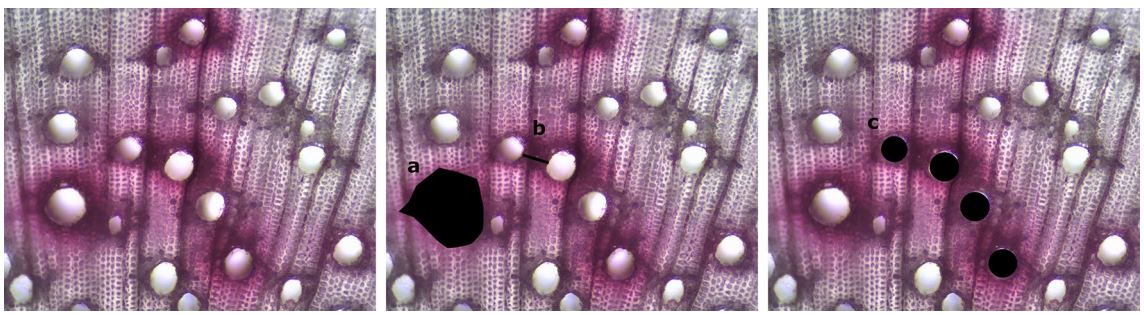

Fig. 2 Safranin stained zone surrounding vessels. The following measurements were made on the photos: Stained zone (**a**), Bridge length (**b**) and Connecting vessels (**c**). Photos were taken at a 40× magnification

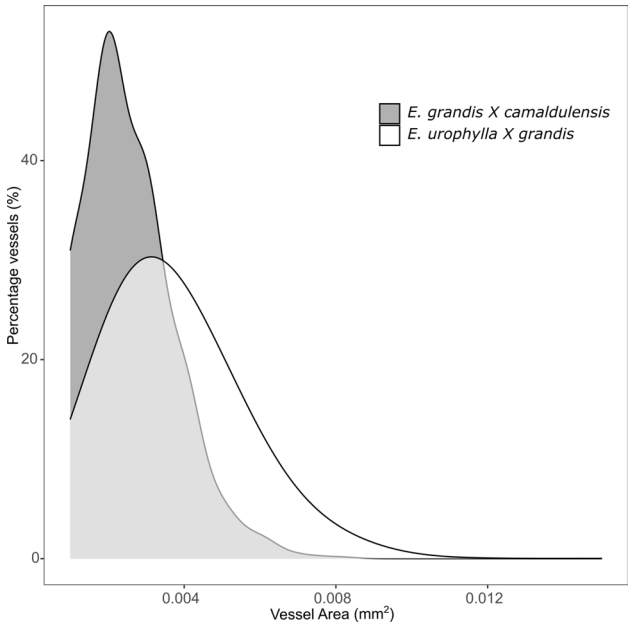

Fig. 3 Vessel area size distribution of *E. urophylla* × *grandis* and *E. grandis* × *camaldulensis* as percentage over vessel area size

the two hybrids. *UG* had a much higher XRI ($H = 3.857$, $p < 0.05$) as compared to *GC* (Fig. 5). It is important to note that both hybrids showed a level of hydraulic recovery, with the measured hydraulic conductivity increasing after rewatering.

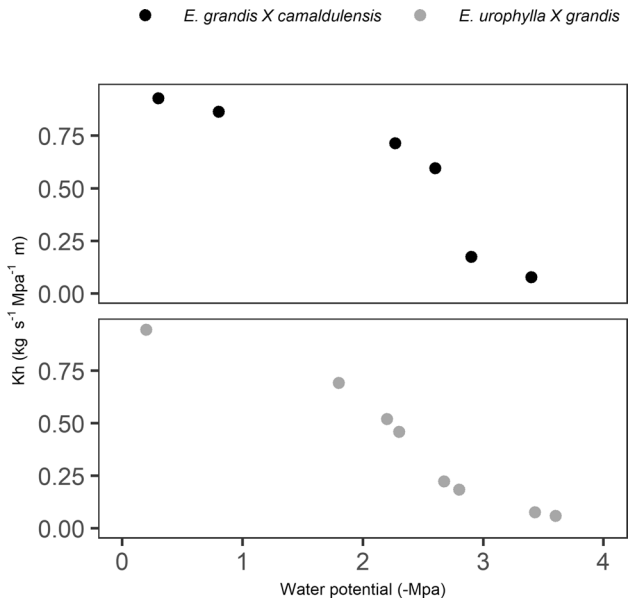

Fig. 4 Vulnerability curves indicating the hydraulic coductivity (K_h: kg m MPa^{-1} s^{-1}) over decrease xylem water potential (Ψx). A significant difference was seen between the curves of the two hybrids ($t = -2.65$, $p = 0.008$)

Functional traits of vessels and surrounding cells

There was a significant difference in the area of safranin staining around vessels between the two hybrids ($H = 52.423$, $p < 0.05$) (Table 1). *UG* showed larger areas of safranin staining when compared with *GC* (Table 1).

The bridge length (continuous stained distance between two vessels) was on average longer in *UG* (mean = 51.38 µm) compared to *GC* (mean = 34.99 µm). The connecting vessels (vessels that are connected by the stained area) were different between the two hybrids ($H = 3.837$, $p = 0.05$), with more connecting vessels seen in *GC*.

For both hybrids, there was a positive relationship between safranin-stained area and vessel size (*UG*: $r_s = 0.312$, $p < 0.05$; *GC*: $r_s = 0.374$, $p < 0.05$). In *GC* the bridge length was significantly correlated to the stained area ($r_s = 0.374$, $p < 0.05$), however this correlation was not seen in *UG* ($r_s = 0.088$, $p > 0.05$). The vessel area and bridge length were not significantly correlated in either hybrid (Tables 2 and 3 in Supplementary material).

Patterns of blue staining was also observed around vessels, when cross-sectional stem segments were stained with a safranin and Alcian blue double stain.

Recovery response

Plants were dehydrated until more than 65% of hydraulic conductivity was lost based on Ψ1 (*UG*: mean = − 2.86 ± − 0.9 MPa; *GC*: mean = − 3.26 ± − 0.23 MPa) and estimated vulnerability

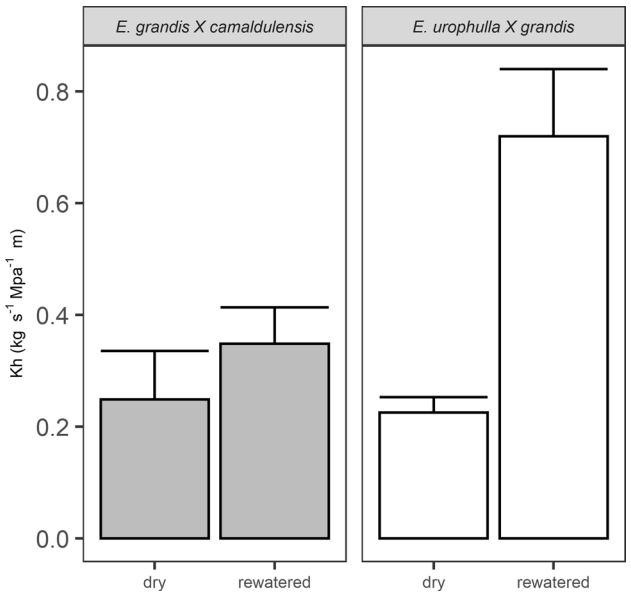

Fig. 5 Mean hydraulic conductivity of stems measured during drought and after rewatering. Error bars show 95% confidence interval

curves. Recovery of Ψl within both species was assessed after 2 h of rewatering (*UG*: mean = − 1.07 ± − 0.64 MPa; *GC*: mean = − 1.13 ± − 0.42 MPa) and 24 h of rewatering (*UG*: − 0.425 ± − 0.26 MPa; *GC*: − 0.5 ± − 0.20 MPa).

From the CT scan results, evidence of vessel refilling was seen for both hybrids (Figs. 6 and 7). When analysing the black/white pixel ratio there was a significant difference in percentage of vessels seen that refilled between the two hybrids ($H = 3.857$, $p < 0.05$), with a higher percentage of vessels refilling in *UG* after 2 h (Fig. 8). Similar trends were, however, clearly seen whether the black/white pixel ratio or the K_h calculated from extracted vessels was used during analysis and it was decided to report results of analysis done on the extracted vessel K_h only (Fig. 8). In both hybrids the K_h that recovered were however small (*UG*: mean = 2.99 ± 3.31%, *GC*: mean = 0.35 ± 0.39%). Vessels were; however, not analysed on a longitudinal axis during CT-scan analysis. No distinguishment was therefore made between complete and partial refilling.

When comparing the percentage extracted vessel K_h to the black/white pixel ratio of the original cross-sectional CT images refilled vessel area was overestimated when analysing the extracted vessel area. During the image analysis in both hybrids there was an overestimate of percentage of vessels that recovered during rewatering with an estimated mean error of 1.31% in measurements of *GC* and an estimated mean error of 2.15% in measurements of *UG* (Fig. 8).

The vessels that embolised in both hybrids were significantly closer to each other as compared to the vessels that refilled (*GC*: $H = 150.58$, $p < 0.05$, *UG*: $H = 86.18$, $p < 0.05$) (Fig. 9).

The vessels that refilled in *UG* were significantly closer to the stem perimeter ($H = 719.79$, $p < 0.5$), however this trend was not seen in *GC* (Fig. 9). The vessels that refilled in both hybrids had significantly smaller k_h than the vessels that stayed embolised (*GC*: $H = 160.65$, $p < 0.05$, *UG*: $H = 343.49$, $p < 0.05$).

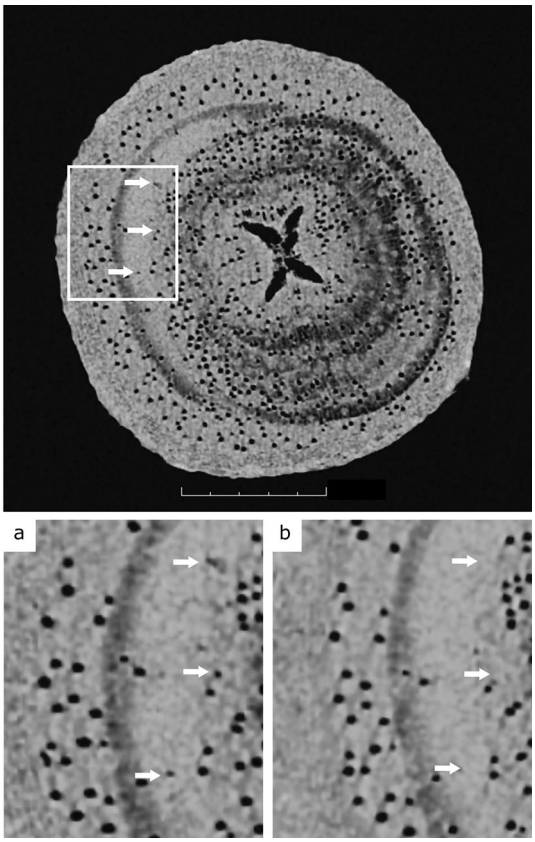

Fig. 7 Images showing refilled vessels during dehydration (**a**) and after 2 h of rewatering (**b**) in *E. grandis* × *camaldulensis*. White arrows indicate examples of refilled vessels. The white box shows area of focus

Discussion

Trade-off between safety, efficiency and recovery

Although the underlying mechanisms relating to embolism

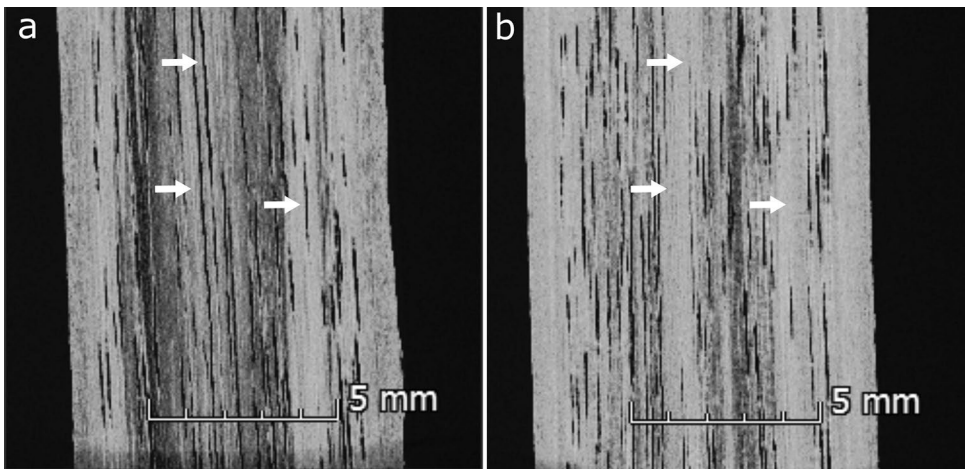

Fig. 6 Longitudinal CT sections showing refilling of vessels in *E. urophylla X grandis*. CT scans show stem when dehydrated (**a**) and 24 h after rewatering (**b**). White arrows indicate areas of clear change seen after rewatering

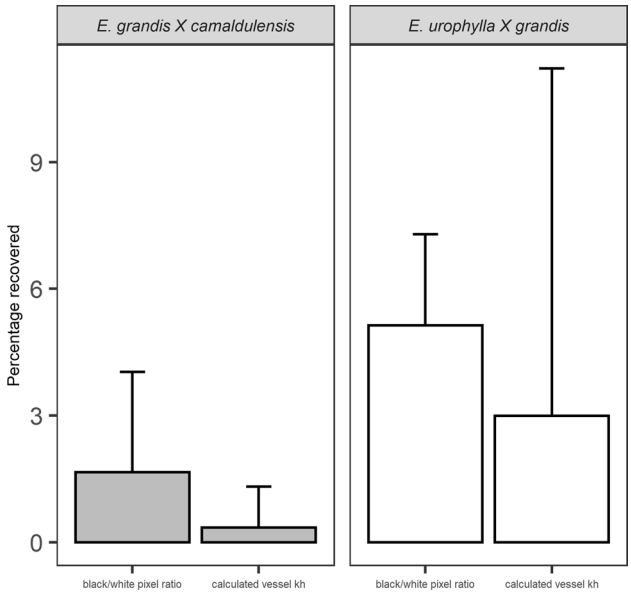

Fig. 8 Mean percentage vessels that refilled of each hybrid after 2 h of re-watering as calculated from black pixels of original CT scans and as calculated from extracted vessels after image processing. Error bars show 95% confidence interval. A significant difference was seen between two hybrids ($H = 3.857$, $p < 0.05$)

recovery are still not well understood, embolism recovery is increasingly considered an important hydraulic strategy used by plants in response to drought (Nardini et al. 2011). Plants often function at Ψx close to hydraulic failure thresholds (Ogasa et al. 2013). Drought levels in the field often exceed P50 values; however, certain plants can nonetheless survive post drought (Klein et al. 2011; Trifilò et al. 2015).

In this study, there was a trade-off seen between resistance to embolism and ability to recover hydraulic conductance following drought. Two distinct hydraulic strategies were observed between the two *Eucalyptus* hybrids, with the hybrid *UG* that is considered more drought-vulnerable (Van der Willigen and Pammenter 1998; Drew et al. 2009) having a higher rate of hydraulic recovery as compared to the embolism resistant hybrid. On the other hand, *GC* showed a greater resistance to embolism and hydraulic loss, an effect also seen by other authors (Van der Willigen and Pammenter 1998; Souden et al. 2020). It has been found that there is a correlation between P50 values and a plants ability to recover embolism (Klein et al. 2018), indicating that there might be a trade-off between hydraulic recovery and vulnerability.

Hydraulic measurements have been criticised for overestimating drought vulnerability due to the introduction of artificial emboli during the cutting procedure (Wheeler et al. 2013; Torres-Ruiz et al. 2015). Although the possibility

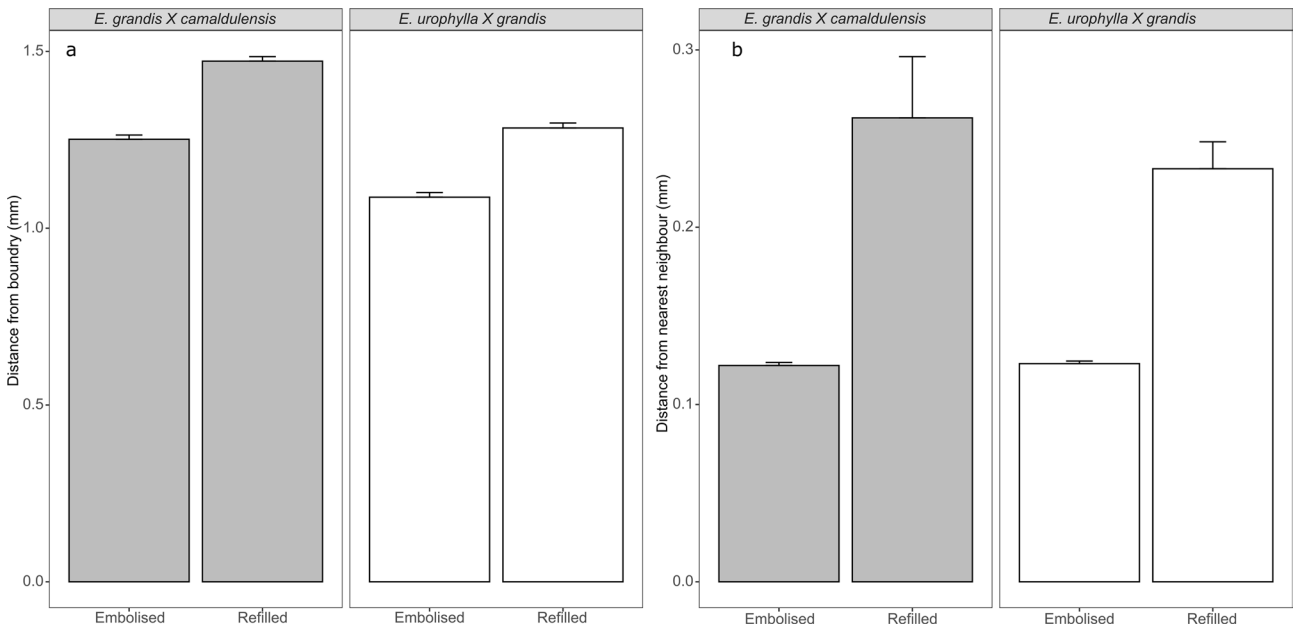

Fig. 9 Figure a show the mean distance of refilled and embolised vessels to stem perimeter; Figure b show the mean distance of embolised and refilled vessels to nearest other vessel. The vessels that embolised in both hybrids were significantly closer to each other as compared to the vessels that refilled (*GC*: $H = 150.58$, $p < 0.05$, *UG*: $H = 86.18$, $p < 0.05$). The vessels that refilled in *UG* were significantly closer to the stem perimeter ($H = 719.79$, $p < 0.5$); however, this trend was not seen in *GC*. All information was extracted from CT scan images after two hours rewatering for both *E. grandis X camaldulensis* and *E. urophylla* × *grandis*. Error bars show 95% confidence intervals

of cutting artifacts could not be excluded from the study, both hybrids were subjected to the same conditions and measurement methods. Different responses could still be seen between the two hybrids further supporting that the responses seen was not due to measurement artifacts. The responses seen in *UG* and *GC* in our study; however, corresponds with the results seen in other studies where it was shown that *GC* is more resistant to embolism formation and drought as compared to *UG* (Van der Willigen and Pammenter 1998; Drew et al. 2009; Saadaoui et al. 2017; Souden et al. 2020), further highlighting the possible link to embolism resistance and recovery.

In our study, larger mean vessel area was seen in the *UG* hybrid that is putatively more vulnerable to drought. This correlation has been seen in other studies (Hacke et al. 2006; Lobo et al. 2018) with the previous studies noting the trade-off between xylem safety and efficiency, but related it to vessel length and not vessel area (Lens et al. 2011). Fernández et al. (2019) found that in several *Eucalyptus* species, vessel safety might be correlated to the area of non-vessel cells surrounding each vessel rather than vessel size.

In the previous studies a trade-off has been observed between efficiency and safety of vessels, with larger vessels compromised by decreases in safety (Gleason et al. 2016). The efficiency of vessels is dependent on their ability to transport water, while safety refers to vessels resisting formation and spread of embolism when soil water decreases (Sperry 2003). A plant's ability to recover hydraulic conductance can, however, also increase a plant's resilience against drought, allowing plants to have high efficiency and resilience regardless of safety (Ogasa et al. 2013).

The two hydraulic strategies seen within this study, highlighted that a high-risk hydraulic strategy might be coupled to a plant's ability to refill embolism. If plants cannot recover hydraulic conductance, they might be more conservative with the hydraulic strategy they use.

Embolism recovery

In our study, embolism recovery took place in both hybrids over short time periods (2–24 h) when plants were rehydrated. It has been previously showed that the recovery of embolism takes place over short time periods by measuring the percentage loss of hydraulic conductance over a drought–recovery cycle (Ogasa et al. 2013; Zeppel et al. 2019); however, in this study the use of successive CT scans on the same samples following rewatering gave further evidence that embolism recovery took place. Although the introduction of artefactual embolisms during sample preparation could not be excluded from the study, both hybrids were subjected to the same conditions and measurement methods. Different responses could still be seen between the two hybrids further supporting that the responses seen was not due to measurement artifacts.

Earlier studies proposed that embolism refilling can occur within 10 min to a few hours indicating that novel refilling is rapid; however, these refilling times have been criticised as possible artifacts of destructive measurements and pressure-induced embolism (Cochard et al. 2000; Hacke and Sperry 2003; Nardini et al. 2011; Duursma et al. 2019). Hydraulic measurements can be used as evidence that hydraulic recovery takes place (Klein et al. 2018); however, the use of in vivo measurements in concert with this approach allows us to independently visually assess the extent of embolism recovery over time (Brodersen and McElrone 2013).

The use of hydraulic measurements in recovery studies have been criticised since stem segments are often cut while the xylem is under tension and it has been suggested that xylem tension should be relaxed before hydraulic measurements take place (Wheeler et al. 2013; Torres-Ruiz et al. 2015). It is suggested that cutting stem segments while xylem is under pressure can lead to the introduction of additional air bubbles into the xylem leading to overestimating xylem vulnerability to drought due to embolism formation (Wheeler et al. 2013). The significance of these artifacts has; however, been questioned (Trifilò et al. 2014; Ogasa et al. 2016). Ogasa et al. (2016) showed that cavitation and refilling is seen when xylem excision takes place while under tension; however, they found that the occurrence of this is not frequent and that artifacts can be minimised by increasing the distance of measurement from the excised end.

The use of micro-CT scans have also cast doubt on the results from studies that used hydraulic measurements in *Laurus nobilis* (Cochard et al. 2015); however, in the study done by Cochard et al. (2015), hydraulic measurements on the same plant material used during the micro-CT scans was not done. A direct comparison could therefore not have been made (Cochard et al. 2015; Nardini et al. 2017). It has also been argued that discrepancies in hydraulic measurements are due to the refilling of embolism during rehydration to relax xylem tension (Nardini et al. 2011; Savi et al. 2016) and should be accompanied by in vivo measurements for validation (Ogasa et al. 2016; Nardini et al. 2017; Nolf et al. 2017).

During this study only a small percentage of hydraulic recovery was seen after two hours using the micro-CT scans. During the hydraulic measurements, a larger recovery was seen after 15 h of rehydration. Concerns regarding cellular damage due to repetitive exposure to radiation during CT scans has been raised by recent studies (Petruzzellis et al. 2018), which could potentially hinder active refilling. During this study, it was therefore important to reduce the exposure of plants to only two CT scans to ensure that cellular damage was kept to a minimum. In the study done by Petruzzellis et al. (2018) they found

that damage was minimal if any was seen after one CT scan; however, cellular damage was seen after the second or third CT scan. During this study, plants were therefore only exposed to one CT scan, before recovery was evaluated during the second scan. During the second scan recovery was still seen in both hybrids; however, to different extents.

It is clear that more studies are needed to understand the source of discrepancies between direct and indirect measurements of hydraulic recovery (Nardini et al. 2017). Although changes in hydraulic measurements can be influenced by artefacts, it has been shown that these are minimal (Ogasa et al. 2016; Nardini et al. 2017) suggesting that large changes in hydraulic measurements after rehydration are due to hydraulic recovery. Hydraulic measurements should therefore also be validated in studies through the use of in vivo measurements, such as micro-CT scans (Brodersen et al. 2010; Choat et al. 2015).

Choat et al. (2018) have found that evidence of refilling seen in cross sectional CT scans in *Eucalyptus* species are often misleading, suggesting that refilled vessels are indications of either partial refilling or a vessel juncture appearing as two embolised vessels. Evidence of partial refilling was seen in *E. saligna* indicating the possibility of an underlying mechanism moving water into embolised vessel. Complete refilling was; however, not seen over a short time frame (Choat et al. 2016). Although the mechanism of refilling can vary between species, the formation of water droplets on the inside of vessels which grows to fill the vessel has been observed in grapevine and laurel (Tyree et al. 1999; Knipfer et al. 2016; Brodersen et al. 2018). In a study done by Knipfer et al. (2016) evidence of partial refilling was seen in grapevines in the absence of root pressure, with evidence that refilling was osmotically driven (Knipfer et al. 2016). A detailed analysis of the same sort in *Eucalyptus* may provide additional insight into the process. In our study no distinction was made between complete and partial refilling. Although there are indications of complete refilling in some vessels (Fig. 6), it is possible that evidence of refilling in other vessels indicate only partial refilling of the vessels.

Excluding the possible regrowth of new hydraulic parthways (Nardini et al. 2014), it has been proposed that embolism recovery can take place either through dissolution of the air bubble when xylem pressures reaches atmospheric pressures or through active or novel refilling (Brodersen and McElrone 2013; Klein et al. 2018), with the latter taking place while the majority of vessels are still under a negative potential (Nardini et al. 2011). There has been a debate on whether embolism refilling can take place under negative tensions (termed novel refilling) (Nardini et al. 2011), with novel refilling only being observed through use of non-invasive measurements in grapevines (Brodersen et al. 2018). We believe our study provides further evidence suggesting that water movement into embolised vessels is a mechanism of hydraulic recovery.

Novel refilling implies that vessels can recover embolism while a large area of functional vessels are still under a negative water potential (Nardini et al. 2011). The physical limitations of refilling under negative tensions have been previously detailed (Vesala et al. 2003); however, it has been suggested that thermodynamic constraints would not allow for novel refilling (Vesala et al. 2003; Zwieniecki and Holbrook 2009; Rockwell et al. 2014). It is significant, in the light of this ongoing discussion, that in our study embolism recovery did apparently take place while a large portion of vessels were still under negative water potantials. This highlights that refilling under negative water potentials could be possible and shows the value of CT scan measurements of embolism refilling (Brodersen and McElrone 2013; Brodersen et al. 2018). Embolism recovery due to an increase in root pressure could be excluded from our study since negative Ψl were still seen in all plants after rewatering.

It has been hypothesized that the role of living cells surrounding vessels (parenchyma, vasicentric tracheids) play an active role in embolism refilling (Nardini et al. 2011; Barotto et al. 2016; Secchi et al. 2021). Nardini et al. (2011) suggests that embolism refilling is a result of sugars and ions being relocated to embolised vessels and changing osmotic gradients. This shift in osmotic gradients drives the flow of water from living cells or neighbouring vessels into embolised vessles (Salleo et al. 2004; Knipfer et al. 2016). The upregulation of certain genes relating to carbohydrate metabolism have also been noted in parenchyma surounding vessels during drought (Secchi and Zwieniecki 2010). The movement of water into tissues immediately surrounding vessels was distinct in our study. This would be expected if the presence of living cells surrounding vessels increases and contributes to the hydraulic conductivity between vessels (Barotto et al. 2016), aiding embolism recovery. Previous studies have shown that the presence of thracheids and parenchyma surrounding vessles improves the hydraulic connectivity between vessles (Salleo et al. 2004; Loepfe et al. 2007; Sano et al. 2011; Barotto et al. 2016).

By increasing the interconnection between vessels, cells surrounding vessels can act as bridges allowing easier water movement between vessels and can contribute to embolism refilling (Barotto et al. 2016). The extent of staining seen was also connected to the percentage of recovery, with *UG* showing larger staining areas as well as increased hydraulic recovery. The staining patterns observed in our study highlights the conductive role of cells surrounding vessels, possibly increasing the connectivity between vessels. Based on the results, it seems likely that cells surrounding vessels will contribute to recovery through increasing hydraulic connectivity.

Conclusion

We observed two distinct hydraulic strategies within *Eucaluptus* hybrids. There was a trade-off between resistance to embolism formation and the ability to recover hydraulic conductivity following drought. A high-risk hydraulic strategy might be linked to embolism recovery, allowing plants to have high hydraulic resistance regardless of safety. While much focus has been given previously to the trade-off between hydraulic efficiency and safety, our results suggest that hydraulic recovery is also an important componant to consider when assessing plant hydraulic strategies. Accordingly, it would be important to understand which taxanomic groups utilise refilling as a hydraulic stratagy to improve vegetation models. The effect of drought stress on production is highly linked to changes in hydraulic conductance. It is important to understand the different mechanisms that govern the responses of plant species to drought stress in order to understand how plant production will be affected by changes in climate.

Previously focus has been given to understand how plant physiology is influenced by drought ultimately leading to tree mortality, with focus often not given to hydraulic recovery after drought. Understanding the hydraulic recovery response of plants, will give further insight into the impact of drought on trees. It is still unclear, whether or not there is a loss of hydraulic conductivity threshold where plants will not be able to recover hydraulic conductance or whether subsequent drougthing events will lead to hydraulic recovery fatigue (Hammond et al. 2019).

Author contribution AS designed the experiment, performed measurements and analysis, and led the writing. DMD contributed to data interpretation, discussion and compiling the final version.

Supplementary Information The online version contains supplementary material available at https://doi.org/10.1007/s00468-021-02188-7.

Acknowledgements We gratefully acknowledge the support of the following people: Sonia Di Buisson (Hans Merensky Holdings) for the provision of the hybrid *Eucalyptus* material used for this study. Dr Leandra Moller for her technical support. Dr Kim Martin for comments and discussions. Dr Anton Du Plessis and Muofhe Tshibalanganda for their assistance in running the CT scans. We would like to thank the anonymous reviewers for all their insightful comments and suggestions.

Funding This work was fully funded by the Hans Merensky Foundation within the Hans Merensky Chair of Advanced Modelling of eucalypt wood formation.

References

Allen CD, Breshears DD, McDowell NG (2015) On underestimation of global vulnerability to tree mortality and forest die-off from hotter drought in the Anthropocene. Ecosphere 6:art129. https://doi.org/10.1890/ES15-00203.1

Anderegg WRL, Plavcová L, Anderegg LDL et al (2013) Drought's legacy: Multiyear hydraulic deterioration underlies widespread aspen forest die-off and portends increased future risk. Glob Chang Biol 19:1188–1196. https://doi.org/10.1111/gcb.12100

Anderegg WRL, Hicke JA, Fisher RA et al (2015) Tree mortality from drought, insects, and their interactions in a changing climate. New Phytol 208:674–683. https://doi.org/10.1111/nph.13477

Barotto AJ, Fernandez ME, Gyenge J et al (2016) First insights into the functional role of vasicentric tracheids and parenchyma in eucalyptus species with solitary vessels: do they contribute to xylem efficiency or safety? Tree Physiol 36:1485–1497. https://doi.org/10.1093/treephys/tpw072

Barotto AJ, Monteoliva S, Gyenge J et al (2018) Functional relationships between wood structure and vulnerability to xylem cavitation in races of *Eucalyptus globulus* differing in wood density. Tree Physiol 38:243–251. https://doi.org/10.1093/treephys/tpx138

Becker P, Gribben RJ, Lim C (2000) Tapered conduits can buffer hydraulic conductance from path-lenght effects. Tree Physiol 20:965–967. https://doi.org/10.1093/treephys/20.14.965

Bonan GB (2008) Forests and climate change: forcings, feedbacks, and the climate benefits of forests. Science (80-) 320:1444–1449. https://doi.org/10.1126/science.1155121

Bourne AE, Creek D, Peters JMR et al (2017) Species climate range influences hydraulic and stomatal traits in *Eucalyptus* species. Ann Bot 120:123–133. https://doi.org/10.1093/aob/mcx020

Brodersen CR, McElrone AJ (2013) Maintenance of xylem network transport capacity: a review of embolism repair in vascular plants. Front Plant Sci. https://doi.org/10.3389/fpls.2013.00108

Brodersen CR, McElrone AJ, Choat B et al (2010) The dynamics of embolism repair in xylem: In vivo visualizations using high-resolution computed tomography. Plant Physiol 154:1088–1095. https://doi.org/10.1104/pp.110.162396

Brodersen CR, Knipfer T, McElrone AJ (2018) In vivo visualization of the final stages of xylem vessel refilling in grapevine (*Vitis vinifera*) stems. New Phytol 217:117–126. https://doi.org/10.1111/nph.14811

Charrier G, Torres-Ruiz JM, Badel E et al (2016) Evidence for hydraulic vulnerability segmentation and lack of xylem refilling under tension. Plant Physiol 172:1657–1668. https://doi.org/10.1104/pp.16.01079

Choat B, Brodersen CR, Mcelrone AJ (2015) Synchrotron X-ray microtomography of xylem embolism in Sequoia sempervirens saplings during cycles of drought and recovery. New Phytol 205:1095–1105. https://doi.org/10.1111/nph.13110

Choat B, Badel E, Burlett R et al (2016) Noninvasive measurement of vulnerability to drought-induced embolism by X-Ray microtomography. Plant Physiol 170:273–282. https://doi.org/10.1104/pp.15.00732

Choat B, Nolf M, Lopez R et al (2018) Non-invasive imaging shows no evidence of embolism repair after drought in tree species of two genera. Tree Physiol 39:113–121. https://doi.org/10.1093/treephys/tpy093

Cochard H, Bodet C, Améglio T, Cruiziat P (2000) Cryo-scanning electron microscopy observations of vessel content during transpiration in walnut petioles. Facts or artifacts. Plant Physiol 124:1191–1202. https://doi.org/10.1104/pp.124.3.1191

Cochard H, Lemoine D, Ameglio T, Granier A (2001) Mechanisms of xylem recovery from winter embolism in *Fagus sylvatica*. Tree Physiol 21:27–33. https://doi.org/10.1093/treephys/21.1.27

Cochard H, Delzon S, Badel E (2015) X-ray microtomography (micro-CT): a reference technology for high-resolution quantification of xylem embolism in trees. Plant Cell Environ 38:201–206. https://doi.org/10.1111/pce.12391

Drew DM, Downes GM, Grzeskowiak V, Naidoo T (2009) Differences in daily stem size variation and growth in two hybrid eucalypt clones. Trees Struct Funct 23:585–595. https://doi.org/10.1007/s00468-008-0303-y

du Plessis A, le Roux SG, Guelpa A (2016) The CT scanner facility at stellenbosch university: an open access X-ray computed tomography laboratory. Nucl Instruments Methods Phys Res 384:42–49. https://doi.org/10.1016/j.nimb.2016.08.005

Duursma RA, Blackman CJ, Lopéz R et al (2019) On the minimum leaf conductance: its role in models of plant water use, and ecological and environmental controls. New Phytol 221:693–705. https://doi.org/10.1111/nph.15395

Fatichi S, Pappas C, Zscheischler J, Leuzinger S (2019) Modelling carbon sources and sinks in terrestrial vegetation. New Phytol 221:652–668. https://doi.org/10.1111/nph.15451

Fernández ME, Barotto AJ, Martínez Meier A et al (2019) New insights into wood anatomy and function relationships: how *Eucalyptus* challenges what we already know. For Ecol Manage. https://doi.org/10.1016/j.foreco.2019.117638

Gleason SM, Westoby M, Jansen S et al (2016) Weak tradeoff between xylem safety and xylem-specific hydraulic efficiency across the world's woody plant species. New Phytol 209:123–136. https://doi.org/10.1111/nph.13646

Hacke UG, Sperry JS (2003) Limits to xylem refilling under negative pressure in *Laurus nobilis* and *Acer negundo*. Plant Cell Environ 26:303–311. https://doi.org/10.1046/j.1365-3040.2003.00962.x

Hacke UG, Sperry JS, Wheeler JK, Castro L (2006) Scaling of angiosperm xylem structure with safety and efficiency. Tree Physiol 26:689–701. https://doi.org/10.1093/treephys/26.6.689

Hammond WM, Yu K, Wilson LA et al (2019) Dead or dying? Quantifying the point of no return from hydraulic failure in drought-induced tree mortality. New Phytol 223:1834–1843. https://doi.org/10.1111/nph.15922

Kim HK, Lee SJ (2010) Synchrotron X-ray imaging for nondestructive monitoring of sap flow dynamics through xylem vessel elements in rice leaves. New Phytol 188:1085–1098. https://doi.org/10.1111/j.1469-8137.2010.03424.x

Klein T, Cohen S, Yakir D (2011) Hydraulic adjustments underlying drought resistance of *Pinus halepensis*. Tree Physiol 31:637–648. https://doi.org/10.1093/treephys/tpr047

Klein T, Zeppel MJB, Anderegg WRL et al (2018) Xylem embolism refilling and resilience against drought-induced mortality in woody plants: processes and trade-offs. Ecol Res 33:839–855. https://doi.org/10.1007/s11284-018-1588-y

Knipfer T, Cuneo IF, Brodersen CR, McElrone AJ (2016) In situ visualization of the dynamics in xylem embolism formation and removal in the absence of root pressure: a study on excised grapevine stems. Plant Physiol 171:1024–1036. https://doi.org/10.1104/pp.16.00136

Kramer PJ, Boyer JS (1995) Water relations of plants and soils. Academic Press Limited, San Diego

Lamarque LJ, Corso D, Torres-Ruiz JM et al (2018) An inconvenient truth about xylem resistance to embolism in the model species for refilling *Laurus nobilis* L. Ann for Sci. https://doi.org/10.1007/s13595-018-0768-9

Lens F, Sperry JS, Christman MA et al (2011) Testing hypotheses that link wood anatomy to cavitation resistance and hydraulic conductivity in the genus Acer. New Phytol 190:709–723. https://doi.org/10.1111/j.1469-8137.2010.03518.x

Liu J, Gu L, Yu Y et al (2019) Corticular photosynthesis drives bark water uptake to refill embolized vessels in dehydrated branches of *Salix matsudana*. Plant Cell Environ 42:2584–2596. https://doi.org/10.1111/pce.13578

Lobo A, Torres-Ruiz JM, Burlett R et al (2018) Assessing inter- and intraspecific variability of xylem vulnerability to embolism in oaks. For Ecol Manage 424:53–61. https://doi.org/10.1016/j.foreco.2018.04.031

Loepfe L, Martinez-Vilalta J, Piñol J, Mencuccini M (2007) The relevance of xylem network structure for plant hydraulic efficiency and safety. J Theor Biol 247:788–803. https://doi.org/10.1016/j.jtbi.2007.03.036

López R, Nolf M, Duursma RA et al (2018) Mitigating the open vessel artefact in centrifuge-based measurement of embolism resistance. Tree Physiol 39:143–155. https://doi.org/10.1093/treephys/tpy083

Martin-StPaul N, Delzon S, Cochard H (2017) Plant resistance to drought depends on timely stomatal closure. Ecol Lett 20:1437–1447. https://doi.org/10.1111/ele.12851

McDowell N, Pockman WT, Allen CD et al (2008) Mechanisms of plant survival and mortality during drought: why do some plants survive while others succumb to drought? New Phytol 178:719–739. https://doi.org/10.1111/j.1469-8137.2008.02436.x

McDowell N, Allen CD, Anderson-Teixeira K et al (2018) Drivers and mechanisms of tree mortality in moist tropical forests. New Phytol 219:851–869. https://doi.org/10.1111/nph.15027

Myburg AA, Grattapaglia D, Tuskan GA et al (2014) The genome of *Eucalyptus grandis*. Nature 510:356–362. https://doi.org/10.1038/nature13308

Nardini A, Lo Gullo MA, Salleo S (2011) Refilling embolized xylem conduits: Is it a matter of phloem unloading? Plant Sci 180:604–611. https://doi.org/10.1016/j.plantsci.2010.12.011

Nardini A, Lo Gullo MA, Trifilò P, Salleo S (2014) The challenge of the Mediterranean climate to plant hydraulics: responses and adaptations. Environ Exp Bot 103:68–79. https://doi.org/10.1016/j.envexpbot.2013.09.018

Nardini A, Savi T, Losso A et al (2017) X-ray microtomography observations of xylem embolism in stems of *Laurus nobilis* are consistent with hydraulic measurements of percentage loss of conductance. New Phytol 213:1068–1075. https://doi.org/10.1111/nph.14245

Niu CY, Meinzer FC, Hao GY (2017) Divergence in strategies for coping with winter embolism among co-occurring temperate tree species: the role of positive xylem pressure, wood type and tree stature. Funct Ecol 31:1550–1560. https://doi.org/10.1111/1365-2435.12868

Nolf M, Lopez R, Peters JMR et al (2017) Visualization of xylem embolism by X-ray microtomography: a direct test against hydraulic measurements. New Phytol 214:890–898. https://doi.org/10.1111/nph.14462

Ogasa M, Miki NH, Murakami Y, Yoshikawa K (2013) Recovery performance in xylem hydraulic conductivity is correlated with cavitation resistance for temperate deciduous tree species. Tree Physiol 33:335–344. https://doi.org/10.1093/treephys/tpt010

Ogasa MY, Utsumi Y, Miki NH et al (2016) Cutting stems before relaxing xylem tension induces artefacts in *Vitis coignetiae*, as evidenced by magnetic resonance imaging. Plant Cell Environ 39:329–337. https://doi.org/10.1111/pce.12617

Petruzzellis F, Pagliarani C, Savi T et al (2018) The pitfalls of in vivo imaging techniques: evidence for cellular damage caused by synchrotron X-ray computed micro-tomography. New Phytol 220:104–110. https://doi.org/10.1111/nph.15368

Pittermann J, Sperry JS, Hacke UG et al (2006) Inter-tracheid pitting and the hydraulic efficiency of conifer wood: The role of tracheid allometry and cavitation protection. Am J Bot 93:1265–1273. https://doi.org/10.3732/ajb.93.9.1265

Rockwell FE, Wheeler JK, Holbrook NM (2014) Cavitation and its discontents: opportunities for resolving current controversies. Plant Physiol 164:1649–1660. https://doi.org/10.1104/pp.113.233817

Saadaoui E, Ben Yahia K, Dhahri S et al (2017) An overview of adaptative responses to drought stress in *Eucalyptus* spp. For Stud 67:86–96. https://doi.org/10.1515/fsmu-2017-0014

Salleo S, Lo Gullo MA, Trifilò P, Nardini & A, (2004) New evidence for a role of vessel-associated cells and phloem in the rapid xylem refilling of cavitated stems of *Laurus nobilis* L. Plant, Cell Environ 27:1065–1076. https://doi.org/10.1111/j.1365-3040.2004.01211.x

Sano Y, Morris H, Shimada H et al (2011) Anatomical features associated with water transport in imperforate tracheary elements of vessel-bearing angiosperms. Ann Bot 107:953–964. https://doi.org/10.1093/aob/mcr042

Savi T, Casolo V, Luglio J et al (2016) Species-specific reversal of stem xylem embolism after a prolonged drought correlates to endpoint concentration of soluble sugars. Plant Physiol Biochem 106:198–207. https://doi.org/10.1016/j.plaphy.2016.04.051

Schneider CA, Rasband WS, Eliceiri KW (2012) NIH Image to ImageJ: 25 years of Image Analysis HHS Public Access

Secchi F, Zwieniecki MA (2010) Patterns of PIP gene expression in *Populus trichocarpa* during recovery from xylem embolism suggest a major role for the PIP1 aquaporin subfamily as moderators of refilling process. Plant Cell Environ 33:1285–1297. https://doi.org/10.1111/j.1365-3040.2010.02147.x

Secchi F, Pagliarani C, Cavalletto S et al (2021) Chemical inhibition of xylem cellular activity impedes the removal of drought-induced embolisms in poplar stems—new insights from micro-CT analysis. New Phytol 229:820–830. https://doi.org/10.1111/nph.16912

Souden S, Ennajeh M, Ouledali S et al (2020) Water relations, photosynthesis, xylem embolism and accumulation of carbohydrates and cyclitols in two *Eucalyptus* species (*E. camaldulensis* and *E. torquata*) subjected to dehydration–rehydration cycle. Trees Struct Funct 34:1439–1452. https://doi.org/10.1007/s00468-020-02016-4

Sperry JS (2003) Evolution of water transport and xylem structure. Int J Plant Sci 164:115–127. https://doi.org/10.1086/368398

Sperry JS, Love DM (2015) What plant hydraulics can tell us about responses to climate-change droughts. New Phytol 207:14–27. https://doi.org/10.1111/nph.13354

Sperry JS, Venturas MD, Anderegg WRL et al (2017) Predicting stomatal responses to the environment from the optimization of photosynthetic gain and hydraulic cost. Plant Cell Environ 40:816–830. https://doi.org/10.1111/pce.12852

Tomasella M, Casolo V, Aichner N et al (2019a) Non-structural carbohydrate and hydraulic dynamics during drought and recovery in *Fraxinus ornus* and *Ostrya carpinifolia* saplings. Plant Physiol Biochem 145:1–9. https://doi.org/10.1016/j.plaphy.2019.10.024

Tomasella M, Petrussa E, Petruzzellis F et al (2019b) The possible role of non-structural carbohydrates in the regulation of tree hydraulics. Int J Mol Sci 21:144. https://doi.org/10.3390/ijms21010144

Tombesi S, Johnson RS, Day KR, Dejong TM (2010) Relationships between xylem vessel characteristics, calculated axial hydraulic conductance and size-controlling capacity of peach rootstocks. Ann Bot 105:327–331. https://doi.org/10.1093/aob/mcp281

Torres-Ruiz JM, Sperry JS, Fernández JE (2012) Improving xylem hydraulic conductivity measurements by correcting the error caused by passive water uptake. Physiol Plant 146:129–135. https://doi.org/10.1111/j.1399-3054.2012.01619.x

Torres-Ruiz JM, Jansen S, Choat B et al (2015) Direct X-ray microtomography observation confirms the induction of embolism upon xylem cutting under tension. Plant Physiol 167:40–43. https://doi.org/10.1104/pp.114.249706

Trifilò P, Raimondo F, Lo Gullo MA et al (2014) Relax and refill: xylem rehydration prior to hydraulic measurements favours embolism repair in stems and generates artificially low PLC values. Plant Cell Environ 37:2491–2499. https://doi.org/10.1111/pce.12313

Trifilò P, Nardini A, Gullo MAL et al (2015) Diurnal changes in embolism rate in nine dry forest trees: Relationships with species-specific xylem vulnerability, hydraulic strategy and wood traits. Tree Physiol 35:694–705. https://doi.org/10.1093/treephys/tpv049

Trugman AT, Detto M, Bartlett MK et al (2018) Tree carbon allocation explains forest drought-kill and recovery patterns. Ecol Lett 21:1552–1560. https://doi.org/10.1111/ele.13136

Tyree MT, Ewers FW (1991) The hydraulic architecture of trees and other woody plants. New Phytol 119:345–360. https://doi.org/10.1111/j.1469-8137.1991.tb00035.x

Tyree MT, Sperry JS (1988) Do woody plants operate near the point of catastrophic xylem dysfunction caused by dynamic water stress? Plant Physiol 88:574–0580. https://doi.org/10.1104/pp.88.3.574

Tyree MT, Salleo S, Nardini A et al (1999) Refilling of embolized vessels in young stems of laurel. Do We need a new paradigm? Plant Physiol 120:11–21. https://doi.org/10.1104/pp.120.1.11

Van der Willigen C, Pammenter NW (1998) Relationship between growth and xylem hydraulic characteristics of clones of *Eucalyptus* spp. at contrasting sites. Tree Physiol 18:595–600. https://doi.org/10.1093/treephys/18.8-9.595

Vazquez-Cooz I, Meyer RW (2002) A differential staining method to identify lignified and unlignified tissues. Biotechinic Histochem 77:277–282

Venturas MD, Sperry JS, Hacke UG (2017) Plant xylem hydraulics: what we understand, current research, and future challenges. J Integr Plant Biol 59:356–389. https://doi.org/10.1111/jipb.12534

Vesala T, Hölttä T, Perämäki M, Nikinmaa E (2003) Refilling of a hydraulically isolated embolized xylem vessel: model calculations. Ann Bot 91:419–428. https://doi.org/10.1093/aob/mcg022

Wheeler JK, Huggett BA, Tofte AN et al (2013) Cutting xylem under tension or supersaturated with gas can generate PLC and the appearance of rapid recovery from embolism. Plant Cell Environ 36:1938–1949. https://doi.org/10.1111/pce.12139

Xiong D, Nadal M (2020) Linking water relations and hydraulics with photosynthesis. Plant J 101:800–815. https://doi.org/10.1111/tpj.14595

Zeppel MJB, Anderegg WRL, Adams HD et al (2019) Embolism recovery strategies and nocturnal water loss across species influenced by biogeographic origin. Ecol Evol 9:5348–5361. https://doi.org/10.1002/ece3.5126

Zwieniecki MA, Holbrook NM (2009) Confronting Maxwell's demon: biophysics of xylem embolism repair. Trends Plant Sci 14:530–534. https://doi.org/10.1016/j.tplants.2009.07.002

Zwieniecki MA, Melcher PJ, Ahrens ET (2013) Analysis of spatial and temporal dynamics of xylem refilling in *Acer rubrum* L using magnetic resonance imaging. Front Plant Sci. https://doi.org/10.3389/fpls.2013.00265

Chapter 4

Stomatal responses of *Eucalyptus* spp. under drought can be predicted with a gain-risk optimisation model

Accepted for publication at *Tree Physiology* on 05 November 2021 (doi.org/10.1093/treephys/tpab145)

Chapter 4: Stomatal responses of *Eucalyptus* spp. under drought can be predicted with a gain-risk optimisation model

Abstract

The frequency and severity of droughting events are expected to increase due to climate change, with optimal environmental conditions for forestry likely to shift. Modelling plant responses to a changing climate is therefore vital. We tested the process-based gain-risk model to predict stomatal responses to drought of two *Eucalyptus* hybrids. The process-based gain-risk model has the advantage that all the parameters used within the model are based on measurable plant traits. The gain-risk model proposes that plants optimise photosynthetic gain while minimising a hydraulic cost. Previous versions of the model used hydraulic risk as a cost function, however, did not account for delayed or reduced hydraulic recovery rates from embolism post-drought. Hydraulic recovery has been seen in many species; however, it is still unclear how this inclusion of a partial or delayed hydraulic recovery would affect the predictive power of the gain-risk model. Many hydraulic parameters required by the model are also difficult to measure and are not freely available. We therefore tested a simplified gain-risk model that includes a delayed or reduced hydraulic recovery component post-drought. The simplified gain-risk model performed well at predicting stomatal responses in both *E. grandis X camaldulensis* (*GC*) and *E. urophylla X grandis* (*UG*). In this study two distinct strategies were seen between *GC* and *UG*, with *GC* being more resistant to embolism formation however could not recover hydraulic conductance, compared to *UG*. The inclusion of a delayed or reduced hydraulic recovery component improved model predictions for *GC* sightly however not for *UG*, which can be related to *UG* being able to recover lost hydraulic conductance and therefore can maintain stomatal conductance regardless of hydraulic risk. Even though the gain-risk model shows promise in predicting plant responses more information is needed regarding hydraulic recovery after drought.

Key words optimisation model, drought stress, stomata regulation, hydraulic risk

Introduction

Shifts in the global hydrological cycle as a result of climate change is an important driver of increasing prevalence and intensities of drought events around the world (Pachauri et al. 2014). Both the increasing intensity and frequency of droughts, or both in combination, have been identified as primary factors leading to global tree mortality in recent years (Allen et al. 2015, Anderegg et al. 2015). A joint international scientific effort towards better understanding these

events across a broad range of forest types are needed (Hartmann et al. 2018). Understanding tree eco-physiological responses to drought is an important part of any such research endeavour, with stomatal conductance being a mechanism of particular importance which plants can use to regulate water loss to the atmosphere in situations of limited water supply or excessive demand from the atmosphere (Sperry et al. 2002, Silva et al. 2004).

Plants are constantly balancing a trade-off between water loss and carbon gain through CO_2 uptake (Xiong and Nadal 2019), with stomatal regulation playing an important role by controlling these two variables. Empirical models for stomatal conductance have been previously used to capture this trade-off (Ball et al. 1987, Ye and Yu 2008, Damour et al. 2010), however these models rely mainly on fitted curves or regression analysis using existing experimental data (Damour et al. 2010). Fitted parameters in empirical models are therefore difficult to quantify and cannot be measured from plant traits (Sperry et al. 2017). They run the risk of not working outside of the parameterisation domain and, as a result, run the risk of being unable to adequately predict stomatal responses, especially in conditions outside of the original parameterisation domain (Powell et al. 2013, Trugman, Medvigy, et al. 2018).

Optimisation models have been proposed as an alternative to empirical approaches (Cowan and Farquhar 1977, Wolf et al. 2016, Sperry et al. 2017). When plants are experiencing drought conditions, optimality theory hypothesises that plants will sacrifice photosynthesis (i.e. production) to minimise water loss, however plants will tolerate water loss to increase photosynthesis when water is more abundant and atmospheric CO_2 levels are limited (Schulze and Hall 1982, Morrison 1987). A convenient way to model this trade-off is to consider that it is controlled by the stomata (Cowan and Farquhar 1977, Katul et al. 2010, Manzoni et al. 2011, Medlyn et al. 2011, Prentice et al. 2014, Wolf et al. 2016, Sperry et al. 2017).

Cowan and Farquhar (1977) first proposed a constrained optimisation model, were photosynthesis (A) is maximised for a set amount of water loss through transpiration (E) over time. The marginal water use efficiency ($\lambda=\partial A/\partial E$) is, therefore, held constant over intervals which remain undefined. Although this model has had similar results as empirical models (Manzoni et al. 2011, Lin et al. 2015), it has not been very widely adopted as it remains unclear how the Lagrangian multiplier (λ) should be interpreted and measured (Medlyn et al. 2011, Buckley 2017). The Lagrangian multiplier has been solved as a function of soil moisture and atmospheric CO_2 respectively (Katul et al. 2010, Manzoni et al. 2011), however λ has to be a function of both water use and CO_2 in order to accurately capture stomatal responses to environmental changes (Wang et al. 2019).

It has also been proposed that plants should rather maximise photosynthesis with increased water loss, when water is readily available (Wolf et al. 2016). Wolf et al. (2016) therefore proposed a gain-risk model where plants maximise A at a level of water potential for a hydraulic cost termed Θ. Although Wolf et al. (2016) did not specify what cost should be included in Θ, it can include cost associated with embolism repair and reduced photosynthetic rates (Brodersen and McElrone 2013, Buckley 2017, Anderegg et al. 2018). Sperry et al. (2017) further developed the gain-risk model and proposed that the hydraulic cost be defined as the increasing damage from cavitation due to embolism formation. It has also been proposed that the hydraulic cost should rather be interpreted as the future opportunistic cost of reduced CO_2 uptake and therefore reduction in photosynthesis (Buckley 2017, Lu et al. 2020).

The gain-risk model has however not been tested on many species at plant-scale. In previous studies the gain-risk model as described by Sperry et al. (2017) has been able to capture stomatal responses in both birch (*Betula occidentalis* Hook.) and aspen (*Populus tremuloides* Michx.) (Venturas et al. 2018, Wang et al. 2019). The model has also been successfully used at ecosystem scale (Sabot et al. 2020), with the model as described by Wolf et al. (2016) successfully being implemented at leaf-scale (Anderegg 2018a, Wang et al. 2020).

Nevertheless, the models did not account for a delayed or reduced hydraulic recovery rates from embolism (Venturas et al. 2018, Anderegg et al. 2018, Wang et al. 2019, Sabot et al. 2020). Hydraulic recovery post-drought has been observed in many species (Nardini et al. 2011, Ogasa et al. 2013, Brodersen and McElrone 2013, Niu et al. 2017, Zeppel et al. 2019, Tomasella, Casolo, et al. 2019), however it is still unclear what the underlying mechanisms of hydraulic recovery are (Klein et al. 2018). Regardless of this, it can be argued that a partial and/or delayed hydraulic recovery should be included in the gain-risk model. During drought conditions plants experience an increased loss of hydraulic conductance (Xiong and Nadal 2019). Reduced hydraulic conductance, due to embolism formation, will persist until there is an increase in available water in the soil. The historic reduction in soil water experienced by a plant during drought will, therefore, influence the hydraulic limitation for as long as embolism persists. Accordingly, it makes sense to include timing of embolism recovery in optimisation models. If embolism recovery takes place immediately after embolism formation at low water potentials, then embolism will recur immediately after recovery. It would therefore be more economical if embolism is only recovered when there is a significant enough increase in soil water potential (Zeppel et al. 2019).

The gain-risk model has the advantage that all the parameters are measurable (Venturas et al. 2018). This makes the model more reliable outside the calibration data range. This is especially important considering the need to predict plant responses under climate change (Menezes-Silva et al. 2019), a problem of particular relevance to growers of commercially significant hardwoods, such as *Eucalyptus* (Iglesias and Wilstermann 2009, Myburg et al. 2014). Although *Eucalyptus* species are natively adapted to a wide range of environmental conditions, some species show highly variable drought responses (Saadaoui et al. 2017). The use of a model that includes measurable physiological parameters will therefore be very useful, considering the variability seen within *Eucalyptus* (Saadaoui et al. 2017) and particularly those used in commercial forest operations.

The wide application of the gain-risk model is, however, still challenging due to the difficulty of measuring some of the hydraulic parameters required (Sabot et al. 2020). The parameters dealing with plant vulnerability are easily accessible for many species (Choat et al. 2012) but estimating the maximum hydraulic conductance (K_{max}) within a plant still poses many challenges (Sabot et al. 2020). In previous studies K_{max} has been inferred from measured transpiration rates and leaf water potential measurements and combining conductivity of the soil and whole plant components (Venturas et al. 2018, Wang et al. 2019). Recently, Sabot et al. (2020) proposed an approach that allows for the simplifying of hydraulic elements from soil to leaves into one element, simplifying the hydraulic side of the gain-risk model.

In that context, we report here the results of applying the gain-risk model to predict stomatal responses in two *Eucalyptus* hybrids during periodic, repeated droughting events. We hypothesised that optimal stomatal behaviour becomes more conservative as soil drying persists and that xylem recovery will only take place when there is a significant increase and/or sustained increase in available water. There were two objectives of the study: (1) to test the gain-risk model of stomatal conductance on *E. grandis x camaldulensis* (*GC*) and *E. urophylla x grandis* (*UG*) hybrids and (2) to test a gain-risk model that accounted for delayed or reduced hydraulic recovery rates and to determine whether this adaptation improved model predictions.

Methods

Model description

The original gain-risk model as described by Sperry *et al.* (2017) states that stomata will respond in such a way as to maximise profit, which can be described as a photosynthetic gain (β) minus a hydraulic cost (θ).

$$Profit = \max\left(\beta\left(\Psi_{leaf}\right) - \theta\left(\Psi_{leaf}\right)\right)$$

where Ψ_{leaf} is the leaf water potential, and β and θ are normalised to one.

The normalised cost (θ) represents the increasing damage of cavitation due to embolism formation and hydraulic conductance is reduced:

$$\theta(\Psi) = \frac{K_{c,max} - K(\Psi)}{K_{c,max} - K_{crit}}$$

where $K_{c,max}$ is the instantaneous maximum hydraulic conductance, K is the hydraulic conductance evaluated at any water potential (Ψ), an K_{crit} is the critical hydraulic conductance at which hydraulic failure is seen. The critical leaf water potential (Ψ_{crit}) indicative of hydraulic failure was set to match 99 % loss of hydraulic conductance.

As soil water decreases, K is reduced due to the formation of embolism and recovers when there is an increase in soil water. The water supply for transpiration therefore dependent on the hydraulic vulnerability of a plant. The cost function is based on the relationship between transpiration (E) and water pressure over time. E is calculated by integrating over the vulnerability curve of a plant:

$$E = \int_{\Psi up}^{\Psi down} K_{max} \cdot \left(e^{-\left(\left(-\frac{\Psi}{b}\right)^{c}\right)}\right) . \, d\Psi$$

where Ψ_{up}-Ψ_{down} is the water pressure gradient seen in the plant, and b and c are Weibull parameters of the vulnerability curve. To scale for leaf area variations, the leaf area to basal area ratio (LA:BA) was used by dividing E by LA:BA.

The hydraulic conductance (K_{max}) can be expressed as the derivative of the transpiration function of water pressure ($K = dE/d\,\Psi$).

We took an approach similar to Sabot et al. (2020), where hydraulic segmentation was removed within the model to allow for a single hydraulic element, which significantly reduces parameterisation of the model. The hydraulic conductance of the whole plant is smoothed across all hydraulic elements (soil, root, stems, leaves). In that way K_{max} represents the maximum hydraulic conductance from soil to leaves.

The normalised gain function (β) is a function of decreasing photosynthetic gain over decrease leaf water potential:

$$\beta(\Psi) = \frac{A(\Psi)}{A_{max}}$$

where A is the photosynthetic uptake evaluated at any water potential (Ψ) and A_{max} is the instantaneous photosynthetic uptake over the entire Ψ range.

Fick's first law is used to calculate the CO_2 flux between the atmospheric (C_a) and intercellular (C_a) CO_2 concentrations:

$$A(\Psi) = G_c(C_{a-} C_i)$$

where G_c is the CO_2 diffuse conductance and C_i is solved by setting the above equation equal to the photosynthetic gain is calculated from the biochemical model of Farquhar *et al.* (1980).

Model adaptation

Vulnerability curves are used to describe the percentage loss of hydraulic conductance (PLC) in response to changes in water pressure (Sperry and Love 2015). This response is seen due to embolism formation within the xylem. E is therefore affected by the decreasing soil water potential, but also post-drought due to the persistence of embolism within the xylem. We therefore propose a model that includes the decrease in PLC due to embolism recovery post drought.

The hydraulic conductance or PLC is influenced by the availability of water within the soil. The availability of soil water can be categorised by two phases: (1) a drought phases, where soil water is decreasing over time and (2) a recovery phase where soil water is increasing over time (Klein et al. 2018).

We propose that recovery will only take place when there is a significant increase and/or sustained increase in available soil water. During drought conditions the PLC at a given water potential ($PLC\,(\Psi_x)$) will not recover and can be defined as the PLC measured in response to the lowest water potential measured (Ψ_{Lx}). The $PLC\,(\Psi_x)$ will therefore increase during drought conditions, due to increased embolism formation over time. When there is a significant and/or sustained increase soil water, $PLC\,(\Psi_x)$ will recover due to embolism recovery (Zeppel et al. 2019). The

repaired PLC however will not be repaired below what the $PLC\,(\Psi_x)$ at that specific time point and water pressure is since new embolism formation will then take place.

The vulnerability curve of a plant at any point in time ($PLC_t(\Psi_x)$) can be modified based on the above-mentioned assumptions.

Drought phase: $\frac{dS}{dt} \leq 0$

$$PLC_t(\Psi_x) = PLC(\Psi_{Lx})$$

Recovery phase: $\frac{dS}{dt} > 0$

$$PLC_t(\Psi_x) = Min\{PLC(\Psi_x)\,;PLC_r\}$$

where S is soil water, t is a time element, $PLC_t(\Psi_x)$ is the PLC at any given time and water pressure, $PLC(\Psi_{Lx})$ is the PLC the plant experienced at the lowest water pressure, $PLC(\Psi_x)$ is the PLC as measured by the specific water pressure and PLC_r is the recovered PLC due to filling of embolisms. PLC_r can be calculated as described in Lu et al. (2020):

$$PLC_r = PLC(\Psi_{Lx}) - [PLC(\Psi_{Lx}) - PLC(\Psi_x)] \times XRI$$

where XRI is the Xylem Recovery Index (Ogasa et al. 2013).

The Xylem Recovery Index can be calculated as the percentage loss of hydraulic conductance when plants are rewatered after drought compared to when plants experienced no drought (Ogasa et al. 2013, Zeppel et al. 2019). The Xylem recovery Index can be calculated as follow:

$$XRI = \frac{PLC_{drought} - PLC_{rewatered}}{PLC_{drought} - PLC_{watered}}$$

where $PLC_{drought}$ is the percentage loss of hydraulic conductance measured during drought, $PLC_{rewatered}$ is the percentage loss of hydraulic conductance measured after rewatering and $PLC_{watered}$ is the percentage loss of hydraulic conductance measured before drought is induced.

Plant material

All work was done on potted rooted cuttings of two *Eucalyptus* hybrids: *E. grandis x camaldulensis* (*GC*) and *E. urophylla x grandis* (*UG*): Prior to the start of the experiment *GC* (n =22) and *UG* (n = 22) plants were grown under shaded netting for two years. Plants were grown in 2 litre pots in a soil mixture ratio of 1:2 fine sand and composted chicken manure. Throughout the growing period all

plants received continuous watering and were fertilised with the controlled release Haifo Multicote 8 (N:15%, P:3%, K:12%, S:7%) prior to any experimental work. The height of plants varied between 0.7 m and 1.2 m with no significant difference seen between hybrids. At the start of the experiment, the average stem diameter for *GC* was 10.29 ± 1.91 mm and *UG* was 8.97 ± 2.07 mm. After the six-week dry-down experiment the average stem diameter for *GC* was 11.10 ± 1.89 mm and *UG* was 9.58 ± 1.91 mm.

Dry-down and re-watering treatments

Twelve (six per hybrid) plants were replanted into 5 l bags of pure sand (pH: 7.55 ± 0.133) and moved into a growth tunnel at the beginning of November 2020 where they could acclimatise for 15 days before the start of any experimental work. All soil was removed from the root system prior to replanting in pure sand. Plants were kept in pots and planted in a randomized 2x6 grid (see Figure 4.9 in supplementary material). All pots were irrigated to field capacity at 07:00, 10:00, 12:00, 14:00 and 17:00 by means of a drip irrigation system prior to the start of the experiment.

To assure that a complete range of physiological responses were observed, two treatments were applied to three plants per treatment: (1) a *control* where plants were irrigated throughout the entire experimental period and (2) a *dry-down - recovery* treatment where plants irrigation was stopped for two days, three days and four days respectfully where plants received no irrigation. Between dry-down events plants were rewatered for five days. All plants were placed on a grid which was lifted above the soil to ensure that plants did not have any additional access to ground water or run-off. Experimental work started on 24th of November 2020.

Model inputs

Hourly values for air temperature, humidity, soil moisture and incoming solar irradiation were averaged from continuous 10 min readings for the entire experimental period. Incoming solar irradiance, temperature and humidity was measured above and below the canopy. Since plants were moved into a growth tunnel, wind speed and precipitation were not logged and assumed to be zero.

Twelve water content reflectometers (model CS655, Campbell Scientific) were used to log soil volumetric water content (SVWC) (m^3 m^{-3}) for every plant. SVWC was logged every hour as an average of 10 min measurements. The van Genuchten model was used to convert soil moisture to soil water pressure (van Genuchten 1980) (see methods 1 in supplementary material). The soil parameters used in the van Genuchten model were determined from the soil texture as described in

the UNSODA Unsaturated Soil Hydraulic Database (Leij et al. 1996). All data was logged on the CR1000X datalogger (Campbell Scientific).

Pre-dawn, midday and afternoon leaf xylem water pressures were taken at the beginning and end of the dry-down experimental period. The soil-canopy K_{max} was calculated from midday (12:00 – 13:00) sap flow measurements (Exoskin Sapflow sensors, Dynamax, Houston, TX, USA) divided by the pressure drop as calculated by pre-dawn and midday xylem water pressures (Sperry and Love 2015). K_{max} was measured before the start of the experiment before any dry-down treatments were applied. A pressure chamber (SKYE plant moisture system, SKPM 1400 series) was used to measure xylem water pressure from excised leaves taken from branches which were placed in a bag with a damp towel and allowed to equilibrate for 30 min. To scale for leaf area variations, the leaf area to basal area ratio (LA:BA) was used.

Vulnerability curves were constructed using the bench dehydration method (Tyree and Sperry 1988) before the start of the drought - recovery experiment. Hydraulic conductance was measured from 15 – 20 cm stem segments of 9 plants per hybrid. The percentage loss of hydraulic conductance was fitted over xylem water pressure using a Weibull function (Hacke et al. 2006). The Xylem Recovery Index (XRI) was calculated from the percentage los of hydraulic conductance as measured on a 15 - 20 cm stem segments under well-watered, drought and re-watered conditions. Plants that were dehydrated during the construction of vulnerability curves were rehydrated through re-watering, to measure the PLC of each species after re-watering.

Maximum carboxylation rate (V_{max25}) and electron transport rate (J_{max25}) at 25°C were calculated from A:Ci curves measured once on 10 random plants for each hybrid before the start of the experiment. A:Ci curve measurements were made using an infrared gas analyser (LiCor 6400) on healthy leaves. The chamber measurements were set as follow: active radiation set at 1500 - 2000 µmol photon m^{-2} s^{-1}, air temperature set at 25°C and VPD set between 1 and 2 kPa. Chamber CO_2 concentrations ranged from 50 – 2000 ppm. The CO2 compensation point at 25°C were taken as a constant as determined from the ACI curves.

The leaf area to basal area ratio (LA:BA) was determined for all plants at the end of the dry-down – recovery experiment. Photos of a representative sample of leaves was taken and analysed using image J software (Schneider et al. 2012) in order to determine leaf area. The representative samples were oven-dried together with the rest of the leaves of the plant. The total leaf area was extrapolated based on the specific leaf area (SLA) as calculated from leaf area over dry mass of leaves. A photo

of all plants and stem diameter of plants was taken once a week throughout the entire experimental period.

All model inputs and parameters can be found table 4.1 and 4.2.

Table 4.1 Physiological parameters used in gain-risk model of all *E. grandis X camaldulens* (*GC*) and *E. urophylla X grandis* (*UG*) plants.

Physiological parameters	***GC***	***UG***
V_{max25} (µmol m^{-2} s^{-1})	43.85 ± 18.84	57.58 ± 23.22
J_{max25} (µmol m^{-2} s^{-1})	144.88 ± 122.01	210.78 ± 66.48
Kmax (kg h^{-1} Mpa^{-1} m^{-2})	857.25	1191.52
Rd (µmol m^{-2} s^{-1})	2.84 ± 1.37	3.84 ± 0.901
XRI	0.18 ± 0.09	0.71 ± 0.26
VC	P50 = -2.72	P50 = -2.33
	P80 = -3.16	P80 = -3.01
LA BA (m^2 m^{-2})	2293.95 ± 1680.13	1794.95 ± 1090.12

Table 4.2 Environmental variables used in the gain risk model

Environmental variables	**Units**
Wind speed	m s^{-1}
Incoming solar irradiance	W m^{-2}
Humidity	%
Soil water pressure	MPa
Atmospheric pressure	kPa
Air Temperature	Degree Celsius

Plant variables

Stomatal conductance (Gw), evapotranspiration (E), and leaf temperature (T_{leaf}) were measured in the morning (08:00- 09:00), midday (12:00 – 13:00) and afternoon (16:00 – 17:00), for most days throughout the entire experimental period. Measurements were taken on five leaves per plant using a LiCor LI-600 Porometer and Fluorometer. Leaf temperature was not modelled during this experiment, and measured leaf temperatures were used within the model. This was done since the aim of the study was to test the gain-risk model and the additional use of the energy balance equations could affect the accuracy of the model.

Statistical analysis

All input variables were tested for normality before analysis. Summary statistics were calculated for all input model variables. A non-parametric Kruskal-Wallis test was used to determine if there was a significant difference in input variables between hybrids, with the letter “H” denotating the test statistic.

Model performances were evaluated for the gain-risk model that assumes complete recovery and partial recovery. The predicted transpiration rate (E) and stomatal conductance was evaluated against measured variables using mean absolute error (MAE), mean absolute percentage error (MAPE) and root mean square error (RMSE). R-squared (R^2) values were also calculated for a linear model between predicted and measured variables. Model performance was averaged across all treatments and plants. A two-way repeated measure ANOVA was used to determine if there was a significant difference between the predicted v. actual measurements of Gw and E over time. Model accuracy was also tested between hybrids.

A Sobol sensitivity analysis was used to assess the effect of the physiological parameters used on the variance seen in the photosynthetic, stomatal and transpiration outputs. All physiological parameters were varied across observed ranges seen during the experimental period and the effect on the variance on predicted outputs was calculated. For the Sobol analysis, confidence intervals were set at 95 % and the number of bootstrap replicates were set at 100. All environmental variables were held constant and not varied since the aim was to test the effect of the physiological variables. The following reference values were used: Incoming solar irradiance set at 1000 W m^{-2}, humidity set at 40%, atmospheric pressure set at 100 kPa, soil water pressure set at 0.3 MPa, air temperature set at 25 degrees Celsius and wind speed set at 0 m s^{-1}.

A Principal component analysis (PCA) was used to determine how environmental changes influenced the degree of MAE for both stomatal conductance and transpiration. All variables were scaled before the PCA to ensure uniformity across variables by subtracting the means of each variable.

Results

Plant characteristics

Based on the vulnerability curves *UG* lost 50 % of its hydraulic conductance at -2.33 MPa while *GC* lost 50 % of its hydraulic conductance at -2.72 MPa. There was a significant difference seen in the recovery response seen between the two hybrids, with *UG* having a higher XRI compared to *GC* ($H = 3.857$, $p = 0.049$). The K_{max} for *UG* was 1191.52 kg h^{-1} Mpa^{-1} m^{-2} and 857.25 kg h^{-1} Mpa^{-1} m^{-2} for *GC* (Table 4.1).

The average V_{max25} for *UG* was 57.57 ± 23.22 µmol m^{-2} s^{-1} and for *GC* was 43.85 ± 18.84 µmol m^{-2} s^{-1}. The average J_{max25} for *UG* was 210.78 ± 66.48 µmol m^{-2} s^{-1} and for *GC* was 144.88 ± 122.01 µmol m^{-2} s^{-1} (Table 4.1). There was no significant difference in V_{max25} and J_{max25} between

the two hybrids (H = 2.287, p = 0.131). The average LA:BA ratio for *UG* 1794.95 ± 1090.12m^2 m^{-2} and for *GC* was 2293.95 ± 1680.13 m^2 m^{-2} (Table 4.1). There was no significant difference seen in the LA:BA ratio (H = 3.69, P = 0.055) and SLA (H = 0.23, P = 0. 631) between the two hybrids.

Treatments

During the experimental period air temperature ranged from 10.11 °C to 44.09 °C. A small discrepancy was seen between absolute humidity measurements taken from the Licor LI600 and the ibuttons placed around the plants, but the instruments showed very similar trends in humidity. It was decided to use the humidity measurements as captured by the Licor LI600 as these values were used by the instrument itself for certain outputs which were subsequently used in modelling work. Humidity measurements ranged from 36.26 % to 68.40 %.

In the control treatment SVWC was kept above 10 % (above -2 MPa soil water pressure), which is the field capacity of sand (Ratliff et al. 1983, Leij et al. 1996). In the dry-down treatment, the SVWC was reduced to various levels below 5 %, which is the permanent wilting point of sand (Ratliff et al. 1983, Leij et al. 1996), during drought phases and then brought back to above 10 % during recovery phases (see Figure 4.10 and Figure 4.11 in supplementary material).

Recovery of pre-dawn leaf water potential (LWP) was seen in all plants within the dry-down treatment with pre-dawn LWP measured at the start of the experimental period (*GC*: -0.60 ± 0.00 MPa and *UG*: -0.8 ± 0.20 MPa) and assessed again at the end of the experimental period (*GC*: -0.67 ± 0.12 MPa and *UG*: -0.8 ± 0.17 MPa).

Model Accuracy

The gain-risk model performed well for both hybrids, with a significant relationship seen between the modelled and predicted transpiration and stomatal conductance measurements with the linear regression slopes being close to 1 ($p > 0.05$) (Figure 4.1 and Figure 4.2). The gain-risk model with complete hydraulic recovery however could not fully capture the transpiration and stomatal responses for *E. urophylla X grandis* when exposed to repeated dry-down treatments, with the R^2 values for transpiration dropping from 60 % for plants in the control treatment to 54 % for plants in the dry-down treatment. A similar trend was seen when the predicted v. actual stomatal conductance measurements with the R^2 values dropping from 57 % to 44 % (Table 4.3).

Table 4.3 Performance of model predictions of transpiration rate (E) and stomatal conductance (Gw) for both *E. urophylla X grandis* (*UG*) and *E. grandis X camaldulensis* (*GC*). RMSE (root mean square error) and MAE (mean absolute error) are given in model output units. R^2 and slope of linear regression between measured and predicted variables are also presented.

Model		**E (mmol $m^{-2}s^{-1}$)**		**Gw (mmol $m^{-2}s^{-1}$)**	
UG		**Dry-down**	**Control**	**Dry-down**	**Control**
gain-risk (with complete hydraulic recovery)	**RMSE**	0.96	1.07	95.89	125.37
	MAE	0.79	0.82	79.27	95.68
	MAPE	30 %	29 %	30 %	32 %
	R^2	54 %	60 %	44 %	57 %
	Slope	0.95	0.91	1.03	1.21
gain-risk (with partial hydraulic recovery)	**RMSE**	1.01	0.99	106.76	132.49
	MAE	0.73	0.71	84.41	103.22
	MAPE	28 %	25 %	33 %	34 %
	R^2	48 %	62 %	34 %	58 %
	Slope	0.93	1.01	1.03	1.35
GC		**Dry-down**	**Control**	**Dry-down**	**Control**
gain-risk (with complete hydraulic recovery)	**RMSE**	0.94	0.64	71.06	78.49
	MAE	0.74	0.47	58.06	53.02
	MAPE	37 %	20 %	29 %	23 %
	R^2	54 %	66 %	65 %	51 %
	Slope	0.98	1.02	1.21	1.11
gain-risk (with partial hydraulic recovery)	**RMSE**	0.92	0.68	73.96	85.57
	MAE	0.72	0.45	61.02	57.36
	MAPE	36 %	19 %	31 %	25 %
	R^2	52 %	64 %	62 %	49 %
	Slope	1.01	1.16	1.19	1.29

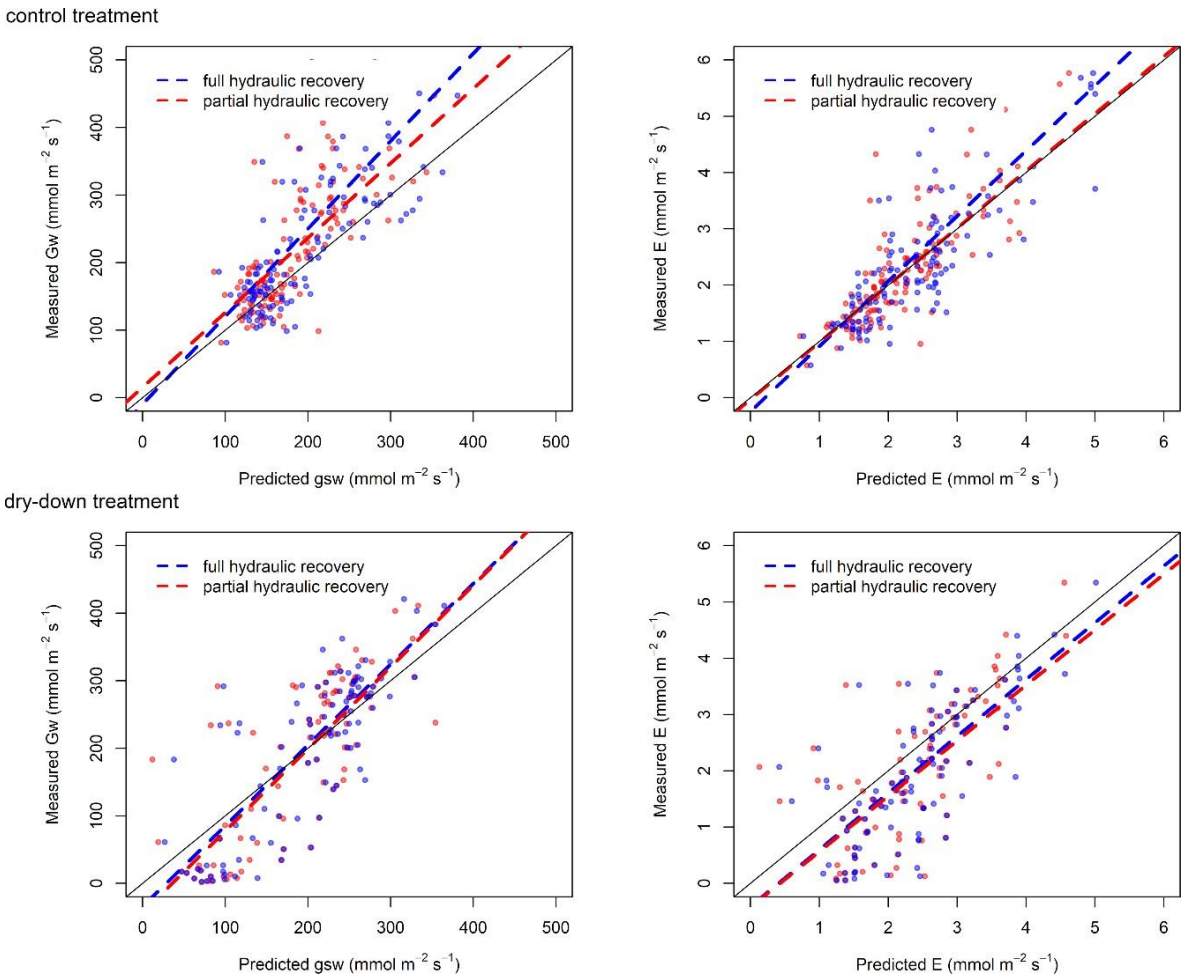

Figure 4.1 Measured vs modelled stomatal conductance (Gw) and transpiration (E) for *E. grandis X camaldulensis* (*GC*). Solid black line indicates 1:1 relationship. Linear regression results for plants in the control treatment were significant for models with complete hydraulic recovery (E: $p < 0.001$, $R^2 = 66$ %; Gw: $p < 0.001$, $R^2 = 51$ %) and with partial hydraulic recovery (E: $p < 0.001$, $R^2 = 64$ %; Gw: $p < 0.001$, $R^2 = 49$ %). Linear regression results for plants in the dry-down treatment were significant for models with complete hydraulic recovery (E: $p < 0.001$, $R^2 = 54$ %; Gw: $p < 0.001$, $R^2 = 65$ %) and with partial hydraulic recovery (E: $p < 0.001$, $R^2 = 52$ %; Gw: $p < 0.001$, $R^2 = 62$ %).

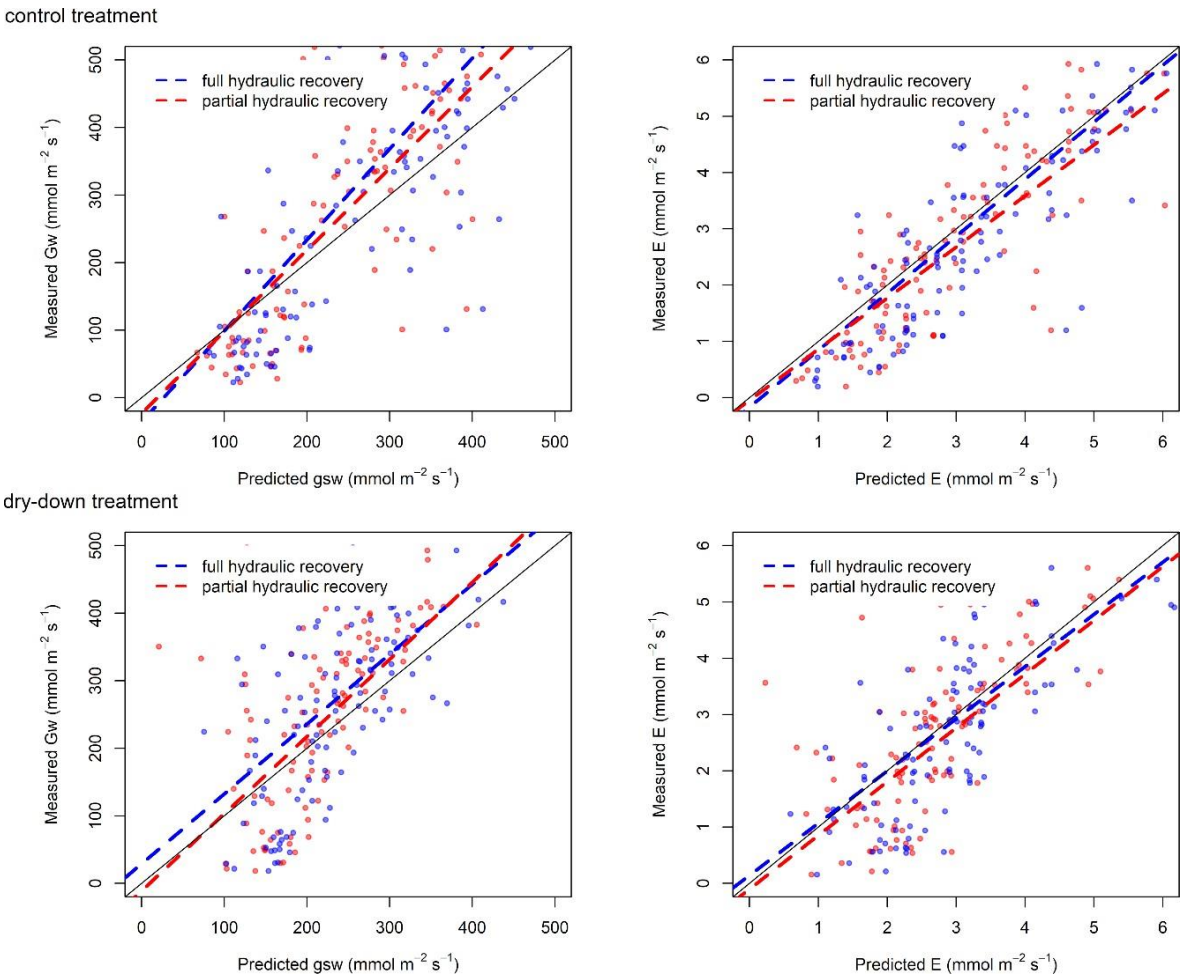

Figure 4.2 Measured vs modelled stomatal conductance (Gw) and transpiration (E) for *E. urophylla X grandis* (*UG*). Solid black line indicates 1:1 relationship. Linear regression results for plants in the control treatment were significant for models with complete hydraulic recovery (E: $p < 0.001$, $R^2 = 60$ %; Gw: $p < 0.001$, $R^2 = 57$ %) and with partial hydraulic recovery (E: $p < 0.001$, $R^2 = 62$ %; Gw: $p < 0.001$, $R^2 = 58$ %). Linear regression results for plants in the dry-down treatment were significant for models with complete hydraulic recovery (E: $p < 0.001$, $R^2 = 54$ %; Gw: $p < 0.001$, $R^2 = 44$ %) and with partial hydraulic recovery (E: $p < 0.001$, $R^2 = 54$ %; Gw: $p < 0.001$, $R^2 = 34$ %).

This was seen for the gain-risk model that only allowed partial hydraulic recovery as well with R^2 values dropping from 62 % to 48 % for transpiration and from 58 % to 34 % for stomatal conductance (Table 4.3). The R^2 values for the gain-risk model with complete hydraulic recovery however only reduced slightly from 66 % to 54 % for transpiration and increasing from 51 % to 65 % for stomatal conductance for *E. grandis X camaldulensis* (Table 4.3). This was also seen for the gain-risk model that only allowed partial hydraulic recovery as well with R^2 values slightly dropping from 64 % to 52 % for transpiration and increasing from 49 % to 62 % for stomatal conductance (Table 4.3).

The two-way repeated measures ANOVA showed that there was not a significant difference in predicted Gw and actual Gw measurements over time for both *GU* and *GC* in the control treatment (*GC*: $F = 0.202$, $df = 41$, $p = 1.000$, *UG*: $F = 1.208$, $df = 35$, $p = 0.221$). There was not a significant

difference in predicted Gw and actual Gw measurements over time for both *GU* and *GC* in the dry-down treatment (*GC*: F = 0.451, df = 33, p = 0.995, *UG*: F = 0.647, df = 35, p = 0.932). The two-way repeated measures ANOVA showed that there was not a significant difference in predicted E and actual E measurements over time for both *UG* and *GC* in the control treatment (*GC*: F = 0.430, df = 41, p = 0.999, *UG*: F = 0.809, df = 35, p = 0.764). There was not a significant difference in predicted E and actual E measurements over time for both *UG* and *GC* in the dry-down treatment (*GC*: F = 0.372, df = 33, p = 0.999, *UG*: F = 0.737, df = 35, p = 0.852) (Figure 4.3 and Figure 4.4).

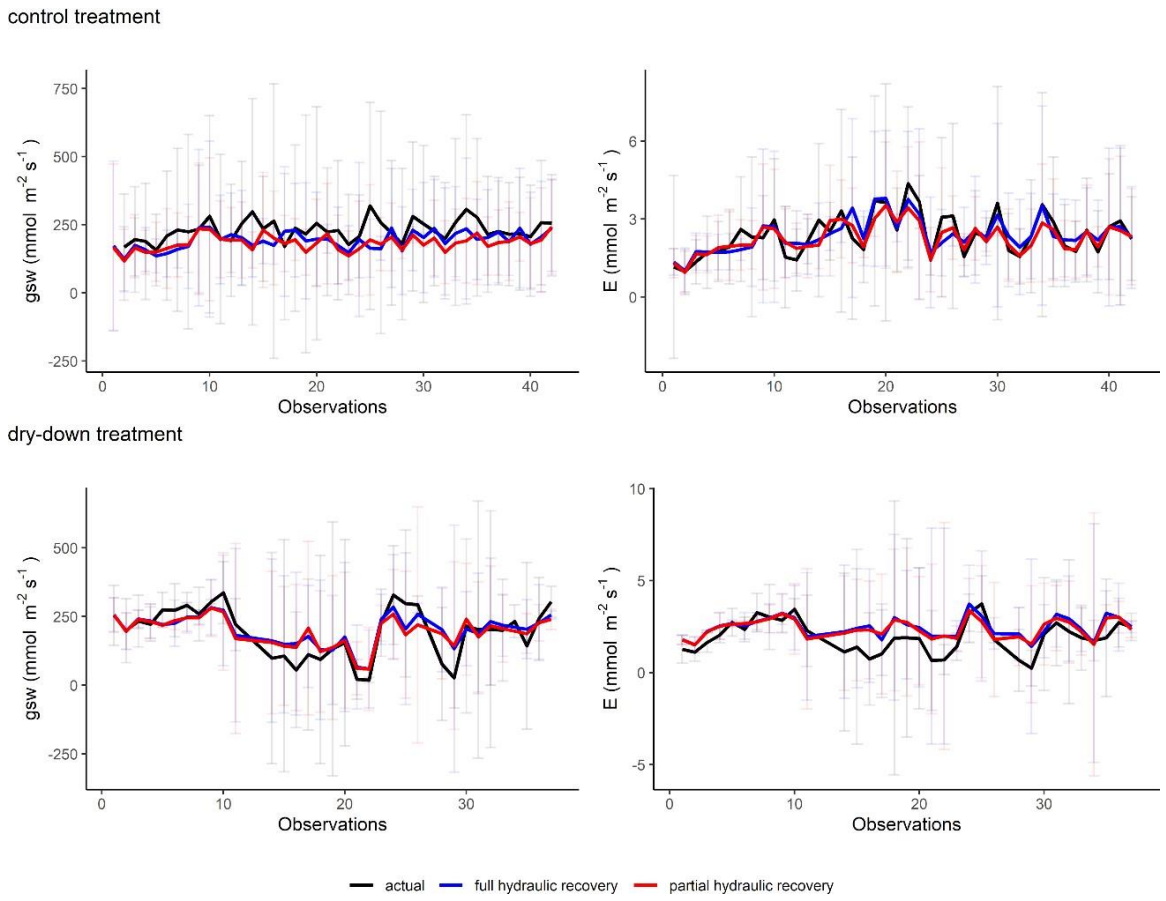

Figure 4.3 The gain-risk model performance of stomatal conductance (Gw) and transpiration rate (E) of *E. grandis X camaldulensis* (*GC*) plants over the experimental period. Measured variables are plotted in black. Predicted variables that is modelled with complete and partial hydraulic recovery is plotted in blue and red respectfully. Mean values with 95 % confidence intervals are plotted.

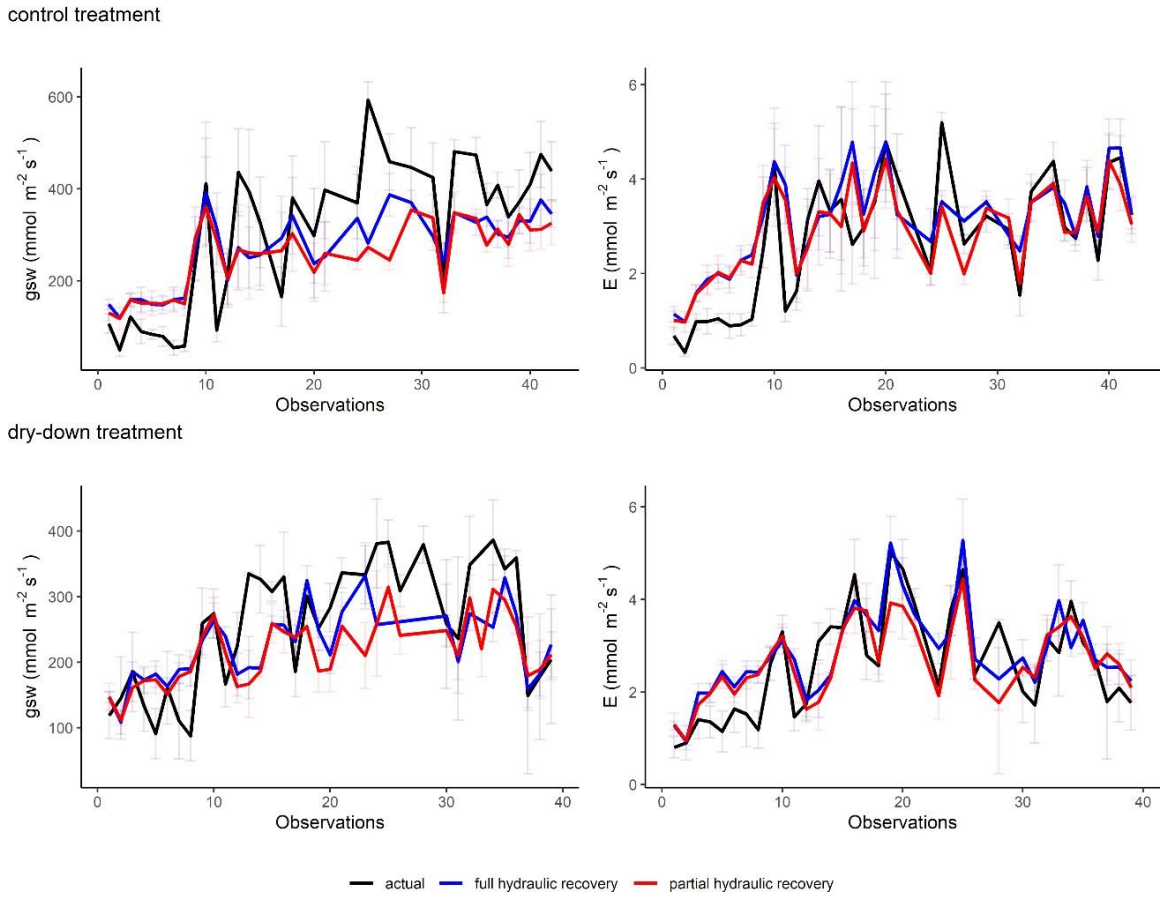

Figure 4.4 The gain-risk model performance of stomatal conductance (Gw) and transpiration rate (E) *of E. urophylla X grandis* (*GC*) plants over the experimental period. Measured variables are plotted in black. Predicted variables that is modelled with complete and partial hydraulic recovery is plotted in blue and red respectfully. Mean values with 95 % confidence intervals are plotted.

The leaf water potential for *GC* was linearly corelated to the soil water potentials for all plants within the control group for the model that allowed for full hydraulic recovery (R^2=0.804, df=121, p < 0.001) as well as for the model that allowed partial hydraulic recovery (R^2=0.826, df=121, p < 0.001). A similar response was seen for *GC* plants in the dry-down treatment with leaf water potential linearly corelated to the soil water potentials for the model that allowed for full hydraulic recovery (R^2=0.785, df=98, p < 0.001) as well as for the model that allowed partial hydraulic recovery (R^2=0.794, df=121, p < 0.001) (Figure 4.5).

The leaf water potential for *UG* was linearly corelated to the soil water potentials for all plants within the control group for the model that allowed for full hydraulic recovery (R^2=0.826 df=110, p < 0.001) as well as for the model that allowed partial hydraulic recovery (R^2=0.928, df=110, p < 0.001). A similar response was seen for *UG* plants in the dry-down treatment with leaf water potential linearly corelated to the soil water potentials for the model that allowed for full hydraulic

recovery (R^2=0.927, df=110, p < 0.001) as well as for the model that allowed partial hydraulic recovery (R^2=0.966, df=110, p < 0.001) (Figure 4.5).

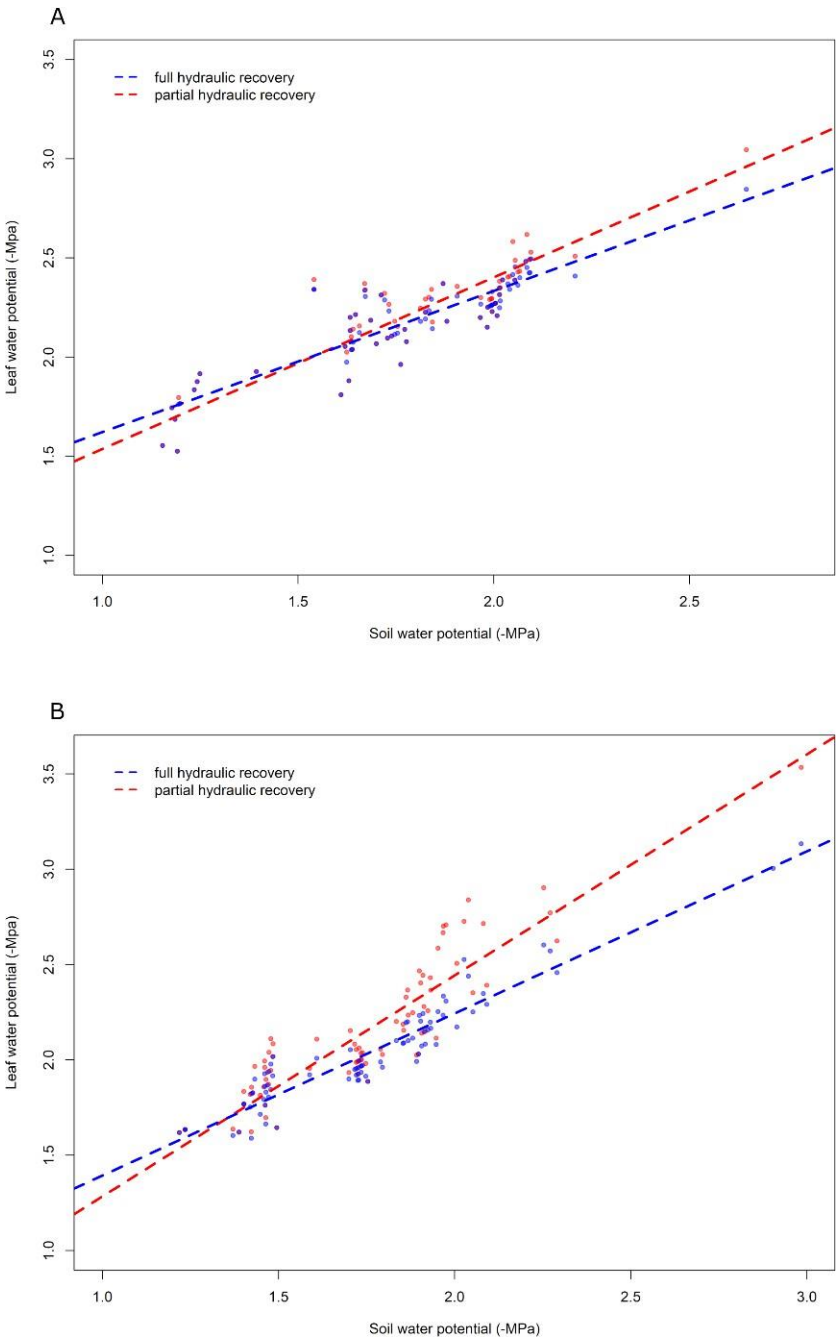

Figure 4.5 Measured soil water potentials vs. modelled leaf water potentials for models with complete hydraulic recovery (blue) and partial/delayed hydraulic recovery (red). Modelled water potentials are given for *E. grandis X camaldulensis* at the top (A) and *E. urophylla X grandis* at the bottom (B).

Complete v. reduced or delayed hydraulic recovery

When delayed/partial hydraulic recovery was included in the gain-risk model the MAE values decreased for both *UG* and *GC* when modelled v. measured transpiration measurements were compared. This trend was however not seen for Gw measurements, with MAE values increasing when delayed/partial hydraulic recovery was included in the gain-risk model.

For *GC*, the R^2 values were similar between the gain-risk model that included full hydraulic recovery as well as delayed/partial hydraulic recovery for plants that received the control treatment as well as the dry-down treatment. This was however not seen in *UG*, where the R^2 values decreased by more than 6 % when delayed/partial hydraulic recovery was included for plants that received the dry-down treatment.

For *UG* the predicted leaf water potentials were more marked when compared with the soil water potentials/pressures for predictions made using the model that allowed for delayed/partial hydraulic recovery, compared to the model that allowed for full hydraulic recovery (Figure 4.5). This was however not the case with predicted leaf water potentials for *GC*, with similar predictions seen form both the model that allowed full hydraulic recovery as well as for the model that allowed for delayed/partial recovery (Figure 4.5).

For *GC* the predicted leaf water pressures did not go below the P50 value for plants in the control group, with the predicted canopy pressures reaching values below P50 only during the drought phases for plants in the dry-down treatment (Figure 4.6). This was however not the case for *UG*, with predicted canopy pressures reaching values below P50 for plants in both the control treatment and the dry-down treatment. It is important to note that only predictions made with the model that allowed for partial/delayed hydraulic recovery predicted leaf water potentials below the P50 value (Figure 4.6)

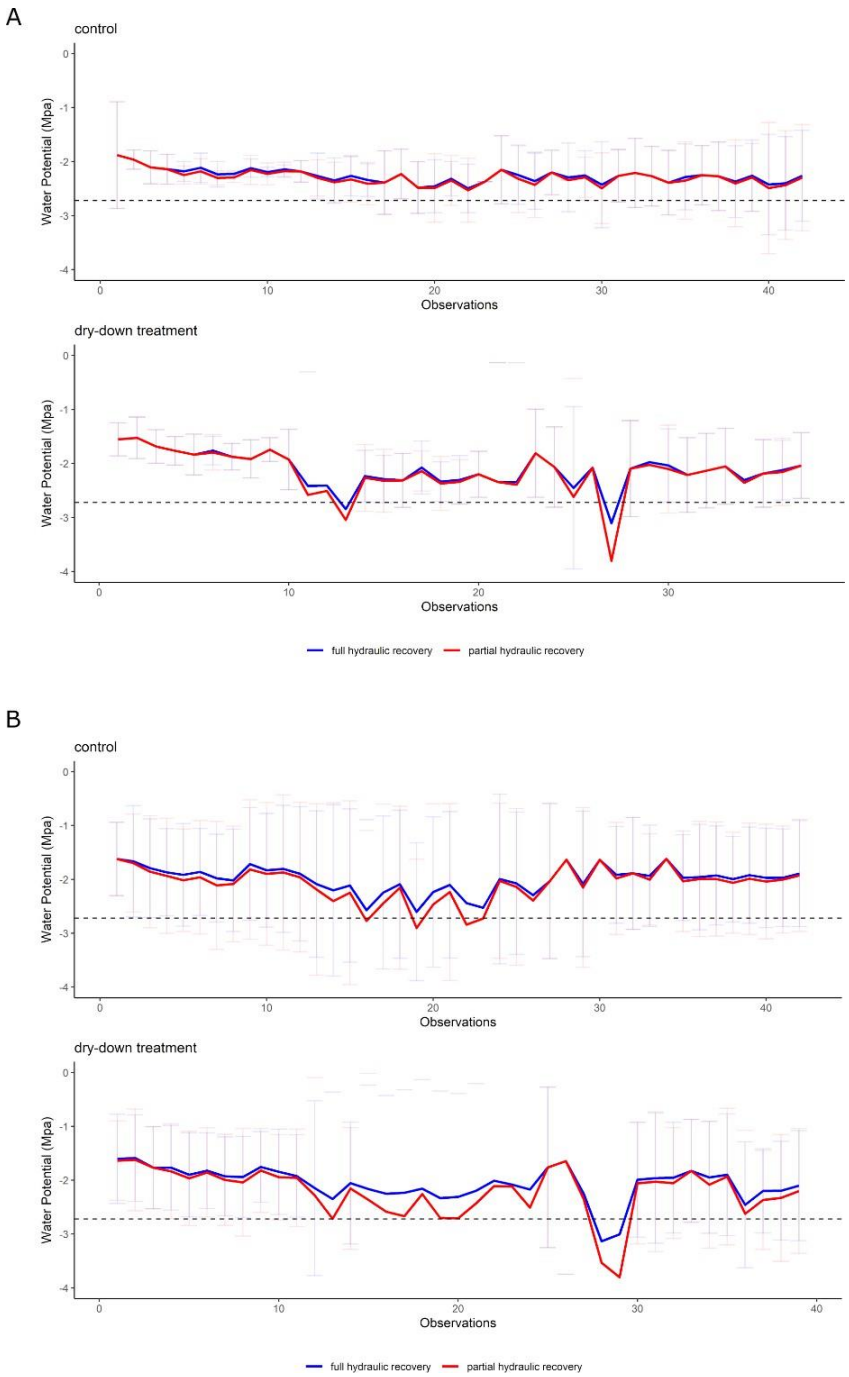

Figure 4.6 The modelled leaf water potentials over time for *E. grandis X camaldulensis* (A) and *E. urophylla X grandis* (B). Modelled values from the model that allows for full hydraulic recovery is given in blue. Modelled values for the model that allows for partial/ delayed hydraulic recovery is given in red. The P50, which indicates pressure/potential at which 50% loss of conductance is seen, is indicated with a dashed line for both hybrids.

Environmental physiological drivers

The Sobol analysis revealed that the physiological parameters influencing the variance in E and An were attributed to K_{max}, LABA and to a lesser extent the Weibull parameters (Figure 4.7).

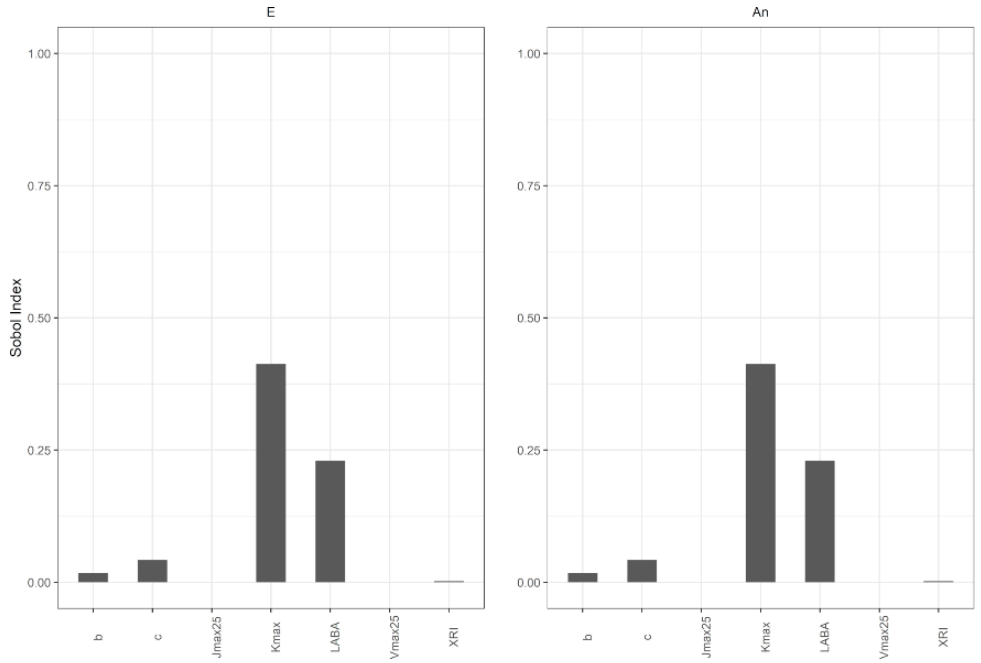

Figure 4.7 Total effects of the Sobol sensitivity analysis testing the gain-risk model that includes the hydraulic limitation. The total effects are plotted for transpiration rates (E) and photosynthesis (An). Physiological parameters on the x-axis include vulnerability curve parameters (b and c), Maximum carboxylation rate (V_{max25}) and electron transport rate (J_{max25}) at 25°C, maximum hydraulic conductance (K_{max}), leaf area to basal area ratio and the xylem recovery index (XRI). The total effects are plotted for transpiration rates (E) and photosynthesis (An).

The PCA for both hybrids showed that the absolute error in predictions for transpiration rate and stomatal conductance increased with a decrease in soil water pressure (Figure 4.8). Components 1 (seemingly related particularly to soil moisture and humidity) and 2 (seemingly related to incoming solar irradiance and air temperature) of the PCA explained 70 % of the variance seen in *GC* and 62 % of the total variance seen in *UG*.

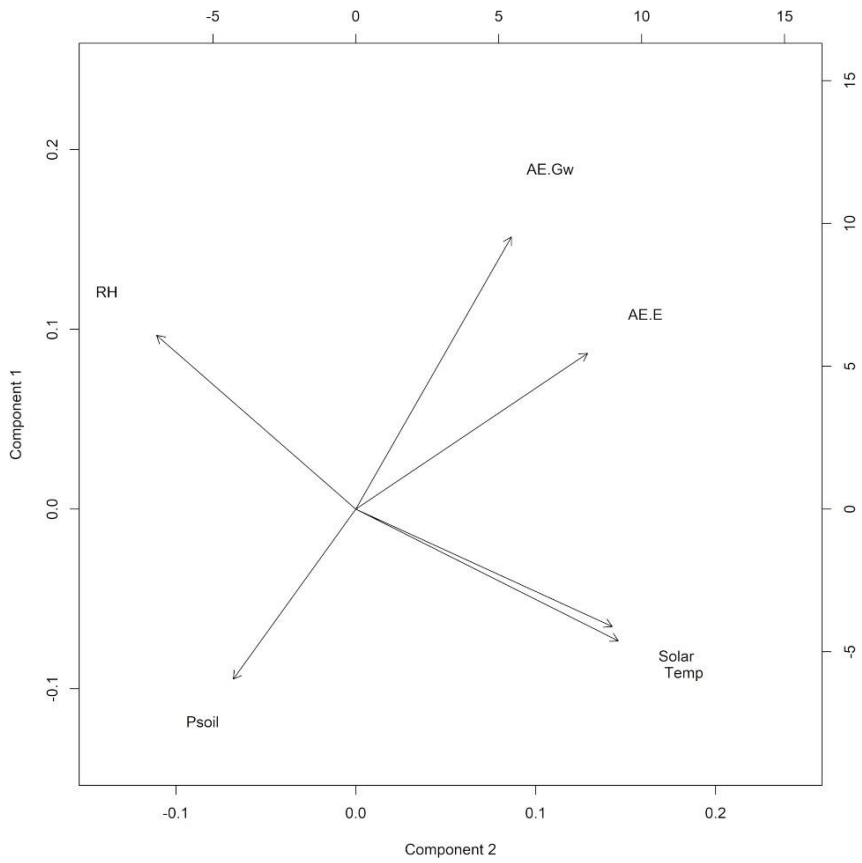

Figure 4.8 Biplot for principal component 1 and 2 yielded by the PCA of the environmental variables measured, and absolute error of predicted transpiration rates and stomatal conductance. Variables include relative humidity (RH), soil water pressure (Psoil), air temperature (Temp), soil irradiance (Solar) and absolute error of model v. measured stomatal conductance (AE.Gw) and transpiration rates (AE.E).

Discussion

In our study the gain-risk model was able to capture stomatal responses of both *GC* and *UG* under periods where soil moisture was decreased, with the model better capturing stomatal responses during the dry-down treatments compared to plants that received continuous watering. The gain-risk model has been used to predict stomatal responses in both birch and aspen (Venturas et al. 2018, Wang et al. 2019), with our study giving further evidence that stomata optimise the trade-off between water loss and carbon gain. To our knowledge, this is the first time the model is being applied at the plant-scale to the important genus *Eucalyptus*, and in particular, to hybrid clonal material of commercial significance.

The use of a model based on physiological process allows for the improvement or adaptation of the model as our understanding of plant responses improves (Wang et al. 2019). Care, however, needs to be taken to ensure that parameters that are difficult to measure are not added to the model especially regarding the hydraulic side of the model since estimating the hydraulic conductance of the soil-plant components can be challenging. In previous studies, the hydraulic conductance of

various elements of the plant (root, stem, leaves) were estimated based on the ratios of transpiration rate and LWP, with these resistance ratios measured using a vacuum method (Venturas et al. 2017, Wang et al. 2019). Sabot et al. (2020) proposed an approach that allows for the simplifying of hydraulic elements from soil to leaves into one element, where the maximum hydraulic conductance of soil-plant-atmosphere continuum (SPAC) as measured under well-watered conditions is used. This reduces the parameterisation of the gain-risk model significantly; however, this simplification runs the risk of predicting plant responses that are less conservative when under drought stress. Drought stress responses will therefore be more marked since hydraulic conductance is smoothed over the entire SPAC within the model (Sabot et al. 2020).

In our study the gain-risk model was able to still predict the trends in plant responses seen even though the hydraulic side of the model was simplified. Plant responses were however more marked when soil moisture was reduced with the absolute error in predicted v. measured variables increasing significantly with a decrease in soil water pressure. This was also seen with predicted leaf water potentials more marked compared to the soil water potentials. Due to the simplification of the hydraulic side of the model, an over-estimation of the pressure drop can be expected as is evident with predicted leaf water potentials reaching below P50 values for both hybrids. It has been proposed that the inclusion of the rhizosphere conductance component should be considered, with other studies showing that the reductions in conductance seen during drought are often more than the resistance created by the cavitation of stems, roots and leaves alone (Venturas et al. 2018). It is however still unclear how the rhizosphere component should be calculated and measured and was therefore not included in this model. Other factors that can influence reductions should also be considered, for example decreases in Rubisco activity has also been observed with increased water stress, which can affect model performance (Zhou et al. 2014).

In previous studies that evaluated the use of a gain-risk model, a larger pressure drop has also been observed for plants that are more resistant to embolism formation as indicated by their vulnerability curves (Venturas et al. 2018). This was evident within this study, with predicted leaf water potentials being more negative for *GC*, which is more resistant to embolism formation compared to *UG*. Some of the main drivers for the gain-risk model was therefore also the vulnerability curve parameters together with the LA:BA as well as the K_{max}. This can be expected at some level since the scaling of these variables being mostly decoupled from other variables and that these non-linearities will increase noise within a model.

The gain-risk model as developed by Sperry et al. (2017) proposed that the plants optimise between a photosynthetic gain and a hydraulic cost and proposed that the hydraulic cost of the model should include the loss of hydraulic conductance during drought. Decreases in stomatal conductance will therefore be observed during drought due to the increased risk of hydraulic failure (Sperry et al. 1993). Plants however use a variety of hydraulic strategies to reduce or mitigate hydraulic failure whether this is through regrowth of hydraulic pathways, resisting embolism formation or refilling embolism post-drought (Ogasa et al. 2013, Sperry and Love 2015). The two *Eucalyptus* hybrids used in our study have been shown to have distinct hydraulic strategies, with *UG* being more drought vulnerable compared to *GC* (Van der Willigen and Pammenter 1998, Saadaoui et al. 2017). A higher rate of recovery was seen in *UG*, with *UG* being able to recover some hydraulic conductance over night after re-watering. This recovery was however not observed within *GC* (Saunders and Drew 2021). Although there is uncertainty around the mechanisms and cost regarding hydraulic recovery (Klein et al. 2018), plants with a more costly recovery method can be expected to be more conservative by closing stomata earlier, during a period of decreasing soil water availability (Lu et al. 2020). This was observed within *GC*, where stomatal conductance decreased as soil moisture decreased, while stomatal conductance trends of *UG* plants seen in the dry-down treatment mimicking the control group.

A more conservative stomatal response can be related to the opportunity cost with increased photosynthesis occurring when soil water is limited (Lu et al. 2020). Plants might favour a strategy relating to avoiding embolism formation instead of tolerating embolism formation if the cost of recovery is too high, compared to the cost of reduced photosynthesis (Lu et al. 2020). Even though the gain-risk model shows promise in predicting plant responses more information is needed regarding hydraulic recovery after drought. Optimisation models that include a cost relating to hydraulic failure due to stress has shown the most promise at predicting stomatal responses (Wang et al. 2020), further highlighting the influence of stomata regulation on the hydraulic vulnerability of a plant, however more research is needed to understand how different recovery strategies will influence plant responses post-drought.

Tight stomatal regulation when soil moisture was decreased was observed with *GC*, suggesting that *GC* uses a resistant strategy. This strategy can be beneficial when periods of decreased soil moisture are short, since it will limit water loss, but will reduce carbon assimilation as well which can lead to carbon starvation if drought periods are prolonged (Martínez-Vilalta and Garcia-Forner 2017, Nolan et al. 2017). This is in contrast with the resilient strategy seen in *UG*, where stomatal conductance is maintained during periods of reduced soil moisture. A resilient strategy will maximise carbon

assimilation during periods of reduced soil moisture, however, increases the risk of mortality due to hydraulic failure if drought persists (Mitchell et al. 2013, Zhang et al. 2016).

In this study the gain-risk model performed better for *GC* during short periods of reduced soil moisture, which suggests that the gain-risk model will perform better for plants that follow a resistant strategy compared to plants that follow a resilient strategy. This may be due to stomatal conductance being maintained during short periods of drought for resilient species, regardless of the risk of hydraulic failure on which the gain-risk model is based. A more in-depth study is therefore needed to understand how the optimisation between water loss and carbon gain based on different water use strategies over various periods of reduced soil moisture will differ. It has also been proposed that a resilient strategy will aid recovery after drought, since the carbohydrate reserves will not be depleted during drought which can help with regrowth of hydraulic pathways post-drought (Mitchell et al. 2013).

In this study the inclusion of a partial and/or delayed hydraulic recovery component performed similarly or slightly better at predicting plant responses during the dry-down treatment for *GC*, however performed worse during the dry-down treatments for *UG*. Although hydraulic recovery has been observed in previous studies as soil water increases, it is still unclear what the underlying mechanisms are (Klein et al. 2018, Zeppel et al. 2019). The gain-risk model relies on a cost function, which was related to the increasing risk of cavitation due to embolism formation during drought (Sperry et al. 2017). In this study, the inclusion of a delayed and/or partial hydraulic recovery did not drastically improve model predictions. Cost associated to embolism recovery was however not considered during this study and can lead to reductions in prediction accuracy.

It has been shown that hydraulic recovery is energy dependent, whether this is through carbon used to regrow hydraulic pathways or changing osmotic gradient by relocating sugars and ions to embolised vessels (Nardini et al. 2011). The upregulating of genes associated with carbohydrate metabolism have also been observed during drought, highlighting that there is another cost involved during embolism recovery (Secchi and Zwieniecki 2010). The inclusion of other cost functions should therefore be considered to improve model predictions, however since it is unclear what these underlying costs are it is difficult to include in the process-based model. In this study focus was therefore given to improve the cost function by including a delayed and/ or partial hydraulic recovery based on the current understanding and knowledge available regarding embolism recovery.

Hydraulic recovery through regrowth, should also be included when predicting plant responses over a larger time frame since this comes with a significant carbon cost (Brodersen and McElrone 2013, Buckley 2017, Anderegg et al. 2018). In fast growing plants such as *Eucalyptus* hybrids, this effect may be particularly important. Other research on *UG* and *GC* clones, and other *Eucalyptus* spp., have shown that very fast rates of growth lead to a highly disproportionate amount of wood with distinctive hydraulic properties forming following release from drought (Drew and Downes 2009, Drew et al. 2009, 2011, Câmara et al. 2021). Xylem growth is also affected by reductions in soil moisture with decreases in vessel density seen in some species, which will affect hydraulic conductance of a plant and should be considered if hydraulic recovery through regrowth is included in the gain-risk model (Tng et al. 2018). In this study, hydraulic recovery through regrowth was however not considered.

The carbon cost of hydraulic recovery was also not considered in this study as there is still a debate regarding how hydraulic recovery takes place (Klein et al. 2018). Besides the carbon cost associated with regrowth of hydraulic pathways, it has been proposed that non-structural carbohydrates can aid hydraulic recovery by changing osmotic gradients (Nardini et al. 2011, Tomasella, Casolo, et al. 2019, Tomasella, Petrussa, et al. 2019). Other factors influencing hydraulic conductance that should also be considered including the loss of water through leaf cuticles and embolism recovery through increase root pressure (Cochard et al. 2001, Secchi and Zwieniecki 2010, Nardini et al. 2011, Duursma et al. 2019, Liu et al. 2019, Tomasella, Petrussa, et al. 2019).

Knowledge gaps in how plants recover hydraulic conductance after drought however still exist, with many researchers still debating whether it is possible over short time periods (Cochard et al. 2001, Nardini et al. 2011, Klein et al. 2018). It has been well established that recovery can take place when soil moisture increases (Ogasa et al. 2013, Klein et al. 2018), and was therefore the only recovery mechanism considered within this study. A better understanding in how plants recover hydraulic conductance, especially over short time periods, can therefore help improve predictions within the gain-risk model. In this model hydraulic recovery was considered when there was an increase in soil moisture. It is however still unclear how plants recover from mild versus severe drought conditions and whether there is a loss of hydraulic conductance threshold from which plants cannot recover (Meinzer and McCulloh 2013, Hammond et al. 2019). Hammond et al. (2019) has shown that 80 % loss of hydraulic conductance was the hydraulic threshold at which plants cannot recover. This work was however done on *Pinus taeda* and determining this threshold within *Eucalyptus* and other species can help improve modelling the hydraulic recovery response within the gain-risk model. It is also still unclear as to whether complete hydraulic recovery is possible

post-drought and whether hydraulic recovery will always be imperfect (Zeppel et al. 2019), and more work is needed to understand whether or not there is a possible threshold of embolism magnitude after which plants will not be able to recover fully.

Conclusion

The gain-risk model has the benefit of being processed-based, with model parameters based on measurable plant characteristics (Venturas et al. 2018). This reduces the assumptions regarding parameterisation, giving it an advantage over empirical models where model parameters are often difficult to quantify (Damour et al. 2010). This allows for the gain-risk model to predict plant responses to future changes in climate, instead of fitting models to known datasets (Sperry et al. 2017). The gain-risk model has however only been tested on a limited amount of species (Venturas et al. 2018, Wang et al. 2019), and focus should be given to test the model on plants with various hydraulic traits and water use strategies (Ciemer et al. 2019). More research is also needed to determine how photosynthetic and hydraulic traits might change over time and affect long-term predictions (Anderegg 2018, Wang et al. 2019, Sabot et al. 2020).

Being trait based, process-based models have the ability to predict plant responses under novel environmental conditions where empirical models have not before been tested (Damour et al. 2010). This is especially important considering the need to capture plant responses in light of climate change (Menezes-Silva et al. 2019). Shifts in precipitation with an increase in droughting events are predicted due to climate change, with areas with optimal environmental conditions for forestry likely to shift (Warburton and Schulze 2008, Pachauri et al. 2014). The need therefore arises to have a model that captures plant responses to changes in climate (Menezes-Silva et al. 2019), with the gain-risk model showing promise as a process-based model.

Supplementary material

Figure 4.9 Experimental design

Figure 4.10 Soil volumetric water content and soil water pressure curve as calculated by the van Genuchten model.

Figure 4.11 Soil water pressure of control and drought-recovery treatment over the experimental period.

Methods 4.1 Van Genuchten model and soil parameters used

Code availability: Code to run the gain-risk model with the hydraulic recovery component (Model1.R) and without the hydraulic recovery component (Model2.R) is available at https://github.com/altazietsman/gain_risk_model.git . All code is written as a function. Please note code is available in only R and was not written for publication.

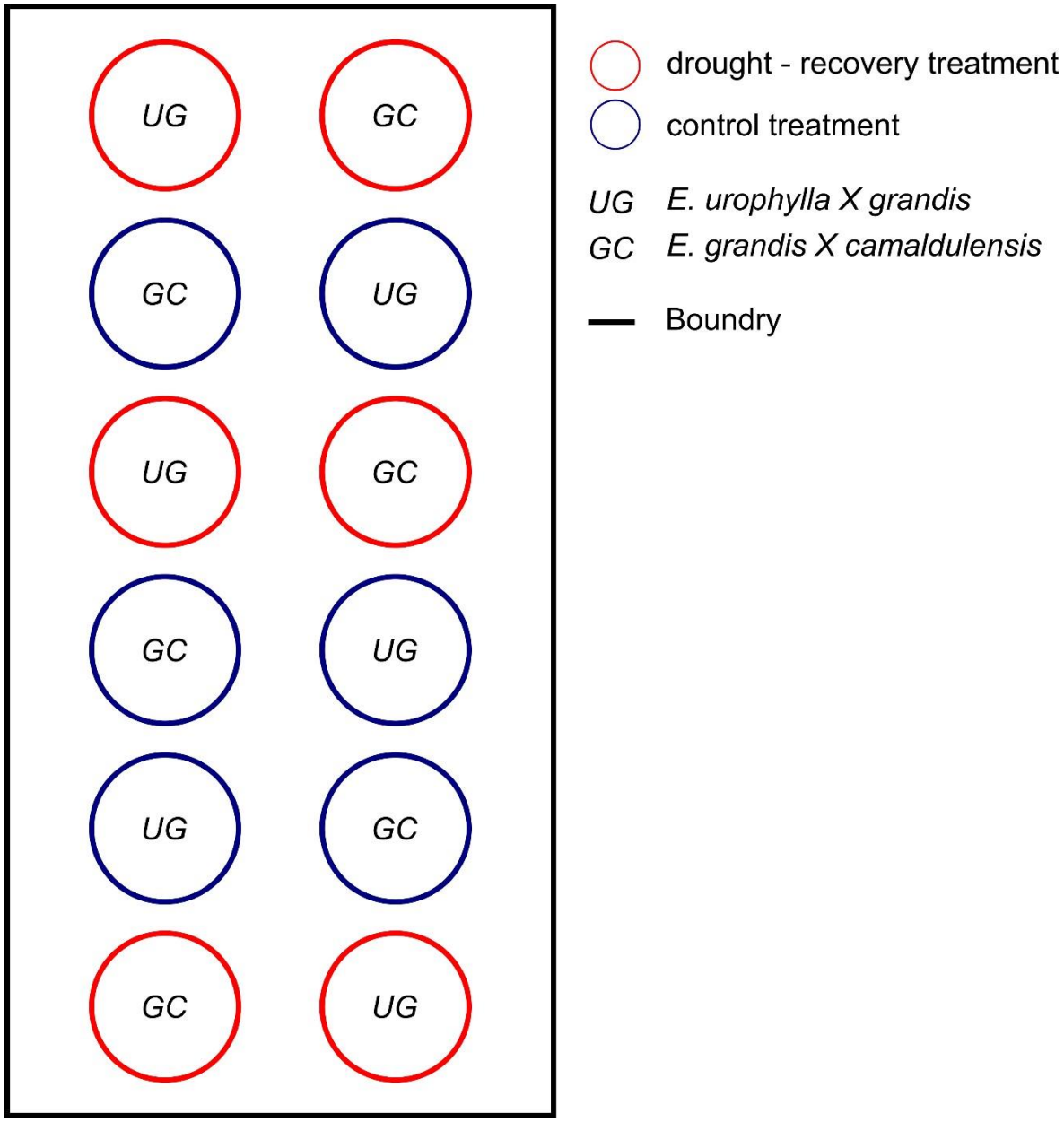

Figure 4.9 Experimental design layout of drought-recovery experiment.

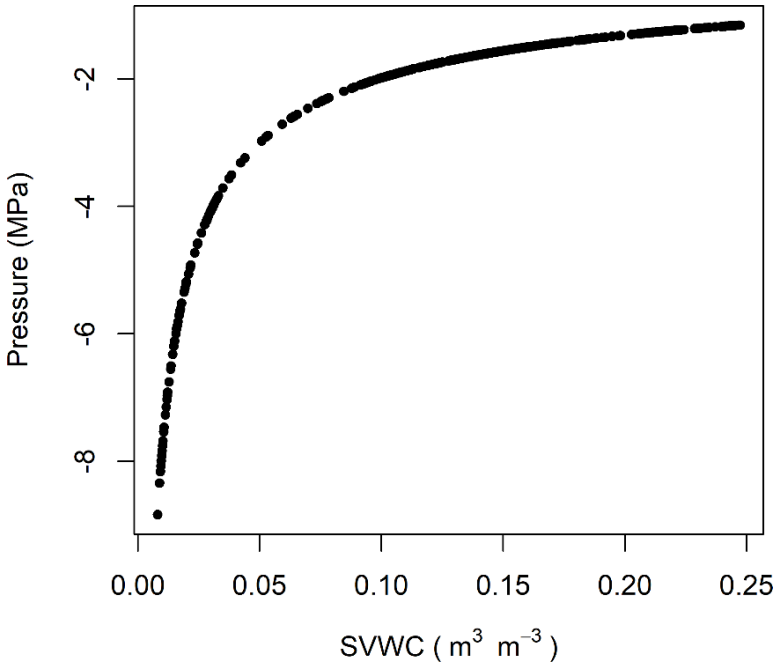

Figure 4.10 Soil volumetric water content and soil water pressure curve as calculated by the van Genuchten model.

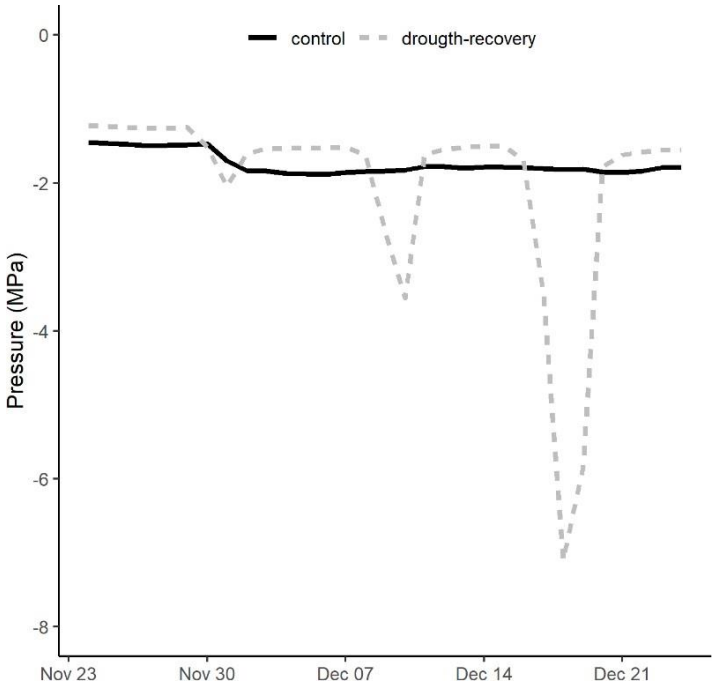

Figure 4.11 Soil water pressure of control and drought-recovery treatment over the experimental period.

Methods 4.1 Soil pressure was calculated using the van Genuchten model (van Genuchten 1980), where the soil moisture (s_ψ) at any given soil water pressure (ψ_s) is calculated as follow:

$$s_\psi = \frac{1}{\left(1 + \left(-\frac{\psi_s}{\alpha}\right)^n\right)^m}$$

where α, n and m are soil parameters based on the soil texture. For this work plants were planted in sand. All soil parameters used was determined from the soil texture as described in UNSODA Unsaturated Soil Hydraulic Database (Leij et al. 1996). The values used for the soil parameters were as follow:

Soil parameter		**Value**
α	→	0.145
n	→	2.68
m (1-1/n)	→	0.626866

Chapter 5

The co-ordination of stomatal regulation, hydraulic properties, and biomass allocation influence drought strategies in two *Eucalyptus* hybrids

Chapter 5: The co-ordination of stomatal regulation, hydraulic properties, and biomass allocation influence drought strategies in two *Eucalyptus* hybrids

Abstract

Drought-induced tree mortality has been linked to decreases in the water transport within plants which, in turn, affects gas exchange and photosynthesis. Increases in global drought events are predicted under climate change, along with increases in drought-induced tree mortality. Considering this, understanding how plant hydraulics and stomatal regulation influence production rates is becoming more important. In this study we therefore compared the patterns of gas exchange and biomass allocation in response to drought between two *Eucalyptus* hybrids: *E. grandis X camaldulensis* (*GC*) and *E. urophylla X grandis* (*UG*). Two drought strategies were observed based on the gas regulation and growth patterns seen during the study: *GC* showed a more resistant strategy where gas exchange was tightly regulated with decreases of growth and production during drought, whereas *UG* showed a more resilient strategy where gas exchange and growth were maintained during drought. The drought responses seen between the hybrids could thus be divided into isohydric vs anisohydric strategies. This study also linked hydraulics and embolism resistance to drought strategies seen between the two hybrids. *GC* was more resistant to embolism formation compared to *UG*, which was related to vessel size and area. During this study drought resistance was therefore related not only to embolism resistance, but also timely stomatal closure and changes in biomass allocation. In light of climate change, understanding how hydraulic and gas exchange traits covary during drought can help improve models for productivity especially in commercially significant hardwoods such as *Eucalyptus*.

Introduction

Understanding how trees respond and function under drought has become more important, with an increase in drought-induced tree mortality seen due to changes in climate (Allen et al. 2010, 2015, Anderegg et al. 2015). Drought-induced tree mortality has been associated with reductions in water transport within the plants (Anderegg et al. 2016). Plants can regulate their water use through changes in their hydraulic properties (conduit diameter etc.) as well as through stomatal regulation (Brodribb 2009, Brodribb and McAdam 2011). Changes in a plant's hydraulic properties can however only provide control in water use after long lag periods, with stomata being much more

dynamic (Aloni, 2015; Tng et al., 2018; Tyree & Sperry, 1988). Understanding how hydraulic traits and stomatal regulation co-vary can help model drought-induced tree mortality in a changing climate (Mcdowell et al. 2013).

Stomatal regulation can help prevent water loss, especially when water is limited, and plays an important role in global hydrological cycles (Silva et al. 2004, Bonan 2008, Bonan et al. 2014). During drought, stomatal regulation ensures that water demand through transpiration does not exceed the water supply, which can otherwise lead to the formation of embolism (Tyree and Sperry 1988, Sperry et al. 2017, Xiong and Nadal 2020). Embolism formation reduces the hydraulic conductivity of a plant, which can ultimately lead to hydraulic failure and tree mortality (Tyree & Sperry, 1988). The ability of a plant to maintain water supply has therefore also been related to embolism resistance, where differences in xylem features allow some plants to resist the formation of embolism as the pressure gradient from roots to leaves increases (Martin-StPaul et al. 2017).

Quantitative wood anatomy traits have given further insight into how trees can respond to drought (Tng et al. 2018). Vessel size, for example, influences water transport capacity, but hydraulic safety can be expected to decline in larger vessels (Gleason et al. 2016) potentially leading to cavitation and desiccation during drought conditions (Lens et al. 2011). Greater hydraulic conductance, however, enables increased growth rates, with the trade-off between hydraulic safety and growth rates being highlighted in previous studies (Hacke et al. 2001, Maherali et al. 2006). Tissues associated with vessels, such as parenchyma and vasicentric tracheids, have also been shown to play a role in the drought response of plants; contributing to water movement between vessels, and playing a role in refilling of embolised vessels (Salleo et al. 2004, Loepfe et al. 2007, Secchi and Zwieniecki 2010, Nardini et al. 2011, Sano et al. 2011, Barotto et al. 2016, Secchi et al. 2021). Leaf and root traits have also been shown to respond to drought. Leaves not only play a role in adjusting their leaf water potential via stomatal control, but reductions in leaf mass during drought (through dropping leaves) can further help to prevent water loss (Mokany et al. 2003, Wolfe et al. 2016). Increased root growth can conversely help to improve the water supply to the plant and canopy (Manzoni et al. 2015).

In previous studies tree mortality has, however, not only been linked to the ability of a plant to regulate its water balance during drought, but also its carbon balance (Allen et al. 2010, Mitchell et al. 2013). Stomatal regulation not only affects water loss, but also regulates carbon gain through CO_2 uptake (Schulze and Hall 1982, Morrison 1987, Xiong and Nadal 2020). It has been shown that stomatal closure due to drought is one of the main limitations of photosynthesis and production

(Flexas and Medrano 2002, Galmés et al. 2007). In addition, the restriction of water movement through the plant also limits the transport of carbohydrates, which decreases metabolism (McDowell et al., 2008; Trugman et al., 2018a). It has, therefore, been proposed that stomatal regulation and hydraulic properties such as embolism resistance are coordinated to ensure that carbon uptake is maximised while still ensuring desiccation does not take place (Brodribb and Feild 2000, Sperry 2004), such that plants close stomata at lower water potential (if they are more resistant to embolism formation) to allow longer periods of carbon uptake (Klein 2014). Evidence of this coordination between stomatal conductance and embolism resistance has been shown in many studies, but predominantly in plant species that have very low resistance to drought (Cruiziat et al. 2002, Mencuccini et al. 2015). However, a recent study by Martin-StPaul et al. (2017) evaluated traits relating to stomatal regulation and embolism resistance for over 100 tree species found evidence challenging this idea. In contrast to stomatal and hydraulic coordination, their findings suggested that increased embolism resistance and early stomatal closure during drought is related (Martin-StPaul et al. 2017), and that timely stomatal closure is necessary to avoid drought-induced tree mortality.

Based on their stomatal responses during drought, plants have often been classified into two main groups: isohydric and anisohydric (Martínez-Vilalta and Garcia-Forner 2017). Anisohydric species maintain stomatal conductance during drought, maximising photosynthesis, but thereby run the risk of hydraulic failure due to embolism formation. Isohydric species, on the other hand, reduce stomatal conductance in order to maintain the water balance, but in doing so sacrifice on carbon assimilation and run the risk of carbon starvation under prolonged droughts (Martínez-Vilalta and Garcia-Forner 2017).

Eucalyptus species typically have high rates of photosynthesis and growth (Whitehead and Beadle 2004), which is accompanied by high rates of stomatal conductance. A wide range of water use strategies have been observed within *Eucalyptus* (Saadaoui et al. 2017), however there is uncertainty as to how hydraulic and stomatal responses of *Eucalyptus* species are coordinated, especially under drought conditions (Zhang et al. 2016). Understanding these phenomena in *Eucalyptus* is of major economic importance, as the genus is widely planted internationally for a range of timber and fiber products (Myburg et al. 2014). There remains a lack of knowledge regarding the mechanism used by species to prevent drought driven mortality (Mitchell et al. 2013) and understanding varying strategies and vulnerability between *Eucalyptus* species and varieties, especially under climate change is particularly important. The aim of this study was, therefore, to better understand the coordination between hydraulic traits and stomatal regulation during drought

for two commercially significant *Eucalyptus* hybrids. The objectives of this study were to (1) determine if drought resistance is related to embolism resistance and/or stomatal regulation, and if so (2) to better understand the influence of hydraulic traits and stomatal regulation on drought resistance and (3) to determine if biomass partitioning during drought is influenced by the drought resistance strategy.

Materials and Methods

Plant material

Eighteen *E. grandis X camaldulensis* (*GC*) and 18 *E. urophylla X grandis* (*UG*) rooted cuttings were grown under shade netting where they received continuous watering and intermitted fertiliser prior to the experimental period. All plants were grown in 2-litre pots in a medium comprising a 2 to 1 ratio of composted pine bark and fine river sand. Plants were grown for two years prior to any experimental work and had a stem diameter of 6.47 ± 0.94 mm.

Experimental design and treatments

Six plants per hybrid were replanted into a coarse sand mixture with a pH of 7.55 ± 0.133 and moved into a growth tunnel where they could acclimatise for 2 weeks. Plants were arranged in a randomised arrangement in a glass house with all pots placed on a raised grid to ensure that plants did not have access to any additional water from below. A cyclic droughting treatment was applied where plants were watered to field capacity for 5 days in between droughting events, applied by drippers. Three droughting cycles were applied of different lengths and severity: plants were completely droughted for 2 days, 3 days and 4 days for each droughting event respectively. Three plants per hybrid received continuous watering throughout the entire 6-week experimental period as a control group. In the control treatment volumetric soil water content (SWC : m^3m^{-3}) was kept above the field capacity of the growing medium, which was 10 % (Ratliff et al. 1983, Leij et al. 1996). During the cyclic drought treatments, the SWC was reduced to below the wilting point (SWC < 5 %) for extended periods of time.

Hourly measurements were taken of SWC, relative humidity (RH : %), air temperature (T_{air} : Celsius) and incoming solar irradiation (Solar : W m^{-2}). Hourly measurements were logged as an average of 10-minute readings using a CR1000X datalogger (Campbell Scientific). SWC was logged for each plant individually using water content reflectometers (model CS 655, Campbell Scientific). T_{air}, RH and Solar was measured above and below the plant canopy. Since all experimental work took place inside a glasshouse, wind and precipitation was not measured and assumed to be zero.

Stomatal conductance (gsw : mmol m^{-2} s^{-1}) and the efficiency of photosystem II (φPSII) was measured during the cyclic drought treatments using a LI-600 Porometer and Fluorometer (Licor). Measurements were taken daily from 5 fully expanded leaves per plant in the morning (08:00 – 09:00), midday (12:00 – 13:00) and in the afternoon (16:00 – 17:00). The predawn leaf water potential (LWP : MPa) measurements were taken once a week using a pressure chamber (Skye plant moisture system, SKPM 1400 series).

At the end of the cyclic drought treatments, all plants were harvested, and all parts oven dried to constant mass. Leaves, stems, and roots were separated, and their dry weights measured. Throughout the experimental period, weekly measurements of stem diameter were taken using an automatic calliper (150 mm Vernier Caliper accurate to 0.01 mm). Marks were made on the stem of each plant to ensure that stem diameter measurements were made at the same place throughout the experimental period.

Hydraulic and Photosynthetic traits

Prior to the cyclic drought treatments measurements relating to photosynthetic and hydraulic traits were taken on a subset of the trees.

The maximum electron transport rate at 25°C (J_{max25}) and the maximum carboxylation rate at 25°C (V_{max25}) was calculated from A:Ci curves for each hybrid. A:Ci curves were constructed for 10 plants per hybrid using a LiCor 6400 Portable photosynthesis system (LiCor Inc). For the derivation of these curves, air temperature was set at 25°C, VPD was set at 1 - 2 kPa, active radiation was set at 1500 - 2000 µmol photon m^{-2} s^{-1} and the CO_2 concentration ranged from 50 - 2000 ppm.

The bench dehydration method was used to construct vulnerability curves for both *GC* and *UG* since it relies on natural desiccation and reduces measurement artifacts (López et al., 2018; Tyree and Sperry, 1988). The hydraulic conductance (K_{int}) was measured on 15 – 20 cm stem segments and different xylem water potentials. The xylem water potential was measured from excised leaves using a pressure chamber (Skye plant moisture system, SKPM 1400 series) after branches have been placed in a black plastic bag with a damp towel and allowed to equilibrate for 30 minutes. Vulnerability curves were constructed as the percentage loss of hydraulic conductance of the maximum hydraulic conductance (PLC) across a range of xylem water potentials. A Weibull function was used to fit the vulnerability curves on the PLC and xylem water potential pairs (Hacke et al. 2006).

Cross sections of stem segments of three plants per hybrid were manually made. Images were acquired and captured using a Motic BA310Pol polarising microscope with a 40x objective. All images were analysed using ImageJ software (Schneider et al. 2012) to measure vessel area (mm^2) of all cross sections. The theoretical hydraulic conductance (k_h) was calculated from the measured vessel area using Hagen-Poiseuille's law (Tyree and Ewers 1991), with the following equation as modified by Tombesi et al. (2010):

$$k_{h=}\left(\frac{\pi\rho}{128\eta}\right)\sum_{i=1}^{n} d_i^4$$

where η is the viscosity of water (1 x 10^{-9} MPa s), ρ is the fluid density of water (1000 kg m^{-3}) and d is the radius of a vessel (m).

Statistical analysis

All variables were tested for normality before the start of analysis. Summary statistics were calculated for all variables measured. A non-parametric Kruskall-Wallis test was used to test for significant difference between hybrids. The dried leaf masses were calculated as a ratio of the dry stem mass for each plant. The percentage reduction in stomatal conductance was calculated as a percentage of the maximum stomatal conductance measured for each plant (Mencuccini et al. 2015, Martin-StPaul et al. 2017). The mean soil water content at which a reduction in stomatal conduction was 50 % and 90 % was calculated for each hybrid. A non-parametric Kruskal-Wallis test was used to determine if there was a significant difference in vessel area and k_h between the two hybrids. Distribution curves were used to compare the vessel size distribution of both hybrids.

A generalised linear model (GLM) with Gaussian distribution was used to test the effect of different variables on stomatal conductance. The Farrar-Glauber test was used to check for collinearity among the predictor variables. Variables that showed collinearity were excluded prior to the GLM; the fixed effects variables were limited to SWC and Solar. The models that best explained the relationship between the predictor variables and gsw were selected on the basis of a minimised Akaike's Information Criterion (AIC). Model weights, AIC differences and maximised log likelihoods were determined for each GLM model. A null model was also included in the analysis.

Results

Experimental treatments

During the cyclic drought experiment, T_{air} ranged between 10.11°C and 44.09°C. The RH ranged between 36.26 % and 68.40 %. The predawn LWP of all plants was recovered before and after

every droughting event. The predawn LWP measurements at the start of the cyclic drought experiment was - 0.60 ± 0.00 MPa for GC and - 0.8 ± 0.20 MPa for UG. The predawn LWP measurements at the end of the experimental period was - 0.67 ± 0.12 MPA for GC and - 0.8 ± 0.17 MPa for UG.

Plant Characteristics

The non-parametric Kruskall-Wallis test revealed no significant differences in the A:Ci curves between the two hybrids (H = 0.29, p = 0.131). The mean V_{max25} and J_{max25} for *UG* was 57.57 ± 23.22 µmol m^{-2} s^{-1} and 210.78 ± 66.48 µmol m^{-2} s^{-1} respectfully. The mean V_{max25} and J_{max25} for *GC* was 43.85 ± 18.84 µmol m^{-2} s^{-1} and 174.88 ± 122.01 µmol m^{-2}.

There was, however, a significant difference in the estimated vulnerability between the two hybrids (H = 3.857, p = 0.008), with *GC* being more resistant to embolism formation. *GC* lost 50 % of its hydraulic conductance (P50) at -2.72 MPa, while the P50 of *UG* was -2.33 MPa. There was also a significant difference seen in the distribution of vessel area between the two hybrids (H= 540.650, p < 0.001). *GC* had a higher count of vessels, while *UG* had larger vessels. A similar trend was seen when the k_h was compared between the two hybrids, with a significantly higher hydraulic conductance seen in *UG* compared to *GC* (Figure 5.1)

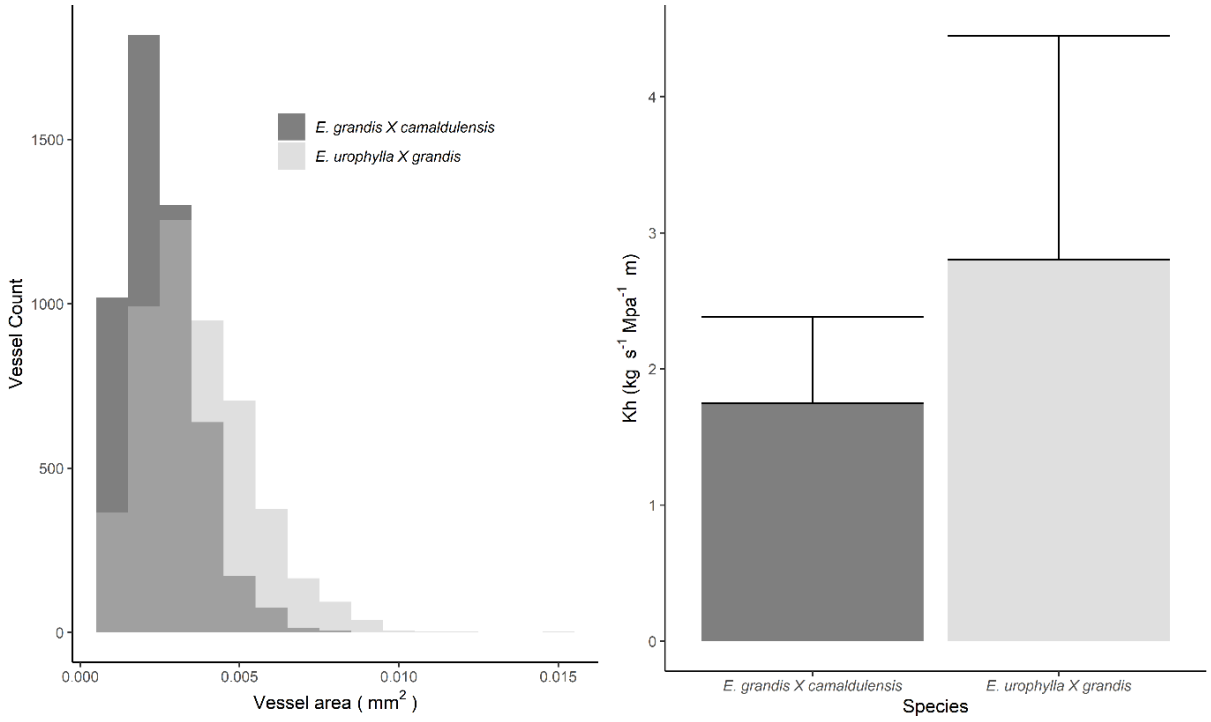

Figure 5.1 Vessel size distribution (left) and hydraulic conductance (right) of E. urophylla X grandis and E. grandis X camaldulensis as calculated based on cross-sections of the stem.

Stomatal responses to drought

There was a clear response seen to drought in *GC*, with gsw reducing soon after a drought was initialised (Figure 5.2). This response was not seen in *UG* with the gsw responses of the plants in the cyclic-drought treatment mimicking the gsw response in the control treatment (Figure 5.2). There was no significant difference seen in the SWC at which 50 % reduction in stomatal conductance and 90 % reduction in stomatal conductance was observed for *GC*, however the SWC at 90 % reduction in conductance was lower (H=3.78, p=0.05188). There was no significant difference seen in SWC at which 50 % reduction in stomatal conductance and 90 % reduction in stomatal conductance was seen for *UG* (H = 0.13, p = 0.722).

There was no significant difference in the SWC at which stomatal conductance dropped to 50 % between the two hybrids (H = 0.009, p = 0.921). Fifty percent reduction in stomatal conductance in *GC* was seen at 0.14 ± 0.07 m^3m^{-3} and 0.16 ± 0.07 m^3m^{-3} for *UG*. There was a significant difference in the SWC at which stomatal conductance is reduced by 90 % between the two hybrids, with 90 % reduction in stomatal conductance in *GC* seen at lower SWC compared to *UG* (H = 5.503, p = 0.019). Ninety percent reduction in stomatal conductance in *GC* was seen at 0.12 ± 0.11 m^3m^{-3} and 0.16 ± 0.07 m^3m^{-3} for *UG*.

The best model for gsw response for both the control *UG* and *GC* plants included only the solar variable (*UG*: AIC model weight = 55 %; *GC*: AIC model weight = 66 %). The model of best fit describing the gsw response for both the droughted *UG* and *GC* plants included only the soil moisture variable (*UG*: AIC model weight = 100 %; *GC*: AIC model weight = 66 %).

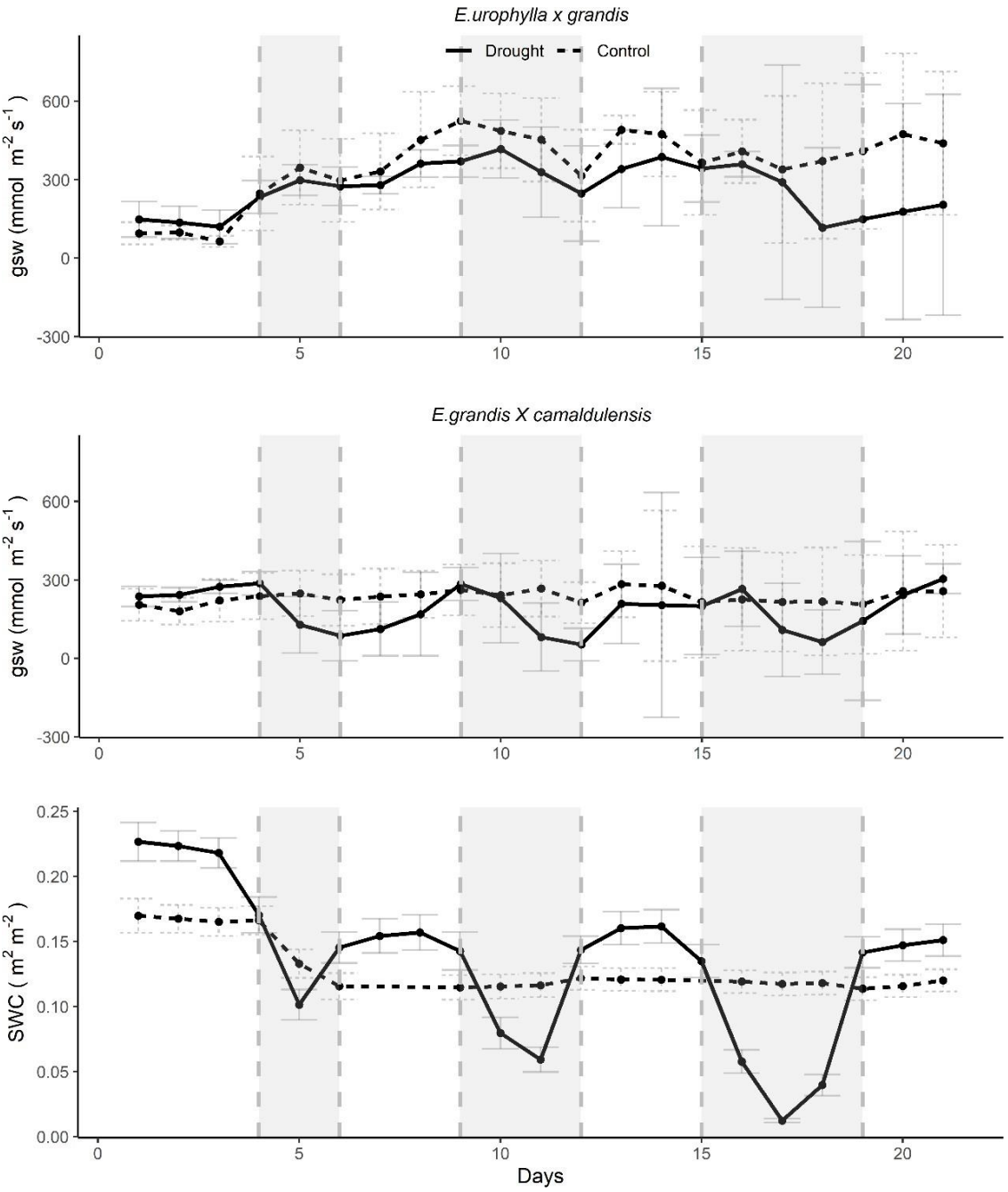

Figure 5.2 Stomatal conductance measurements for *E. urophylla X grandis* (top) and *E. grandis X camaldulensis* (bottom) of plants in the control group that received continuous watering (Control) and plants that were subjected to a cyclic-drought treatment (Drought). The volumetric soil moisture content for the experimental period is also given (bottom). The dashed grey lines indicate the periods of a droughting events. Means with 95% confidence intervals are given.

Production and photosynthetic response to drought

There was a significant difference in the cumulative increase in stem diameter between the droughted and controlled plants for *GC*, with the stem diameter increasing more in the control group (H = 5.83, p = 0.02). There was no significant difference seen between the cumulative increase in stem diameter for *UG* (H = 0.15, p = 0.22) (Figure 5.3).

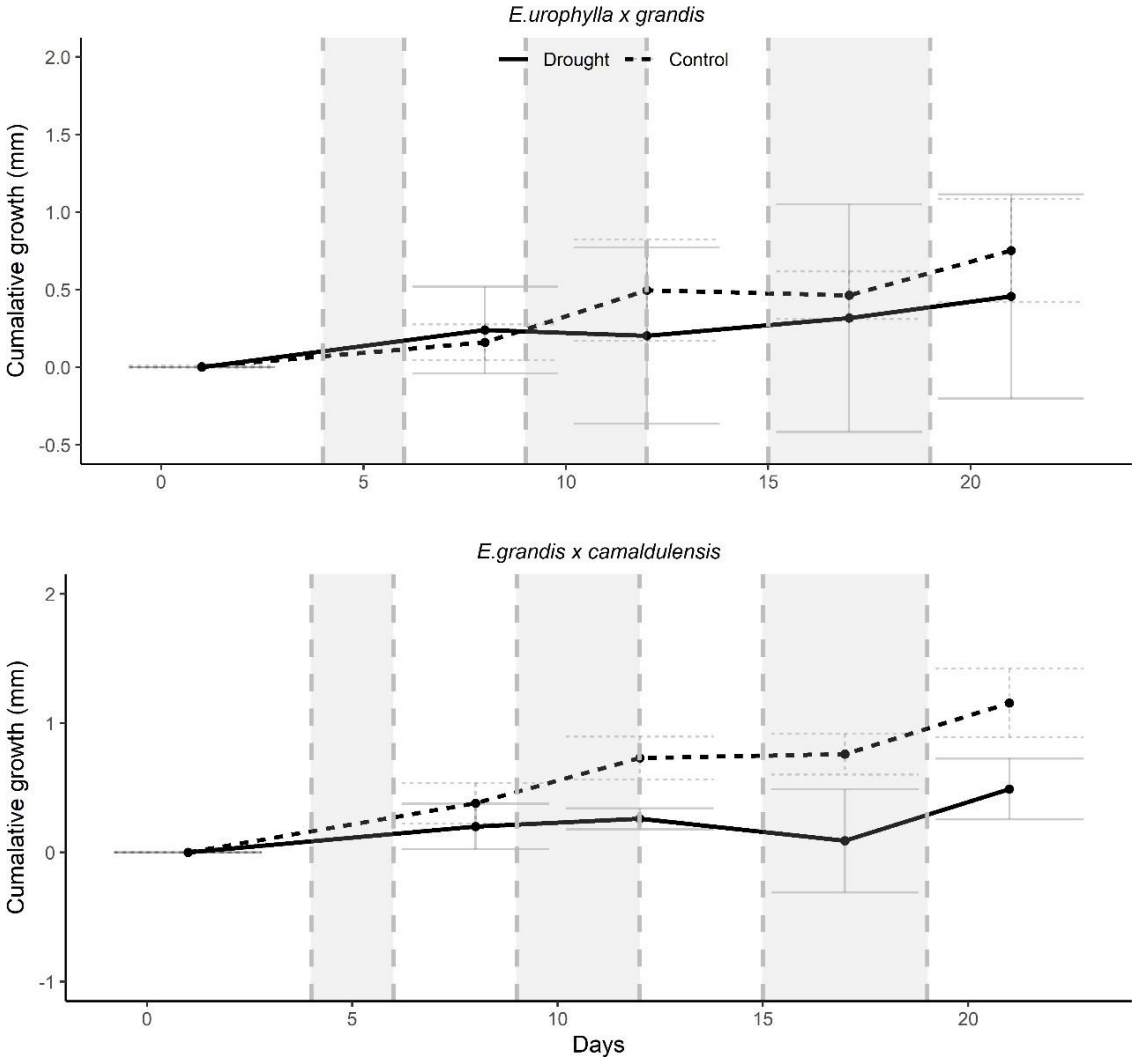

Figure 5.3 Cumulative growth for *E. urophylla X grandis* (top) and *E. grandis X camaldulensis* (bottom) of plants in the control group that received continuous watering (Control) and plants that were subjected to a cyclic-drought treatment (Drought). Means and standard deviation are given.

There was a significant difference in the dried leaf weight ratios between the droughted and control plants for *GC*, with a significant reduction in relative leaf to stem weight seen in the droughted plants (H = 3.86, p = 0.049) (Figure 5.4). While there was some reduction in dried leaf weight ratios between droughted and control plants for *UG*, the difference was not significant (H = 2.33, p =

0.13). There were no differences in dried root weight ratios between the droughted and control plants for *GC* (H = 0.05, p = 0.83). There was, however, a significant difference in the dried root weight ratios between the droughted and control plants for *UG*, with a significant increase in relative root to stem weight seen in the droughted plants (H = 3.86, p < 0.049) (Figure 5.4).

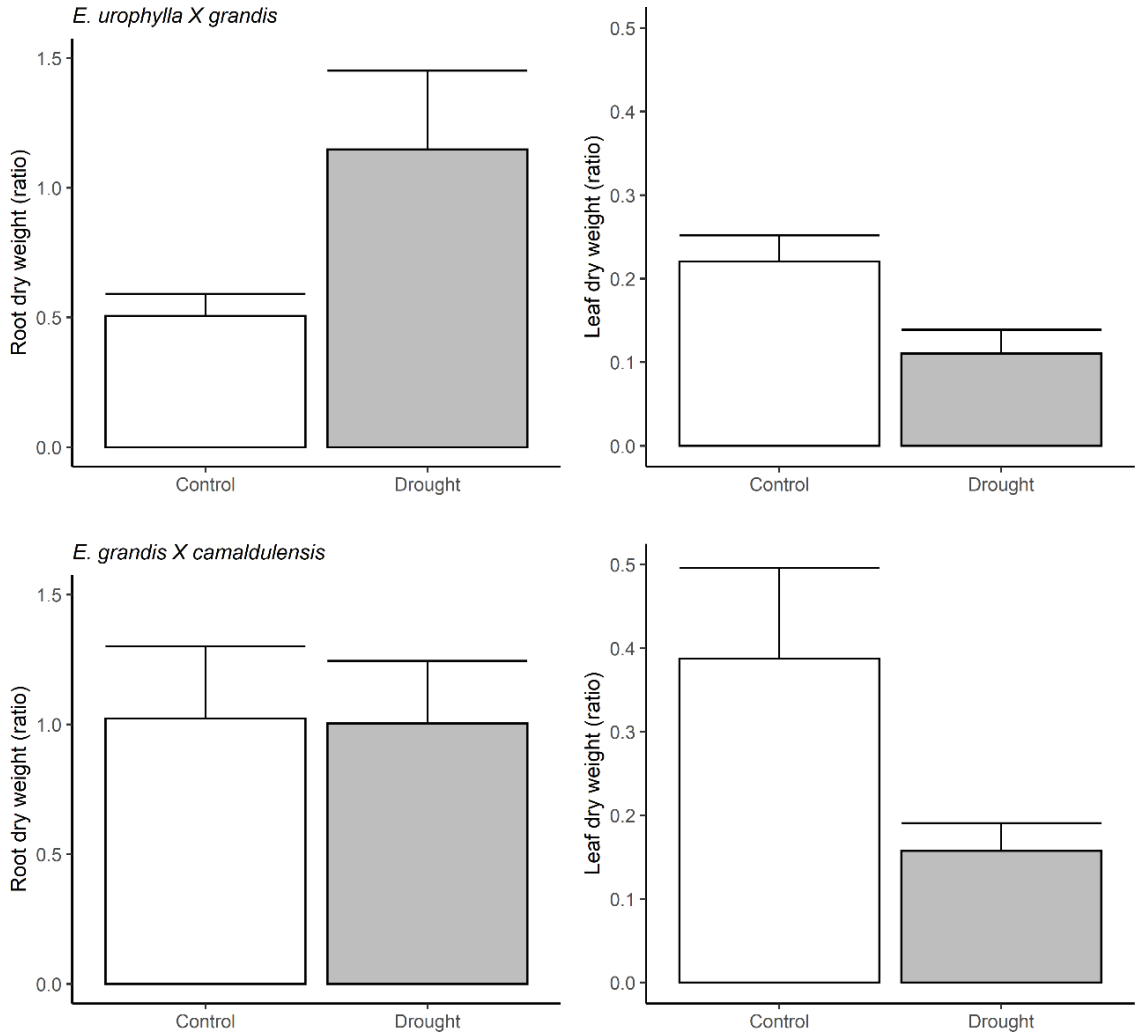

Figure 5.4 The dried root-stem ratio and the dried leaf-weight ratio for *E. urophylla X grandis* (top row) and *E. grandis X camaldulensis* (bottom row) plants of the control treatment (Control) and cyclic drought-recovery treatment (Drought). Mean and standard errors given.

Discussion

Water-use strategies during drought

Stomatal responses regulate the water use and balance of plants during drought, with differences in these responses being a major determinant of the plant's water use strategy (Mitchell et al. 2013). We observed two distinct water-use strategies between the two *Eucalyptus* hybrids based on their stomatal responses during drought (Figure 5.5). *E. urophylla X grandis* maintained stomatal conductance and gas exchange during drought (maintaining growth, and risking hydraulic failure),

while *E. grandis X camaldulensis* tightly regulated stomatal conductance in response to drought (reducing water loss, and risking carbon starvation) (McDowell et al. 2008, Martínez-Vilalta and Garcia-Forner 2017).

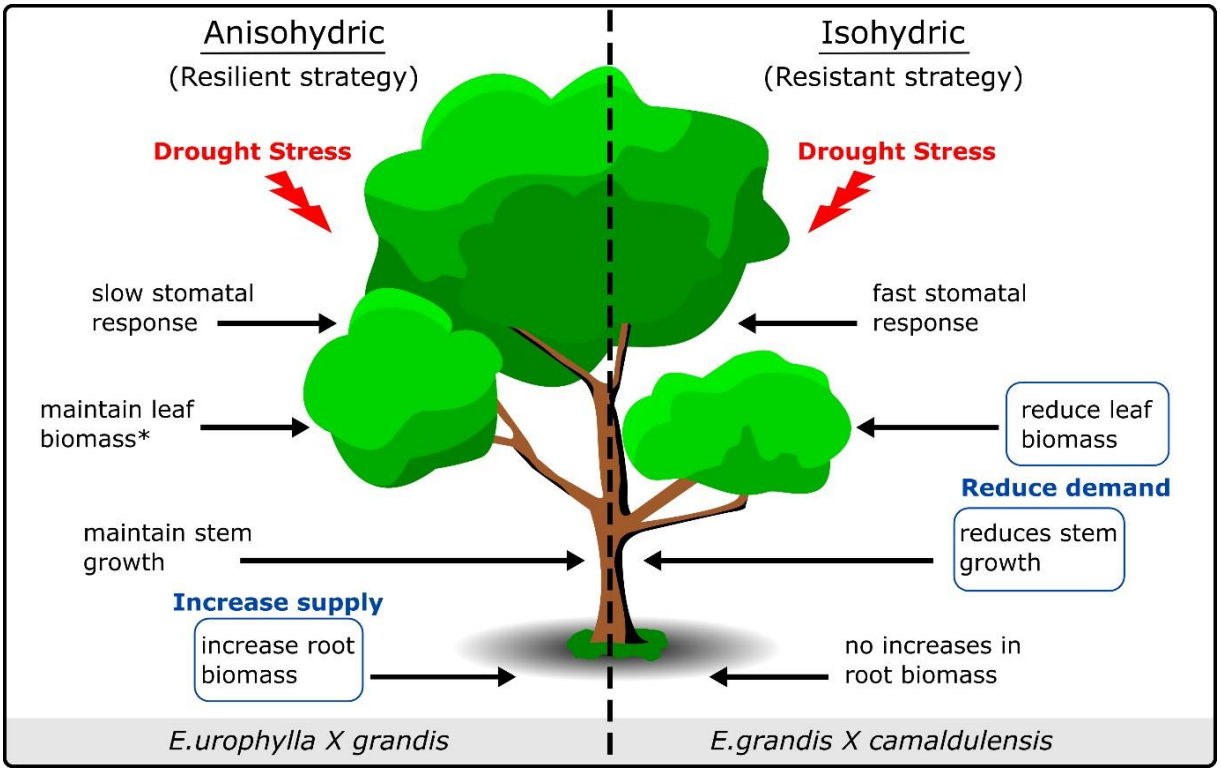

Figure 5.5 Schematic representation of the two distinct responses to drought observed between two Eucalyptus hybrids: *E. grandis X camaldulensis* and *E. urophylla X grandis*. *reductions in leaf biomass was seen, however it was not significant

In trying to understand these differences, it is useful to consider these stomatal responses as the balance of a trade-off between water loss and carbon gain (McDowell et al. 2008). The question arises as to where the two varieties lie on a spectrum between so-called anisohydric and isohydric strategies (Martínez-Vilalta and Garcia-Forner 2017). Isohydric plants will close stomata earlier in response to drought, thereby limiting water use, but also reducing carbon assimilation. Anisohydric plants, on the other hand, will maintain stomatal conductance during drought, maximising carbon assimilation, but running the risk of hydraulic failure (McDowell et al. 2008, Martínez-Vilalta and Garcia-Forner 2017). Previous studies have shown that *E. urophylla* exhibits certain anisohydric traits (Zhang et al. 2016) while *E. camaldulensis* is more isohydric (Nolan et al. 2017). This is in line with the findings we have presented for responses in the *UG* and *GC* hybrids.

The *GC* strategy can be considered more ‘resistant’, with conservative growth patterns and tight stomatal regulation in response to drought (Figure 5.5). A resistant strategy can be beneficial during

short drought periods, protecting against loss of conductive vessels to embolism. It can, however, hinder recovery after drought due to carbon starvation (Mitchell et al. 2013). This is in contrast with the 'resilient' strategy seen by *UG*, where growth is maintained, running the risk of mortality due to hydraulic failure if drought periods persist. A resilient strategy can however aid recovery after drought since the needed carbohydrate reserves will be maintained (Mitchell et al. 2013). In line with this finding, *UG* has been shown to have a good water use efficiency compared with other *Eucalyptus* species, with some studies suggesting that moderate drought might even favor *UG* hybrids (Maseyk et al. 2011, Otto et al. 2014, Zhang et al. 2016). The underlying mechanism for this is, however, still not clear and needs further investigation.

Drought resistance, embolism resistance and stomatal regulation

During this study two distinct hydraulic strategies were seen between the two *Eucalyptus* hybrids, with *UG* known to be more vulnerable compared to the embolism-resistant hybrid *GC* (Van der Willigen and Pammenter 1998, Drew et al. 2009, Saadaoui et al. 2017). The embolism-resistance seen in the *GC* hybrid was accompanied by sensitive stomatal regulation, with stomatal conductance decreasing markedly with decreases in soil moisture (Figure 5.5). These stomatal trends are similar to what was described by Nolan et al. (2017), where they found a steady decrease in stomatal conductance in response to drought in *E. camaldulensis*. They related this decrease in stomatal conductance during drought to an increase in abscisic acid (ABA) concentrations in the leaves, which controls stomatal conductance in isohydric species (Nolan et al. 2017). This was however not seen in *UG*, with stomatal conductance staying stable throughout the droughting events, despite *UG* being considered to be more vulnerable to embolism than *GC* (Saadaoui et al. 2017). This is in contrast with other studies that suggest stomatal closure will be delayed in plants that are more resistant to embolism formation, to allow for longer periods of photosynthesis and carbon assimilation during drought (Cruiziat et al., 2002; Tyree & Sperry, 1988).

P50 values derived from vulnerability curves have previously been related to drought resistance (Martin-StPaul et al. 2017), with studies proposing that embolism-resistant plants will be able to photosynthesize longer during drought, since reducing stomatal conductance is not as critical to prevent hydraulic failure (Cruiziat et al., 2002; Tyree & Sperry, 1988). It has been suggested that drought-driven mortality is not due to desiccation, but rather hydraulic failure, which reduces assimilation and carbon metabolism within plants (McDowell et al., 2008; Sala et al., 2012; Sevanto et al., 2014). Reductions in hydraulic conductance reduce assimilation rates within plants due in part to the need for a sufficient water supply for transport of metabolites. Trees can however recover hydraulic conductance through regrowth, given sufficient carbohydrate reserves (Brodersen

and McElrone 2013, Buckley 2017, Anderegg et al. 2018). In research done on *Eucalyptus* hybrids including *GC* and *UG*, increases in wood formation with distinctive hydraulic properties have been seen after drought (Drew and Downes 2009, Drew et al. 2009, 2011, Câmara et al. 2021). Recovery through regrowth post-drought is however carbon-intensive, with reductions in carbon uptake during and after drought being attributed as the cause of the drought-driven tree mortality due to carbon 'starvation' (Trugman, Detto, et al. 2018).

It can be proposed that a preferred strategy for trees experiencing drought would therefore minimise losses in hydraulic conductance due to embolism formation, if the carbon cost of regrowth after drought might be too severe (Trugman, Detto, et al. 2018). During this study, a decrease in stomatal conductance was seen in the more drought- and embolism-resistant hybrid, *GC*. Stomatal control not only regulates water loss, but also carbon uptake (Flexas and Medrano 2002) and stomatal closure is one of the main limitations of photosynthesis, metabolism and ultimately plant growth (Kramer and Boyer 1995, Becker et al. 2000, Flexas and Medrano 2002, McDowell et al. 2008, Anderegg et al. 2015, Trugman et al. 2018a, Trugman et al. 2008b). Stomatal regulation, therefore, is a trade-off between carbon gain and water loss (Xiong and Nadal 2020), which has led to the idea that stomatal conductance tends to operate close to hydraulic failure thresholds (Cruiziat et al., 2002; Tyree & Sperry, 1988). In contrast to this view, in *GC* we show an example of a strategy where a hybrid with a high hydraulic failure threshold (high embolism resistance) simultaneously demonstrates conservative stomatal regulation, while in *UG* we have a hybrid with a lower hydraulic failure threshold (lower embolism resistance) which shows little stomatal regulation in response to drought. This trend gives further support that drought resistance is not only related to embolism resistance, but also to timely stomatal closure (Bartlett et al. 2016, Martin-StPaul et al. 2017).

Recent work that suggests that *UG* may be able to partially recover the function of embolised vessels may provide some explanation for the paradoxical observations in the latter case, as they suggest that *UG* is able to recover without being entirely reliant on carbon-intensive regrowth (Saunders and Drew 2021). A more conservative stomatal regulation response to decreases in soil moisture can therefore be expected of plants with a more costly recovery method (Lu et al. 2020).

The hydraulic system and stomatal conductance is closely linked, with the hydraulic system ensuring sufficient water supply to leaves, while stomata regulate the demand (Tardieu and Davies 1993, Ding et al. 2020). Embolism resistance and stomatal regulation are two key plant traits coupled to drought-resistance of plants (Choat et al. 2012), but there remains a lack of

understanding as to how these traits interact and changes with relation to each other, especially on a global scale (Mcdowell et al. 2013). Our study has highlighted and characterised the quite distinct hydraulic strategies utilised by *GC* and *UG*.

Embolism resistance and hydraulic properties

Embolism resistance has been previously connected to vessel length and vessel area (Lens et al. 2011), with larger vessels being more efficient, although with a decrease in safety (Hacke et al. 2006, Lobo et al. 2018). In this study, smaller vessel average area was seen in *GC*, which was found to be less vulnerable to embolism. The hybrid *UG* had larger vessels and was more vulnerable to embolism formation. Larger vessels seen in *UG* in this study were also associated with increased hydraulic conductance. This trade-off between vessel safety and efficiency has been found in other studies (Gleason et al. 2016), however Fernández et al. (2019) found that non-vessel cells surrounding vessels can help improve the safety of vessels regardless of vessel size. It has been proposed that plants can also change their hydraulic properties through growth in responses to drought (Tng et al. 2018). Increases in vessel area have been seen in both *E. grandis* and *E. grandis X camaldulensis* in response after drought periods when water availability increased, with the authors suggesting that this was to improve water uptake due to increased demands (transpiration) (February et al. 1995). In previous studies, increased vessel area has also been correlated to increases in hydraulic conductance and efficiency for *E. urophylla* (Zhang et al. 2016).

Drought resistance and biomass partitioning

To prevent starvation due to reductions in hydraulic conductance following drought, trees can also deploy other strategies to reallocate carbon resources adaptively (Trugman, Detto, et al. 2018), including reducing the water demand by reducing leaf area (by shedding leaves), or increasing root biomass in order to increase the supply of water (Mokany et al. 2003, Manzoni et al. 2015). There were significant reductions in leaf mass seen during drought for *GC*, which was not the case in *UG*. This trend was observed in previous studies as well, where an increase in root to shoot ratios was seen during drought for *E. camaldulensis*. These increases were however attributed to leaf shedding as a result of increases in ABA concentrations seen in the canopy (Nolan et al. 2017). During this study both hybrids deployed different strategies of biomass allocation in response to drought, with *GC* decreasing leaf biomass (demand) while *UG* increased root biomass (supply) (Figure 5.5).

Plants subjected to drought stress have been shown to increase root biomass while maintaining leaf biomass, which can help recovery post-drought (Poorter et al. 2012). During this study only *UG* was seen to significantly increase root biomass, highlighting that this response might be considered

as an extension of the anisohydric strategy (in contrast to the isohydric *GC*, which showed no change in root biomass). Changes in biomass allocation have been seen in species that are not adapted to variable soil moisture, with species adapted to variable soil moisture maintaining their root to shoot ratios during drought (Poorter et al. 2012).

Maintaining leaf biomass can help ensure enough carbon uptake for regrowth of lost hydraulic pathways post-drought (Anderegg, Plavcová, et al. 2013). During this study the stem growth rate decreased in *GC* during drought, while the droughted *UG* plantsmaintained stem growth, highlighting the likely carbon allocation to repair hydraulic pathways in *UG*. In a study done by Mitchell et al. (2013), it was also shown that reduced stem growth decreases the carbon demand for species that have a conservative water-use strategy. During this study, plants were subjected to cyclic droughting events over short time periods. Carbon allocated to leaves during drought would only put a plant in a positive carbon balance if soil moisture were restored relatively soon. During prolonged droughts, this strategy would increase xylem tension reducing carbon assimilation even further (Anderegg et al. 2012). Carbon allocation strategies employed by plants during drought, can therefore explain post-drought tree mortality or, alternatively, recovery (Trugman, Detto, et al. 2018)

Conclusion

During this study two different strategies in response to drought were observed between *GC* and *UG*. Although *GC* was more resistant to embolism formation, reductions in stomatal conductance were more marked in response to drought compared to *UG*. The contrasting stomatal responses seen could be related to the anisohydric behavior of *UG* and isohydric behavior of *GC* (Zhang et al. 2016, Nolan et al. 2017). This study shows that drought resistance is not only related to embolism resistance in *Eucalyptus* hybrids, but also related to timely stomatal closure in response to drought. This study further highlights the difference in biomass allocation seen during drought between the two hybrids, with *GC* reducing leaf biomass and therefore reducing water demand, while *UG* increased root biomass (increasing the supply of water), further accentuating the respective difference between isohydric and anisohydric responses.

Carbon allocation and hydraulic traits are connected to the drought-resistance of plants and can have a significant effect on post-drought recovery. Stomatal regulation helps balance between water loss and carbon gain, influencing carbon allocation and growth, as well as hydraulic conductance and water supply. Differing stomatal regulation strategies used by plants in response to drought can have a significant impact on ecosystem scale patterns of carbon and hydrological cycles (Nolan et

al. 2017). Increases in droughting events due to climate change is predicted (Pachauri et al. 2014). It is predicted that anisohydric species will be more productive during increased periods of drought, however, increases in tree mortality due to hydraulic failure might be expected during periods of prolonged droughts (Roman et al. 2015), compared to isohydric species. Understanding how isohydric and anisohydric species respond to drought is important to model productivity in response to climate change, especially in commercially significant hardwoods like *Eucalyptus*.

Chapter 6

Machine learning models perform better than traditional empirical models for stomatal conductance when applied to multiple tree species across different forest biomes

Published in *Trees, Forest & People* on 10 September 2021 (doi.org/10.1016/j.tfp.2021.100139)

Trees, Forests and People 6 (2021) 100139

Contents lists available at ScienceDirect

Trees, Forests and People

journal homepage: www.sciencedirect.com/journal/trees-forests-and-people

Machine learning models perform better than traditional empirical models for stomatal conductance when applied to multiple tree species across different forest biomes

Alta Saunders [a], David M. Drew [a], Willie Brink [b]

[a] Department of Forest and Wood Science, Stellenbosch University, Private Bag X1, Stellenbosch South Africa
[b] Department of Mathematical Sciences, Stellenbosch University, Private Bag X1, Stellenbosch South Africa

ARTICLE INFO

Keywords:
Stomatal conductance
Machine learning
Climate data

ABSTRACT

Stomatal closure decreases water loss and is one of the main mechanisms that trees can use to mitigate drought-induced physiological stress. The adaptability of trees to drought is likely to be of increasing importance as climate changes occur around the world. Modelling stomatal regulation can help improve our understanding of how forests respond to their environment. Traditionally, empirical models have been used to model stomatal responses, however these models cannot always capture nonlinear responses and their parameters are often difficult to measure. In this study various machine learning (ML) models were able to capture stomatal responses of multiple tree species. We showed that ML can be a useful tool for predicting stomatal response based on climate variables and species traits. A random forest model performed the best with an R^2 of 75 %, compared to the empirical Ball-Berry stomatal conductance model (BWB) (R^2 = 41 %). In this study, the use of a combined dataset consisting out of data from multiple studies were successfully used, showcasing the use of data across studies. This also allowed for an ML model to be trained on 36 tree species from 5 forest biomes, from measurements taken across 6 continents, instead of being limited to one species, increasing the versatility of the model. The importance of species-specific stomatal responses was highlighted, with the drought strategies used by plants significantly influencing stomatal responses and predictions. ML models were able to capture these trends parsimoniously without prior knowledge of the underlying physiology of the tree species. The quality of combined datasets are however still not desirable, and long-term data collection using standardized measuring protocols are required to increase the strength of ML models. Data taken across different climatic regions and vegetation types can also help improve the adaptability of ML models. Regardless of limitations on data accessibility, ML shows promise in modelling plant responses to changes in climate. Focus on the use of ML together with traditional models can help give further insight into various ecological mechanisms.

1. Introduction

Greater evaporative demand due to increasing temperature, in concert with decreased soil water availability during more frequent or intensive droughts (Pachauri and Mayer, 2014) will increase tree stress and can ultimately be expected to reduce forest productivity (Anderegg et al., 2013; Park Williams et al., 2013). In order to properly predict these changes, accurate models of plant responses to water limitations and other environmental changes are therefore becoming increasingly important for effective forest management (Chen et al., 2020).

Stomatal closure is one of the main mechanisms that plants use to mitigate drought-induced physiological stress (Buckley, 2017; Silva et al., 2004; Sperry et al., 2002). Stomatal closure, however, also decreases CO_2 uptake and reduces photosynthetic productivity (Xiong and Nadal, 2020). Stomatal regulation can play an important role in how plants respond to environmental stress, with stomatal closure often being used as an indication of plant stress during drought (Blonquist et al., 2009; Martin-StPaul et al., 2017). Modelling stomatal regulation can help improve our understanding of how trees and forests respond to their environment, especially as stomata are sensitive to many environmental parameters (Damour et al., 2010).

Traditionally, empirical models, such as the Ball-Berry (BWB) model, have been used to model stomatal conductance (gsw), however these models are limited to prior experimental work focussing on how plants

E-mail addresses: drew@sun.ac.za (D.M. Drew), wbrink@sun.ac.za (W. Brink).

https://doi.org/10.1016/j.tfp.2021.100139
Received 14 July 2021; Received in revised form 3 September 2021; Accepted 6 September 2021
Available online 10 September 2021

would respond to different environmental variables (Ball et al., 1987; Jarvis, 1976; Macfarlane et al., 2004; Monteith, 1995). Parameters used in empirical models are also difficult to quantify, as they are determined through regression analysis or curve fitting on existing datasets and cannot be directly measured (Hastie et al., 2001). These models, therefore, run the risk of not fully capturing stomatal responses when used for datasets where the parameterization domain changed; for example measurements in different climatic conditions, compared to the datasets on which these models were developed (Jung et al., 2001; Powell et al., 2013; Trugman et al., 2018). Empirical models also struggle to capture responses when multiple factors are included (Chen et al., 2020; Damour et al., 2010). Besides empirical models, process-based approaches have also been proposed to model stomatal responses, as the parameters used are related to plant traits (Sperry et al., 2017). Process-based models are, however, still not widely used as many of the parameters are difficult to measure and not widely available for many species (Choat et al., 2012; Sabot et al., 2020).

An important development in predicting plant responses over the last few years has been the increasing use of machine learning (ML) approaches (Chen et al., 2020; Johnson et al., 2016; Kurz et al., 2009; Liu et al., 2018; Pan et al., 2020; Papalem and Valentini, 2003; Périé and de Blois, 2016; van Klompenburg et al., 2020). ML models have been widely shown to improve predictions, especially when multiple environmental factors are included (Elavarasan and Vincent, 2020; Ellsäßer et al., 2020; Houshmandfar et al., 2021; Liu et al., 2018; Silva et al., 2019; van Klompenburg et al., 2020; Vitrack-Tamam et al., 2020). In forest science, the use of ML models has also been increasing as they are more adaptable than traditional approaches and can assist with making more rapid decisions in forest management (Liu et al., 2018). For example, ML models have been used to predict species distribution in response to changes in climate (Benito Garzón et al., 2008; Périé and de Blois, 2016; Vaca et al., 2011) and to model carbon cycles (Kurz et al., 2009; Papalem and Valentini, 2003; Tramontana et al., 2016, 2015), with ML working well even when combined with process-based models (Shoemaker and Cropper, 2010).

ML is, however, still not widely used to model fine-scale physiological processes like transpiration rate and stomatal response to environmental shifts (Ellsäßer et al., 2020; Houshmandfar et al., 2021; Liu et al., 2018; Pan et al., 2020; Vitrack-Tamam et al., 2020). One of the main limitations to applying ML to these problems is the availability of suitable datasets for training (Silva et al., 2019). This problem was highlighted in recent studies where ML was used to model gsw only on cotton and palm trees (Ellsäßer et al., 2020; Vitrack-Tamam et al., 2020) which significantly reduced the versatility of these models to predict stomatal responses outside of the two tested regions and plant species. Furthermore, Elläßer et al. (2020) struggled with prediction accuracy, relating it back to insufficient datasets containing concurrent gsw measurements and remotely sensed spectral and meteorological measurements.

There is also limited information available regarding how ML models compare to traditional models of stomatal conductance such as the Ball-Berry model, especially when more than one plant species is included. Previous ML models also focussed on training individual models for individual species, rather than aiming for one model that learns from the data of many different species (Ellsäßer et al., 2020; Houshmandfar et al., 2021; Liu et al., 2018; Pan et al., 2020; Vitrack-Tamam et al., 2020). There is wide variability between plant physiological traits, which can significantly influence how different species respond to environmental changes. For that reason it is important to develop models over a wide range of species and plant functional types (Smith and Dukes, 2013).

In light of these issues, we report here the results of a study that aimed to develop a global model for predicting stomatal responses of multiple tree species across various forest biomes. The aim of the research was to (1) evaluate the use of various ML models to predict stomatal responses of multiple tree species, (2) compare the performance of ML model predictions to the empirical Ball-Berry model for stomatal conductance (Ball et al., 1987) and (3) evaluate the use of compiled datasets of gsw measurements from different studies.

2. Methods

Described here is the dataset used, variable selection, training, and testing of models as well as the approach for assessing model accuracy (Fig. 1).

2.1. Stomatal conductance measurements and datasets

Existing datasets of stomatal conductance (gsw: mol m^{-2} s^{-1}) measurements with concurrent measurements of various environmental parameters were used for this study. These datasets were identified in the review by Anderegg et al. (2018), and are accessible via the "Figshare Repository" with DOI 10.6084/39.figshre.6066449 (Anderegg, 2018). In addition, gsw measurements from a 6-week drought-recovery study, where measurements were taken for *E. grandis X camaldulensis* and *E. urophylla X grandis* were included (Saunders et al., unpublished data). Access to the complete gsw dataset including code for model development can be found at https://github.com/altazietsman/ML-stomatal-conductance-models.git. The overall compiled dataset consists out of 4202 measurements across 36 different species (Table 1).

2.2 Data analysis

The use in our study of a combined datasets from multiple studies allowed for a ML model that was trained on 36 different species, across 5 forest biomes and 6 continents (Fig. 2) representing a wide range of environmental conditions.

The first step during model development was selecting appropriate predictor variables, with one of the main limitations being the availability of data. All data used in this study were compiled from a literature search done by Anderegg et al. (2018), with the exception being data for *E. grandis X camaldulensis* and *E. urophylla X grandis*. Since data came from various studies that used different experimental designs, environmental variables that were the most common across all the datasets were used as predictor variables. These variables included incoming solar irradiation (Solar: W/m^2), volumetric soil water content (SWC: m^3/m^3) and the vapour pressure deficit (VPD: kPa) (Fig. 3). Limited information regarding plant physiological traits was available for the species in the compiled dataset. It was therefore decided to include species names as the only categorical variable (Table 1). Missing values seen in the SWC measurements were replaced with soil water content values calculated based on the predawn leaf water potential as calculated using the van Genuchten model (van Genuchten, 1980). Missing values were not seen in any of the other parameters.

Dummy variable encoding was used to transform the species names into binary variables. Every species name was encoded to an (n-1)-dimensional binary feature vector, where n is the number of species. Outliers with a z-score (how many standard deviations a data observation is from the mean) of more than 3 was removed from the dataset.

All predictor variables were standardized before model development. Data were randomly split into a training and testing dataset with a ratio of 80:20 (80 % of data used for training and 20 % of data used for testing). Various ML models were trained on the compiled dataset with gsw as the main output and environmental variables and species names used as the predictor variables.

2.3. Models

Focus was given to test some of the most used models for predicting plant responses to environmental variables seen within the literature. These included Random Forest models (RF) since this model is often used in other studies and the model does not make any assumptions regarding the relationship between dependent and independent

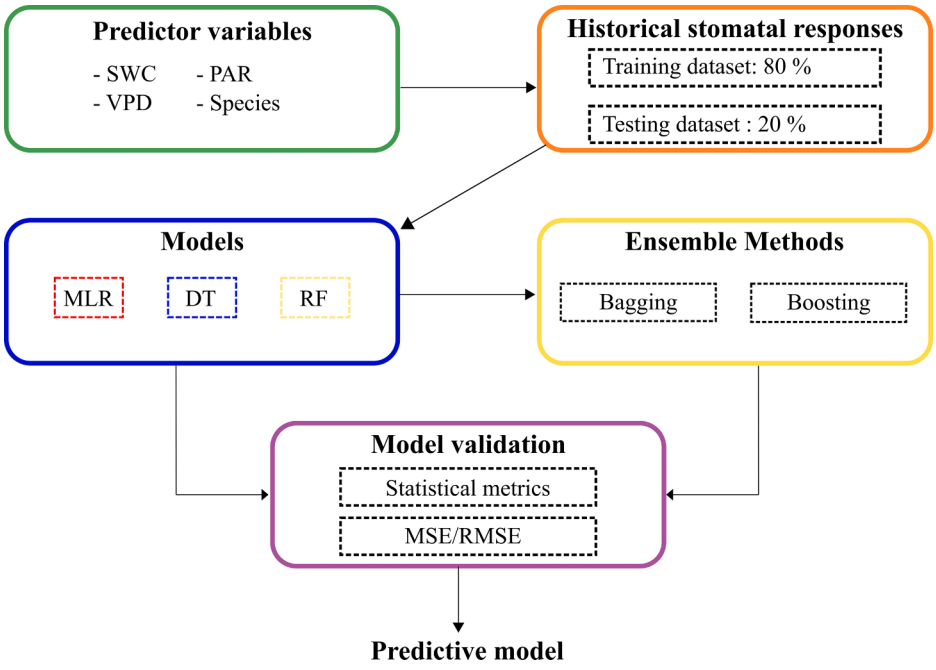

Fig. 1. Modelling flowchart for predicting stomatal response to environmental variables. The environmental variables used as predictor variables include vapour pressure deficit (VPD), volumetric soil water content (SWC) and incoming solar irradiation (Solar). Species names were included as the only categorical predictor variable. The following models were trained and tested: multiple linear regression (MLR), decision trees (DT) and random forest (RF). Bagging (bootstrap aggregating) and boosting were used as ensemble methods. Models were evaluated using root mean square error (RMSE) and statistical metrics.

variables or the distribution patterns of data (Breiman, 2001). A Decision Tree (DT) was also tested since random forest models are ensembles of decision trees. Multiple Linear Regression (MLR) was used as the baseline model to compare all other ML models to. The same training dataset was used for all models with no additional data processing taking place.

We constructed 3 machine learning models to predict gsw. The gsw data was randomly split into a training and testing dataset with a ratio of 80:20 (80 % of data used for training and 20 % of data used for testing). The following machine learning models were constructed on the training data using 5-fold cross-validation: MLR, DT and RF. For the DT and RF model no restriction was put on the depth of trees and nodes were allowed to expand until it consisted out of one observation (also considered as pure). The default quality criterion for a data split, Gini Impurity, was used during model development (Pedregosa et al. 2011). The criterion splits observations into separate nodes by measuring the probability of incorrect classification of an observation and splitting observations to minimize that probability (Pedregosa et al., 2011). The default settings, as specified in the Scikit-learn library, were used for all other hyperparameters within the DT and RF. The number of trees in the RF models were limited to 100.

During the 5-fold cross-validation, the training data was randomly divided into 5 subsets, where random combinations of 4 subsets were used to make predictions for the 5th subset. To help reduce model variance and bias, two ensemble methods (bagging and bootstrap aggregating) were used with RF as the base model. All results were aggregated. During model development the open-source Scikit-learn library for Python was used, which allows for easy use of various ML algorithms (Pedregosa et al., 2011).

Since all species are not equally represented, which can lead to model bias, a RF model was also trained on only species that had 100+ observations within the dataset and the model performance was evaluated against the model performance when all species were included in the training set.

2.4. Empirical Ball-Berry stomatal conductance

All ML model performances were compared against the empirical Ball-Berry stomatal conductance model, which is widely used to model plant responses (Ball et al., 1987; Miner et al., 2017). Stomatal conductance could be calculated as follow:

$$gsw = g_0 + g_a \frac{A_{net} \cdot RH}{C_a}$$

where g_0 and g_a are parameters fitted to the data, A_{net} is net photosynthesis, C_a is the CO_2 concentration at leaf surface and RH is relative air humidity. If available in the dataset, photosynthesis measurements were used, otherwise photosynthesis was calculated using the biochemical photosynthetic model developed by Farquhar et al. (1980). The fitted g_0 and g_a model parameters were optimized through a grid search to minimize mean absolute error between the measured and predicted gsw on the training dataset only.

2.4. Model performance and statistical analysis

The prediction accuracy for all ML models were evaluated first during the cross-validation and then again using the independent testing dataset, which was not seen during the model training phase. Before ML model training, all predictor variables were standardized. The Ball-Berry stomatal conductance model with optimized fitted parameters was only tested once against the independent testing data.

Model predictions were compared to actual measurements within the testing dataset and evaluated using the root mean square error (RMSE). The R^2 values were also used to describe the variance seen between the predicted and measured gsw measurements. To determine how the size of the training data affected model outputs, an RF model was trained on training datasets of different sizes. The R^2 values were calculated for the RF model performance as the size of the training data increased.

The features (predictor variables) that had the most significant impact on model performance were extracted. The coefficients of the MLR model, which show the slope of the linear relationship between each predictor variable and dependent variable, were used to determine feature importance of predictor variables. The Gini impurity score, which was used to split data observations, was used to determine the feature importance of the predictor variables for DT as well as RF (Pedregosa et al., 2011). A hierarchical clustering was used to cluster stomatal observation of species in responses to environmental changes. The Euclidean distance metric was used as a measure of dissimilarity

Table 1
List of tree species included in training dataset together with the number observations within the dataset, biomes of trees, continent where measurements were made as well as the common names of trees. The biomes are as follow: Broadleaf Deciduous Temperate (BDT), Tropical Evergreen (TPE), Tropical Deciduous (TPD), Broadleaf Evergreen Temperate (BET) and Needleleaf Evergreen Temperate (NET).

Species name	Common Name	N of observations	Biomes	Continent
Acer campestre	Field Maple	41	BDT	Europe
Acer pseudoplatanus	Sycamore Maple	39	BDT	Europe
Alphitonia excelsa	Red Ash/ Soap Tree	173	TPE	Australia
Anacardium excelsum	Wild Cashew	14	TPE	North America
Annona hayesii	Hayes' Custard Apple	46	TPE	North America
Astronium graveolens	Glassywood	91	TPE	North America
Austromyrtus bidwillii	Python Tree	35	TPE	Australia
Brachychiton australis	Broad-leaved Bottle Tree	100	TPD	Australia
Bursera simaruba	Copperwood	101	TPD	North America
Carpinus betulus	European Hornbea,	48	BDT	Europe
Cavanillesia platanifolia	Bongo/ Macondo	41	TPD	North America
Cochlospermum gillivraei	Kapok	75	TPD	Australia
Cojoba rufescens	-	319	TPE	North America
Cordia alliodora	Spanish Elm	18	TPD	North America
Corylus avellana	Common Hazel	35	BDT	Europe
Eucalyptus globulus	Southern Blue gum	73	BET	Europe
Eucalyptus grandis X camaldulensis	Blue gum hybrid	252	BET	Africa
Eucalyptus urophylla X grandis	Blue gum hybrid	252	BET	Africa
Ficus insipida	-	14	TPE	North America
Fraxinus excelsior	European Ash	40	BDT	Europe
Genipa americana	Genipa	109	TPD	North America
Juniperus monosperma	One-Seed Juniper	576	NET	North America
Juniperus osteosperma	Utah Juniper	34	NET	North America
Phillyrea angustifolia	Narrow-leaved Mock Privet	17	BET	North America
Picea abies	Norway Spruce	544	NET	Europe
Pinus edulis	Colorado Pinyon	511	NET	North America
Pinus ponderosa	Ponderosa Pine	146	NET	Europe
Pistacia lentiscus	Mastic Tree	23	BET	North America
Populus balsamifora	Balsam Poplar	29	BDT	North America
Populus tremuloides	Quaking Aspen	43	BDT	North America
Prosopis velutina	Velvet mesquite	23	BDT	North America
Quercus douglasii	Blue Oak	166	BDT	North America
Quercus gambelii	Gamble Oak	12	BDT	North America
Quercus ilex	Evergreen Oak	110	BET	North America
Schefflera morototoni	Matchwood	19	TPE	North America
Tapirira guianensis	-	33	TPE	North America

between observations.

Pearson correlation was used to determine if gsw measurements were significantly correlated to any of the climate variables. This was done after data were standardized.

3. Results

3.1. Environmental predictors

3.1. Stomatal response predictions

Comparing model predictions with the independent testing dataset used for model validation, showed that all ML models performed better at predicting gsw for multiple species compared to the empirical BWB model. The R^2 for the BWB model was 41 %, compared to 77 % for the boosting ensemble model with RF used as the base learner, which was the best performing model. The output accuracy of all ML models was compared with the MLR model used as the baseline model. Model predictions were tested on an unseen testing dataset, which contained 20 % of the data observations randomly selected from the original dataset. Fig. 4 shows the predicted versus actual measurements, with a 1:1 ratio line added to better compare model predictions.

The MLR model was not able to successfully predict the stomatal responses of various plant species based on climate variables (Fig. 4). The MLR model only explained 56 % of the variance seen. A similar trend was seen with the DT model, which explained 54 % of the variance seen (Fig. 4). The RMSE values for both the MLR and DT models were 0.096 mol m^{-2} s^{-1} and 0.098 mol m^{-2} s^{-1}, respectively (Table 2).

The RF model explained 75 % of the model variance and achieved an RMSE of 0.072 mol m^{-2} s^{-1}, which decreased to 0.071 mol m^{-2} s^{-1} with the boosting ensemble model that used RF as the base learner model. Both ensemble models that used the RF model as the base learner performed well, explaining more than 75 % of the variance seen (R^2 of boosting model: 76 %, R^2 of bagging model: 75 %).

The accuracy of model predictions increased as the training data size increased. The R^2 value increased from 66 % to 79 % as the training dataset increased from 840 data observations to 3781 data observations.

When assessing model accuracy per forest biome, model predictions were more accurate for trees within the Broadleaf Deciduous Temperate, Needleleaf Evergreen Temperate and Broadleaf Evergreen Temperate biomes (R^2 = 81 %) compared to model predictions for trees in the Tropical Deciduous (R^2 = 35 %) and Tropical Evergreen biomes (R^2 = 69 %) (Fig. 5).

Since we used a compiled dataset, certain species were underrepresented during the training phase of the models. To ensure that the trained model was not biased towards species that had better representation in the dataset, an RF model was also trained on a dataset that only included species with 100 + observations. The R^2 was reduced from 75 % to 68 % when the model only included well-represented species. However, RMSE remained the same whether the training data included all species or only well-represented species (RMSE: 0.0.72).

3.3. Importance of environmental predictors

The Pearson correlation showed that there was a significant positive correlation between gsw and SWC ($r = 0.365$, $t = 25.446$, $p < 0.001$). There was a significant negative correlation between gsw and VPD ($r = -0.364$, $t = -25.323$, $p < 0.001$), as well as between gsw and Solar ($r = -0.238$, $t = -15.889$, $p < 0.001$).

In the MLR model, the most important environmental feature influencing model performance was SWC (Table 3). The top environmental feature that had the most influence on model performance for the DT and RF models was SWC (Table 3).

Eucalyptus globulus, Populus balsamifora, E. urophylla X grandis, E. grandis X camaldulensis and Q. douglassi emerged in this dataset as the top five species that had stomatal behaviour that was out of the ordinary. The Gini impurity score for these species varied from 0.045 to 0.125,

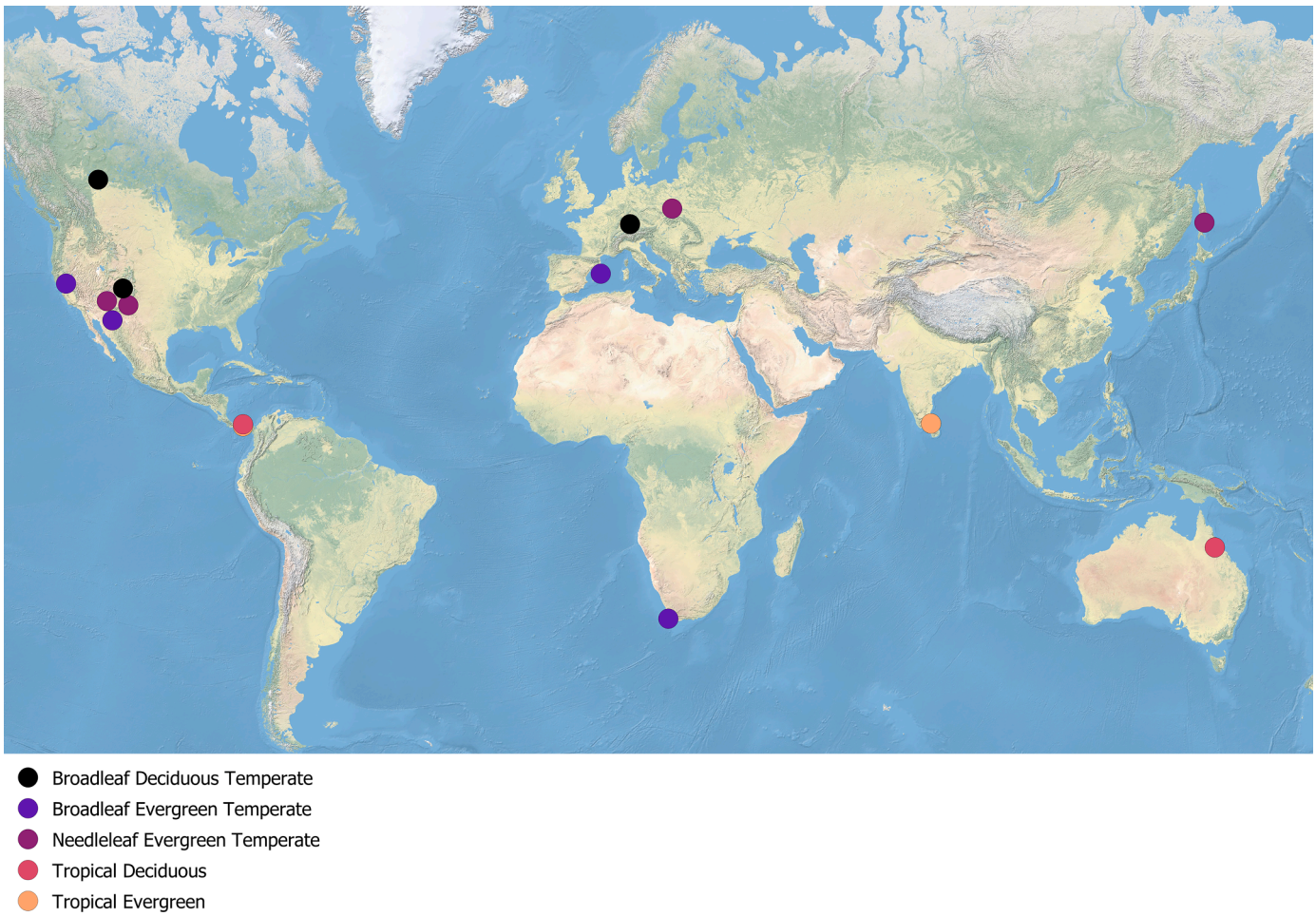

Fig. 2. A map indicating the measurement areas for all datasets used in the study. Colour codes indicate the broad forest biome/type of each tree species measured at each study site.

which highlighted the top 5 feature importance scores of all species. The importance of stomatal responses of these species were further highlighted with the hierarchical clustering, where the above-mentioned species were not clustered together with any other species, but rather clustered to their own branches. This was seen for all species, except for *E. grandis X camaldulensis* and *E. urophylla X grandis* which were clustered together on the same branch (Fig. 6). *Q. gambelii* was the only species that emerged as unique during the hierarchical cluster analysis, which did not have a high feature importance within the RF model.

4. Discussion

4.1. A global model for predicting stomatal responses

In this study we presented findings of using a set of ML models to predict stomatal conductance. These outperformed the more traditionally used empirical BWB model, even though model parameters for the BWB model were fitted to the dataset. This improvement is in all likelihood because plant responses to climate variables are not inherently linear (Alvarez, 2009; Cai et al., 2019), and ML methods are far more suited to capture these nonlinear responses (Cai et al., 2019; Kaul et al., 2005; Li et al., 2007). We were able to successfully train models to predict stomatal responses of multiple species across 5 forest biomes, instead of focussing on only one species which is far more common (Ellsäßer et al., 2020; Houshmandfar et al., 2021; Liu et al., 2018; Pan et al., 2020; Vitrack-Tamam et al., 2020). As a result, this study was able to highlight that ML can be a viable solution to predict plant responses on a global scale.

The developed model was trained on 36 different tree species from natural or managed forest biomes occurring on multiple continents and under very different conditions. The versatility of this type of model can help with improving simulations of gas exchange and carbon cycles, where empirical models are often used. The packaged model together with an example dataset is available for further testing and development and can be found at https://github.com/altazietsman/ML-stomatal-conductance-models.git.

4.2. Data availability and training: limitations and opportunities

Although ML has been shown to increase prediction accuracy, the performance of ML models is dependent on the quality of data used during training. ML models require large training datasets across different environmental conditions to adequately predict plant responses (Houshmandfar et al., 2021; Papale et al., 2015; Tramontana et al., 2015, 2016); . This has been highlighted particularly as an issue to predict stomatal responses and transpiration rates (Ellsäßer et al., 2020). Difficulties in sample size as well as the need to have concurrent gsw responses and environmental variable measurements have been highlighted as one of the main limitations (Ellsäßer et al., 2020). The use of remote sensing to gather information such as normalized difference vegetation index (NDVI), photochemical reflectance index (PRI) and infrared temperature measurements of plant canopies can give further insight into stomatal responses and help improve predictions (Blonquist et al., 2009; Panda et al., 2014).

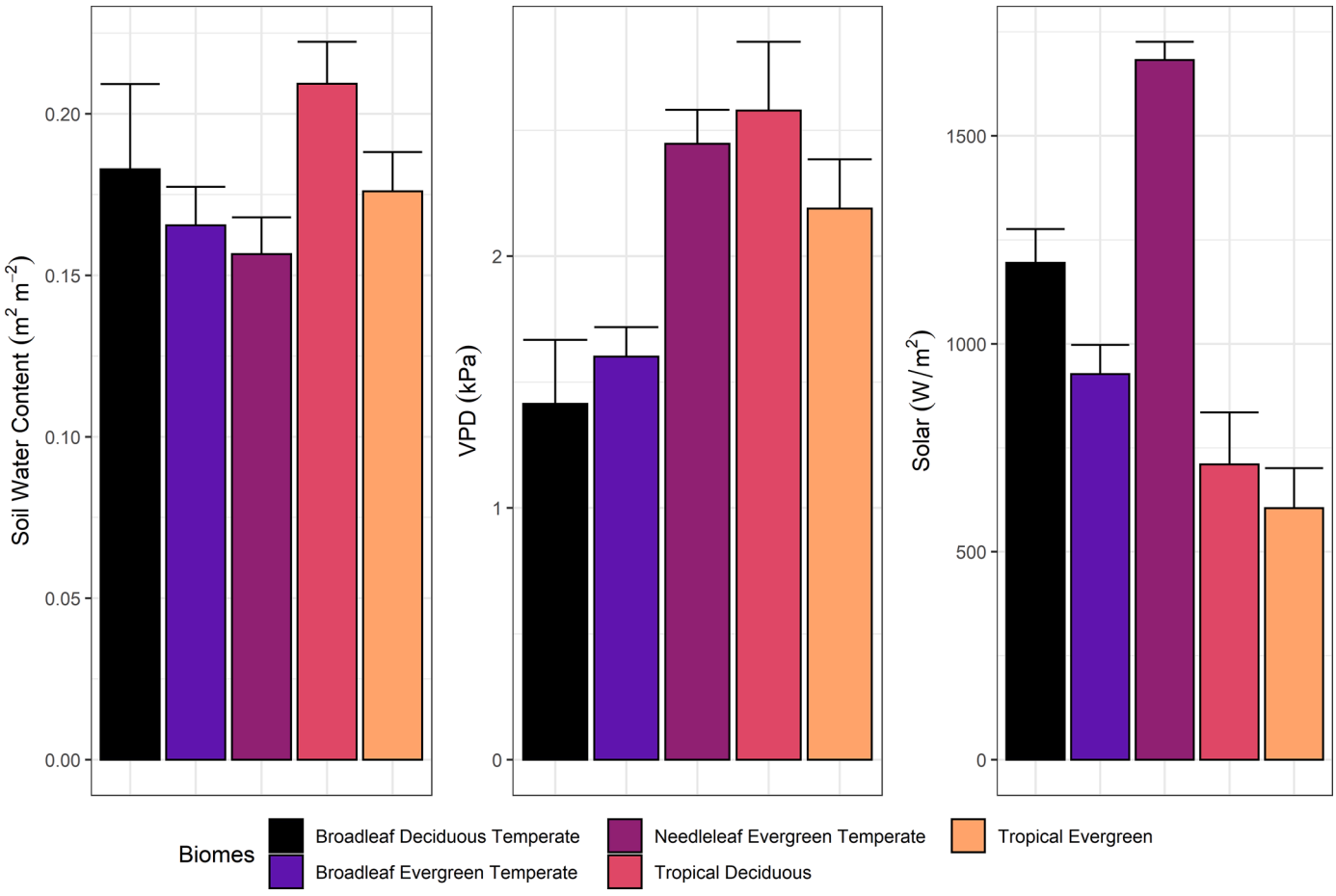

Fig. 3. Mean with 95 % confidence intervals of soil water content, vapour pressure deficit and incoming solar irradiance used as predictor variables per biome.

A study done by Papale et al. (2015) further highlighted that data from more study sites, especially across different vegetation types and climatic regions, are required to accurately predict changes in global carbon cycles. Tramontana et al. (2016) also highlighted the need to increase data collection across various regions to ensure the adaptability of ML models. Access to suitable training datasets can also be improved through the sharing of data (Liu et al., 2018). In our study, for example, we used a dataset compiled from a literature review done by Anderegg et al. (2018). This resulted in measurements from 36 different species across 5 forest biomes.

The use of combined datasets across species can however lead to class imbalance with observations not being equally distributed across all species/biomes. In that case, certain species would be underrepresented in the compiled dataset, which is the case in this study, and can lead to the trained ML model being biased towards the most represented species (He and Garcia, 2009). It has, however, been suggested that ensemble methods as used in our study, can help with this class imbalance problem (Galar et al., 2012). Although class imbalance can lead to model bias, the information gained from the underrepresented classes in the training dataset will generally still lead to prediction improvements for ML models (He and Garcia, 2009). This was evident in our study, with the ML model trained on a dataset that included all species outperforming the ML model that was trained on a dataset where only species with 100+ observations were included. The value gained by including less represented species was further highlighted with the *P. balsimifora* feature variable having one of the highest Gini impurity scores, which is used to split data at nodes within decision trees, even though it was one of the least represented species in the dataset (with only 32 observations).

Although data sharing can be an effective solution, the quality of shared data still poses many challenges. Different experimental designs and sampling rates make it difficult to compile datasets (Silva et al., 2019) with many ML models developed for single studies only (van Dijk et al., 2021). This was true in our study, with missing values for some data observations. To increase the accuracy and strength of ML models, long-term data collection is required across multiple environmental conditions using standard measurement protocols (Pieruschka and Schurr, 2019). Within the forestry sector this is often difficult due to financial constraints, limitations of equipment, or equipment failure (Liu et al., 2018). Advances in ML can, however, solve some of these problems (Dahmen et al., 2019). Synthetically creating training data, based on parametric model simulations, can potentially solve the problem of access to suitable (in terms of quantity as well as quality) datasets (Dahmen et al., 2019).

4.3. Statistical inference from ML-derived models

Another limitation is that ML models do not lend themselves to standard statistical inference, making it difficult to get reliable confidence parameters such as confidence intervals and p-values (Azodi et al., 2020; van Dijk et al., 2021). ML models often act as a 'black box', where it is difficult to understand the internal logic within the model (Azodi et al., 2020). Incorporating prior knowledge of trends or correlations into ML models are therefore challenging, limiting the use of ML as a method to build on results from previous studies (van Dijk et al., 2021).

It is also an important consideration that the use of ML models for ecological or forestry modelling remains dependent on the skill set of the user, with a level of programming experience required. The development of various tools such as the open-source Scikit-learn library developed for Python (Pedregosa et al., 2011), which was showcased in

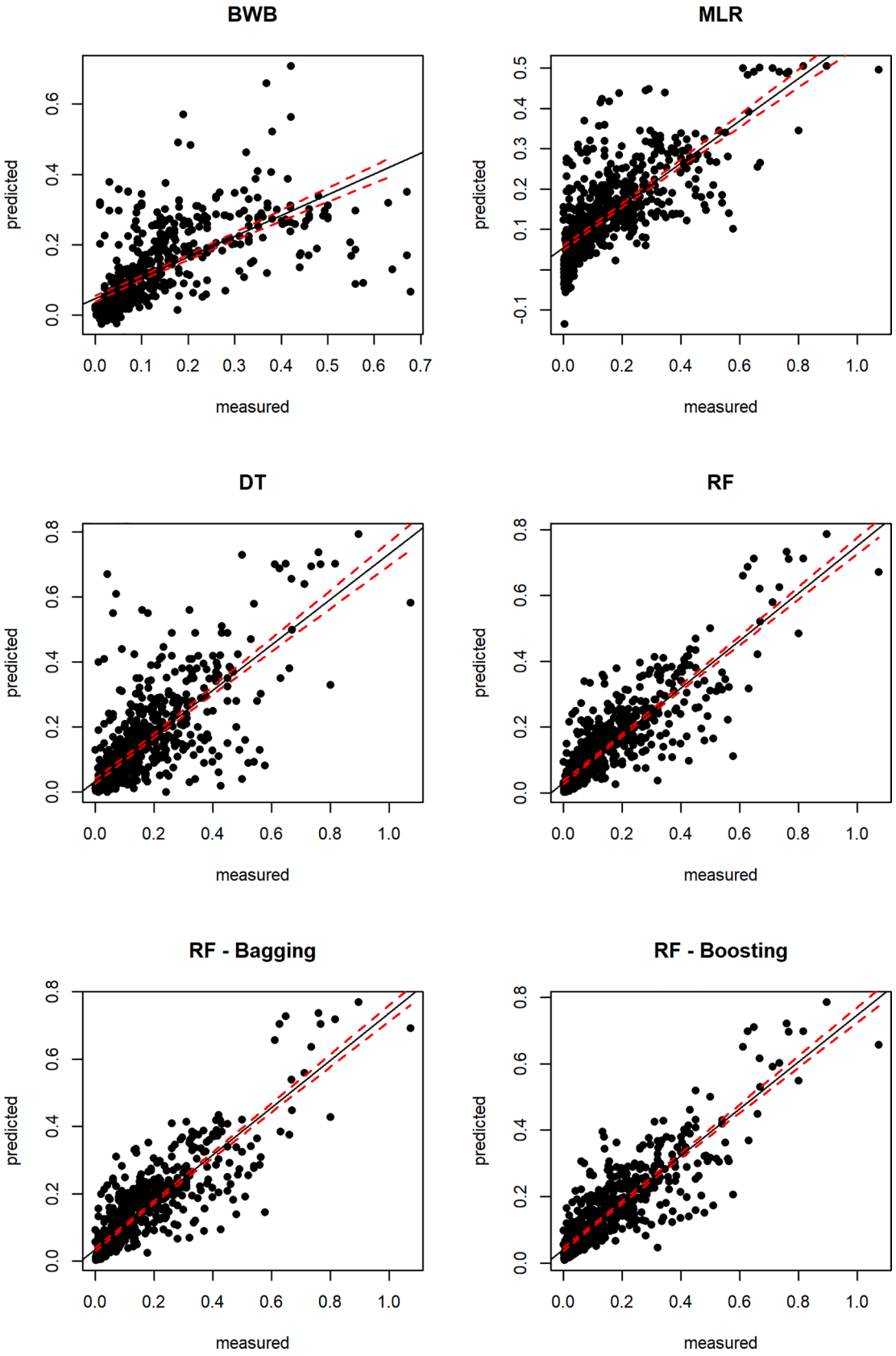

Fig. 4. Predicted versus modelled stomatal conductance (mol m^{-2} s^{-1}) for the following models Ball-Berry model (BWB): multiple linear regression (MLR), decision tree (DT), random forest (RF), bagging ensemble model with RF as base model (Bagging) and boosting ensemble model with RF as base model (Boosting). The regression slope (solid lines) and the 95% confidence intervals (dashed lines) are also included.

Table 2
Performance of model predictions for the following models: Ball-Berry model (BWB), multiple linear regression (MLR), decision tree (DT), random forest (RF), bagging ensemble model with RF as base model (Bagging) and boosting ensemble model with RF as base model (Boosting). RMSE (root mean square error) is given in model output units. R^2 between measured and predicted variables are also presented.

ML model	RMSE (mol $m^{-2}s^{-1}$)	R^2
MLR	0.096	56%
DT	0.098	54%
RF	0.072	75%
Bagging	0.073	75%
Boosting	0.071	76%
BWB	0.009	41%

our study, makes the use of ML more accessible. Programming experience as well as a certain level of mathematical proficiency is however still needed to build efficient models, debug model parameters and prevent problems like overfitting (Liu et al., 2018).

4.4. Predictor variables and differences between species

In our study only three environmental variables were used, due the access and availability of datasets across different studies which is a potential shortcoming within our model. Although the environmental variables used during model training in this study were limited, we were still able to get good model predictions for stomatal conductance.

Form these three environmental variables the most important environmental features across all ML models were SWC and VPD. This selection corresponds with other studies which used features relating to water availability (rainfall, SWC, etc.) (Kisi and Cimen, 2009; van Klompenburg et al., 2020). For gsw specifically, VPD, SWC and Solar were strongly linked to stomatal responses (Ellsäßer et al., 2020). This finding makes sense when considering that stomata are constantly trying to optimize between photosynthetic gain through carbon uptake while minimizing water loss (Xiong and Nadal, 2020). It can be argued that stomata have evolved to regulate photosynthesis as well as regulate or maintain the plant water status (Cowan and Farquhar, 1977). Temperature should however also be considered when modelling stomatal responses since it affects both photosynthesis (Schulze and Hall, 1982) as well as transpiration rates which are connected to the water status of a plant, with both processes regulated by the stomates (Urban et al., 2017). Other factors such as increased atmospheric CO_2 should also be considered in light of climate change, since reductions in stomatal regulation has been observed with increases in atmospheric CO_2 (Bunce, 2004).

Table 3
The ranking of environmental features and their significance on model development and predictions. For multiple linear regression (MLR), the coefficient (r), t-statistic (t) and p-values (p) are given. For the DT and RF models the Gini impurity score is given.

	MLR	DT	RF
1. SWC	r = 0.323, t = 20.517, p < 0.001	0.255	0.233
2. VPD	r = -0.212, t = 15.428, p < 0.001	0.169	0.231
3. Solar	r = 0.072, t = 5.711, p < 0.001	0.103	0.101

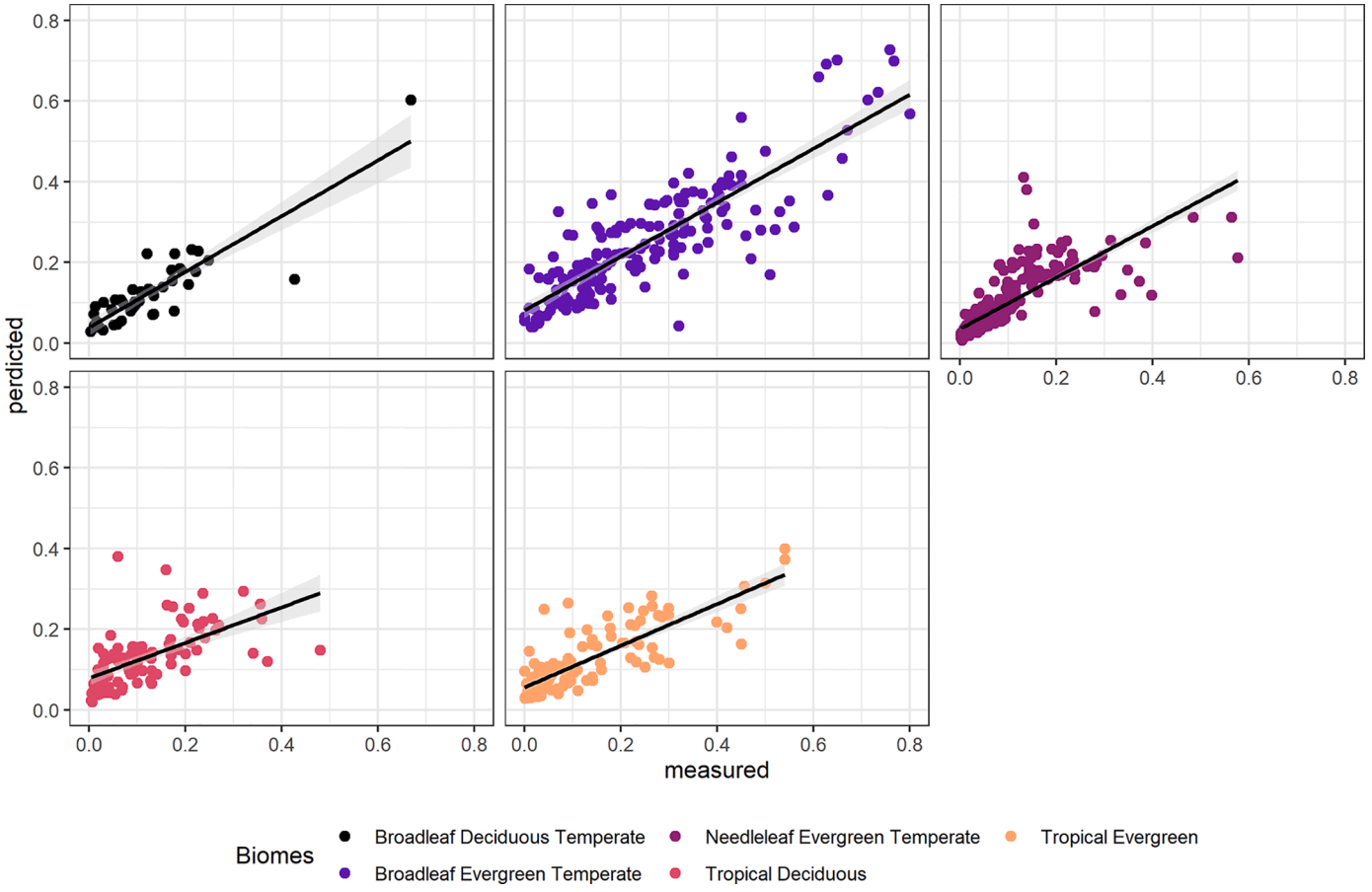

Fig. 5. Predicted versus modelled stomatal conductance (mol m-2 s-1) per forest biome for the Boosting Ensemble model with Random Forest as the base learner. Linear regression and 95 % confidence intervals are shown.

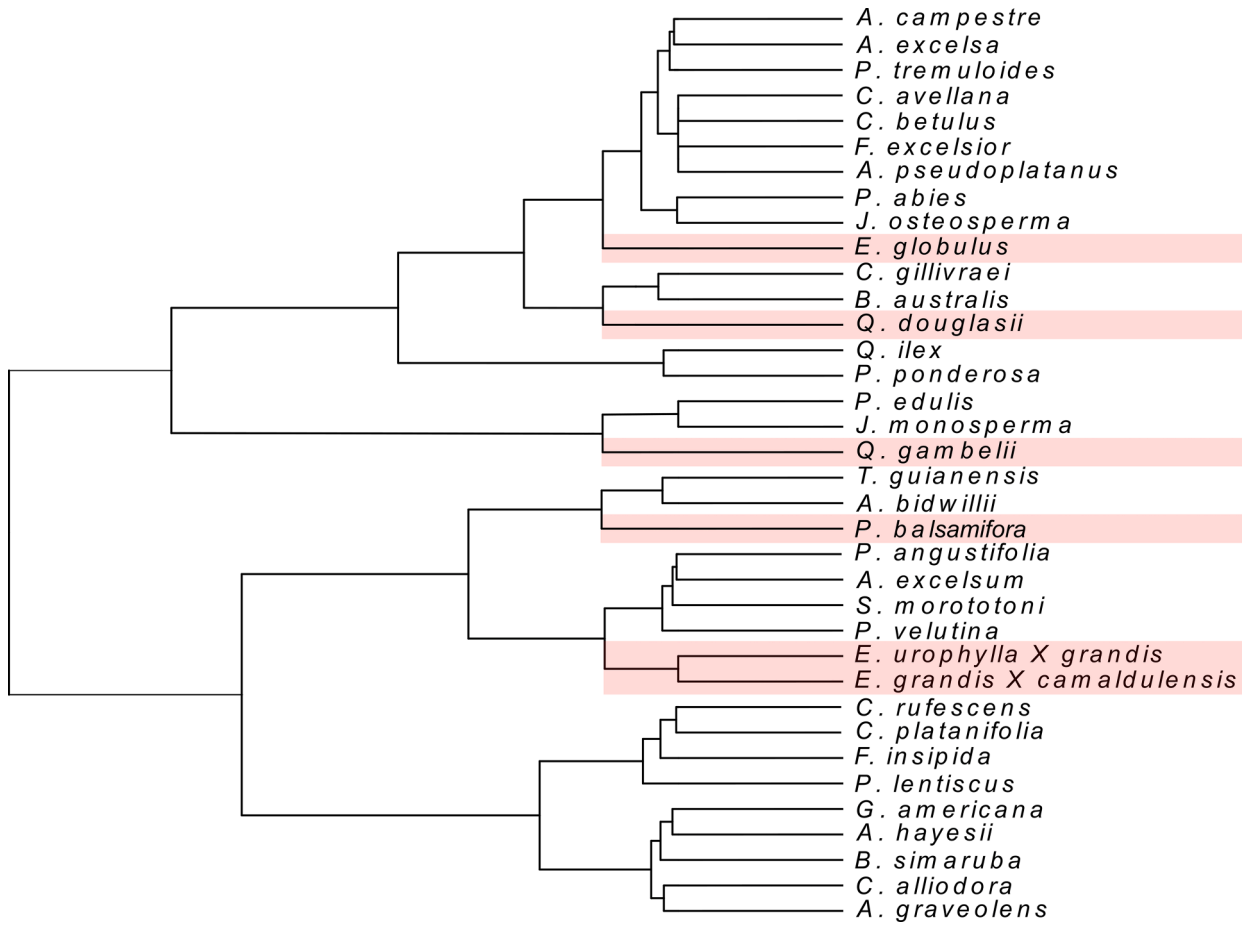

Fig. 6. Dendogram indicating the hierarchical clustering of stomatal responses of all tree species included within the study. Species dedicated to their own clusters/ branches are highlighted in red.

It was clear from our results that some species exhibited unique stomatal responses, linked in some way to ecological or drought-avoidance strategies or underlying physiology. These species included all *Eucalyptus* species, two *Quercus* species as well *P. balsamifora.* The importance of these species' stomatal responses was further highlighted by the cluster analysis. *Eucalyptus* species have high rates of photosynthesis and growth (Whitehead and Beadle, 2004), which are accompanied by high rates of stomatal conductance. A wide range of water use strategies have however been observed within *Eucalyptus* (Saadaoui et al. 2017) which can lead to unique stomatal responses. It is important to note that the only two *Eucalyptus* hybrids included in the study both clustered together. This could be related to a similar underlying physiological response since both hybrids included *E. grandis* as part of the hybrid cross.

The species that emerged with high feature importance in model predictions represented fast-growing tree species with high resource efficiency, which can be linked to their stomatal responses to drought. This was seen not only with the *Eucalyptus* species, but also the *Quercus* and *Populus* species (Abrams, 1990; Almeida-Rodriguez et al., 2010; Xu and Baldocchi, 2003). The stomatal responses seen of these species may be linked to these species choosing a drought tolerance strategy, which favours high stomatal conductance and growth rates during drought.

The importance of these species-unique response was highlighted further when considering that the above-mentioned species were not even the most represented in the training data used for model development. Stomatal responses between species can be unique, and data collected from a wide range of tree species can help improve model predictions, especially when the model is applied across multiple plant functional types, or groups where experimental data regarding their underlying physiology is lacking (Smith and Dukes, 2013). Traits associated with the different species, including physiological and growth characteristics, and which have been important features in ML models (van Klompenburg et al. 2020) should also be taken into account. Hydraulic traits, such as vessel size and distribution, have been related to stomatal responses in plants (Bartlett et al., 2016; Brodribb and Holbrook, 2003; Fernandes et al., 2016) ; and should also be considered when modelling stomatal responses to climate. In our present study we captured these effects parsimoniously by using only species names as an additional effect in the models and captured species-level stomatal responses without necessarily having to understand the underlying physiology. It is therefore clear that species-specific responses to water availability is important in understanding and modelling drivers of forest dynamics and should be included during model development.

4.5. *Stomatal responses and predictions per biome*

By using models relating to water availability, the ML model was able to predict stomatal responses for trees in the Broadleaf Deciduous Temperate, Broadleaf Evergreen Temperate as well as the Needleleaf Evergreen Temperate biomes. The model struggled however to make accurate predictions for species within the Tropical Deciduous and Tropical Evergreen biomes. This would suggest that more data is needed from these biomes to improve model predictions, or other variables such as temperature should also be considered when modelling stomatal responses for trees found in these two biomes. Although variables related to water availability have been shown to be one of the main drivers of forest dynamics (Zhao et al., 2021), it has been shown that a 40 % decrease in average growth of tropical forests can be expected due to

increasing temperatures (Aubry-Kientz et al., 2019). This is important as increases in droughts as well as increases in temperature are predicted due to climate change (Pachauri et al., 2014). We expect that ML models including not only variables relating available water, but also temperature can help to improve the prediction of forest responses to climate change.

4.6. ML complementarity with process-based models

Process-based models have been suggested as an alternative to modelling stomatal responses, since these models are based on physiological principles with the model parameters being trait-based and therefore measurable (Sabot et al., 2020; Sperry et al., 2017; Wang et al., 2019). These models are, however, not widely used since many of the parameters are difficult to measure (Sabot et al., 2020). The underlying mechanisms of stomatal responses are also not well known, limiting the use of models based on our understanding of plant physiology (Damour et al., 2010; Wang et al., 2019).

Perhaps for this reason, most models for stomatal responses remain empirical or semi-empirical, but based to some extent on physiological principles combined with empirical functions (Damour et al., 2010). These models often focus on stomatal responses based on only one or two environmental variables, with many models focussing on the relationship between the availability of soil water and gsw (Jarvis, 1976; Macfarlane et al., 2004; Misson et al., 2004; Stewart, 1988). Although stomatal responses to environmental conditions have been studied extensively (Jarvis, 1976; Monteith, 1995), there are still knowledge gaps regarding the underlying mechanism driving stomatal responses (Damour et al., 2010). These models struggle to include multiple environmental factors that might influence stomatal responses, with some environmental interactions not accounted for (Damour et al., 2010).

ML provides an approach that can help overcome some of these issues, bringing multiple environmental conditions together with physiological plant characteristics to model stomatal responses. ML can also help to gain a better understanding of the underlying interactions behind stomatal responses and environmental variables (Liu et al. 2018, Silva et al. 2019, Elavarasan and Durairaj Vincent 2020, van Klompenburg et al. 2020). The ML models used in this study were focussed on making gsw predictions, rather than extracting information regarding the underlying mechanism which drives gsw. Regardless of this, the ML models were able to outperform the empirical BWB model and could therefore be used as a viable option to replace empirical models in larger systems. While ML can be an effective tool to model plant responses, traditional models for stomatal responses can still have the advantage that they give better insight into the underlying mechanisms and drivers of plant responses (Houshmandfar et al., 2021). There is, perhaps, a place for both approaches in this area of research.

5. Conclusion

In this study we were able to train a ML model to capture stomatal responses of multiple tree species across 5 different forest biomes, which increased the versatility of this model to be applied on a global scale. This study showed that ML can be a useful tool for predicting stomatal response based on climate variables and species traits, outperforming the empirical BWB model. ML shows potential for ecological modelling, however it is still not widely used with the access to suitable data often being one of the main limitations (Silva et al., 2019). In our study a combined dataset consisting out of data from multiple studies was successfully used. The quality of combined dataset often lacks since measurements are taken across multiple experimental designs and timescales, potentially leading to missing data points. To increase the strength of ML models, long-term data is required using standardized measuring protocols (Pieruschka and Schurr, 2019). Data taken across different vegetation types and climatic regions can also help improve the adaptability of ML models (Papale et al., 2015; Tramontana et al., 2015, 2016); . In previous studies ML has been successfully combined with process-based models and empirical models (Houshmandfar et al., 2021; Shoemaker and Cropper, 2010). More focus on the use of ML together with traditional models can help give further insight into various ecological mechanisms.

Funding

This work was fully funded by the Hans Merensky Foundation within the Hans Merensky Chair of Advanced Modelling of eucalypt wood formation.

Declaration of Competing Interest

All authors declare that they have no conflict of interest.

Acknowledgements

We gratefully acknowledge the support of the following people:

Sonia Di Buisson (Hans Merensky Holdings) for the provision of the hybrid *Eucalyptus* material used for this study.

Dr Leandra Moller for her technical support.

References

Abrams, M.D., 1990. Adaptations and responses to drought in Quercus species of North America. Tree Physiol. 7, 227–238.

Almeida-Rodriguez, A.M., Cooke, J.E.K., Yeh, F., Zwiazek, J.J., 2010. Functional characterization of drought-responsive aquaporins in Populus balsamifera and Populus simonii×balsamifera clones with different drought resistance strategies. Physiol. Plant. 140, 321–333. https://doi.org/10.1111/j.1399-3054.2010.01405.x.

Alvarez, R., 2009. Predicting average regional yield and production of wheat in the Argentine Pampas by an artificial neural network approach. Eur. J. Agron. 30, 70–77. https://doi.org/10.1016/j.eja.2008.07.005.

Anderegg, L.D.L., Anderegg, W.R.L., Berry, J.A., 2013. Not all droughts are created equal: translating meteorological drought into woody plant mortality. Tree Physiol. 33, 672–683. https://doi.org/10.1093/treephys/tpt044.

Anderegg, W., 2018. AllData_EcologyLetters_Figshare_v1_3-18.csv. figshare. Dataset. https://doi.org/10.6084/m9.figshare.6066449.

Anderegg, W.R.L., Wolf, A., Arango-Velez, A., Choat, B., Chmura, D.J., Jansen, S., Kolb, T., Li, S., Meinzer, F.C., Pita, P., Resco de Dios, V., Sperry, J.S., Wolfe, B.T., Pacala, S., 2018. Woody plants optimise stomatal behaviour relative to hydraulic risk. Ecol. Lett. 21, 968–977. https://doi.org/10.1111/ele.12962.

Aubry-Kientz, M., Rossi, V., Cornu, G., Wagner, F., Hérault, B., 2019. Temperature rising would slow down tropical forest dynamic in the Guiana Shield. Sci. Rep. 9 https://doi.org/10.1038/s41598-019-46597-8.

Azodi, C.B., Tang, J., Shiu, S.-H., 2020. Opening the Black Box: Interpretable Machine Learning for Geneticists. Trends Genet. 36, 442–455. https://doi.org/10.1016/j.tig.2020.03.005.

Ball, J.T., Wood, I.E., Berry, J.A., 1987. A Model Predicting Stomatal Conductance and its Contribution to the Control of Photosynthesis Under Different Environmental Conditions. J., in: Progress in Photosynthesis Res. 221–224.

Bartlett, M.K., Klein, T., Jansen, S., Choat, B., Sack, L., 2016. The correlations and sequence of plant stomatal, hydraulic, and wilting responses to drought. Proc. Natl. Acad. Sci. 113, 13098–13103. https://doi.org/10.1073/pnas.1604088113.

Benito Garzón, M., Sánchez de Dios, R., Sainz Ollero, H., 2008. Effects of climate change on the distribution of Iberian tree species. Appl. Veg. Sci. 11, 169–178. https://doi.org/10.3170/2008-7-18348.

Blonquist, J.M., Norman, J.M., Bugbee, B., 2009. Automated measurement of canopy stomatal conductance based on infrared temperature. Agric. For. Meteorol. 149, 2183–2197. https://doi.org/10.1016/j.agrformet.2009.10.003.

Breiman, L., 2001. Random Forests. Mach. Learn. 45, 5–32. https://doi.org/10.1023/A:1010933404324.

Brodribb, T.J., Holbrook, N.M., 2003. Stomatal Closure during Leaf Dehydration, Correlation with Other Leaf Physiological Traits. Plant Physiol. 132, 2166–2173. https://doi.org/10.1104/pp.103.023879.

Buckley, T.N., 2017. Modeling stomatal conductance. Plant Physiol. 174, 572–582. https://doi.org/10.1104/pp.16.01772.

Bunce, J.A., 2004. Carbon dioxide effects on stomatal responses to the environment and water use by crops under field conditions. Oecologia. https://doi.org/10.1007/s00442-003-1401-6.

Cai, Y., Guan, K., Lobell, D., Potgieter, A.B., Wang, S., Peng, J., Xu, T., Asseng, S., Zhang, Y., You, L., Peng, B., 2019. Integrating satellite and climate data to predict wheat yield in Australia using machine learning approaches. Agric. For. Meteorol. 274, 144–159. https://doi.org/10.1016/j.agrformet.2019.03.010.

Chen, J., Yang, H., Man, R., Wang, W., Sharma, M., Peng, C., Parton, J., Zhu, H., Deng, Z., 2020. Using machine learning to synthesize spatiotemporal data for modelling DBH-

height and DBH-height-age relationships in boreal forests. For. Ecol. Manage. 466, 118104 https://doi.org/10.1016/j.foreco.2020.118104.
Choat, B., Jansen, S., Brodribb, T.J., Cochard, H., Delzon, S., Bhaskar, R., Bucci, S.J., Feild, T.S., Gleason, S.M., Hacke, U.G., Jacobsen, A.L., Lens, F., Maherali, H., Martínez-Vilalta, J., Mayr, S., Mencuccini, M., Mitchell, P.J., Nardini, A., Pittermann, J., Pratt, R.B., Sperry, J.S., Westoby, M., Wright, I.J., Zanne, A.E., 2012. Global convergence in the vulnerability of forests to drought. Nature 491, 752–755. https://doi.org/10.1038/nature11688.
Cowan, I.R., Farquhar, G.D., 1977. Stomatal function in relation to leaf metabolism and environment. Symp. Soc. Exp. Biol. 471–505.
Dahmen, T., Trampert, P., Boughorbel, F., Sprenger, J., Klusch, M., Fischer, K., Kübel, C., Slusallek, P., 2019. Digital reality: a model-based approach to supervised learning from synthetic data. AI Perspect. 1, 2. https://doi.org/10.1186/s42467-019-0002-0.
Damour, G., Simonneau, T., Cochard, H., Urban, L., 2010. An overview of models of stomatal conductance at the leaf level. Plant. Cell Environ. 33 https://doi.org/10.1111/j.1365-3040.2010.02181.x no-no.
Elavarasan, D., Vincent, P.M.D., 2020. Crop Yield Prediction Using Deep Reinforcement Learning Model for Sustainable Agrarian Applications. IEEE Access 8, 86886–86901. https://doi.org/10.1109/ACCESS.2020.2992480.
Ellsäßer, F., Röll, A., Ahongshangbam, J., Waite, P.-A., Hendrayanto, Schuldt, B., Hölscher, D., 2020. Predicting Tree Sap Flux and Stomatal Conductance from Drone-Recorded Surface Temperatures in a Mixed Agroforestry System—A Machine Learning Approach. Remote Sens. 12, 4070. https://doi.org/10.3390/rs12244070.
Farquhar, G.D., Von Caemmerer, S., Berry, J.A., 1980. A Biochemical Model of Photosynthetic CO 2 Assimilation in Leaves of C 3 Species. Planta.
Fernandes, T., Campo, A., García-Bartual, R., González-Sanchis, M., 2016. Coupling daily transpiration modelling with forest management in a semiarid pine plantation. iForest - Biogeosci. For. 9, 38–48. https://doi.org/10.3832/ifor1290-008.
Galar, M., Fernandez, A., Barrenechea, E., Bustince, H., Herrera, F., 2012. A review on ensembles for the class imbalance problem: Bagging-, boosting-, and hybrid-based approaches. IEEE Trans. Syst. Man Cybern. Part C Appl. Rev. https://doi.org/10.1109/TSMCC.2011.2161285.
Hastie, T., Tibshirani, R., Friedman, J., 2001. Springer Series in Statistics The Elements of Statistical Learning Data Mining, Inference, and Prediction. Springer, New York.
He, H., Garcia, E.A., 2009. Learning from imbalanced data. IEEE Trans. Knowl. Data Eng. 21, 1263–1284. https://doi.org/10.1109/TKDE.2008.239.
Houshmandfar, A., O'Leary, G., Fitzgerald, G.J., Chen, Y., Tausz-Posch, S., Benke, K., Uddin, S., Tausz, M., 2021. Machine learning produces higher prediction accuracy than the Jarvis-type model of climatic control on stomatal conductance in a dryland wheat agro-ecosystem. Agric. For. Meteorol. 304–305, 108423 https://doi.org/10.1016/j.agrformet.2021.108423.
Jarvis, P.G., 1976. The Interpretation of the Variations in Leaf Water Potential and Stomatal Conductance Found in Canopies in the Field. Philos. Trans. R. Soc. London. Ser. B 273 (273), 593–610.
Johnson, M.D., Hsieh, W.W., Cannon, A.J., Davidson, A., Bédard, F., 2016. Crop yield forecasting on the Canadian Prairies by remotely sensed vegetation indices and machine learning methods. Agric. For. Meteorol. 218–219, 74–84. https://doi.org/10.1016/j.agrformet.2015.11.003.
Jung, M., Reichstein, M., Bondeau, A., 2001. Towards global empirical upscaling of FLUXNET eddy covariance observations: validation of a model tree ensemble approach using a biosphere model. Biogeosciences.
Kaul, M., Hill, R.L., Walthall, C., 2005. Artificial neural networks for corn and soybean yield prediction. Agric. Syst. 85, 1–18. https://doi.org/10.1016/j.agsy.2004.07.009.
Kisi, O., Cimen, M., 2009. Evapotranspiration modelling using support vector machines /Modélisation de l'évapotranspiration à l'aide de 'support vector machines. Hydrol. Sci. J. 54, 918–928. https://doi.org/10.1623/hysj.54.5.918.
Kurz, W.A., Dymond, C.C., White, T.M., Stinson, G., Shaw, C.H., Rampley, G.J., Smyth, C., Simpson, B.N., Neilson, E.T., Trofymow, J.A., Metsaranta, J., Apps, M.J., 2009. CBM-CFS3: A model of carbon-dynamics in forestry and land-use change implementing IPCC standards. Ecol. Modell. 220, 480–504. https://doi.org/10.1016/j.ecolmodel.2008.10.018.
Li, A., Liang, S., Wang, A., Qin, J., 2007. Estimating crop yield from multi-temporal satellite data using multivariate regression and neural network techniques. Photogramm. Eng. Remote Sens. 73, 1149–1157, 0099-1112/07/7310–1149/$3.00/0.
Liu, Z., Peng, C., Work, T., Candau, J.-N., DesRochers, A., Kneeshaw, D., 2018. Application of machine-learning methods in forest ecology: recent progress and future challenges. Environ. Rev. 26, 339–350. https://doi.org/10.1139/er-2018-0034.
Macfarlane, C., White, D.A., Adams, M.A., 2004. The apparent feed-forward response to vapour pressure deficit of stomata in droughted, field-grown Eucalyptus globulus Labill. Plant, Cell Environ. 27, 1268–1280. https://doi.org/10.1111/j.1365-3040.2004.01234.x.
Martin-StPaul, N., Delzon, S., Cochard, H., 2017. Plant resistance to drought depends on timely stomatal closure. Ecol. Lett. 20, 1437–1447. https://doi.org/10.1111/ele.12851.
Miner, G.L., Bauerle, W.L., Baldocchi, D.D., 2017. Estimating the sensitivity of stomatal conductance to photosynthesis: a review. Plant Cell Environ. https://doi.org/10.1111/pce.12871.
Misson, L., Panek, J.A., Goldstein, A.H., 2004. A comparison of three approaches to modeling leaf gas exchange in annually drought-stressed ponderosa pine forests. Tree Physiol. 24, 529–541. https://doi.org/10.1093/treephys/24.5.529.
Monteith, J.L., 1995. A reinterpretation of stomatal responses to humidity. Plant, Cell Envirotimerit 18, 357–364.
Pachauri, R.K., Mayer, L., 2014. Intergovernmental Panel on Climate Change. Climate change 2014 : synthesis report. Geneva, Switzerland.
Pan, S., Pan, N., Tian, H., Friedlingstein, P., Sitch, S., Shi, H., Arora, V.K., Haverd, V., Jain, A.K., Kato, E., Lienert, S., Lombardozzi, D., Nabel, J.E.M.S., Ottlé, C., Poulter, B., Zaehle, S., Running, S.W., 2020. Evaluation of global terrestrial evapotranspiration using state-of-the-art approaches in remote sensing, machine learning and land surface modeling. Hydrol. Earth Syst. Sci. 24, 1485–1509. https://doi.org/10.5194/hess-24-1485-2020.
Panda, S., Amatya, D.M., Hoogenboom, G., 2014. Stomatal Conductance, Canopy Temperature, and Leaf Area Index Estimation Using Remote Sensing and OBIA techniques. J. Spatial Hydrol.
Papale, D., Black, T.A., Carvalhais, N., Cescatti, A., Chen, J., Jung, M., Kiely, G., Lasslop, G., Mahecha, M.D., Margolis, H., Merbold, L., Montagnani, L., Moors, E., Olesen, J.E., Reichstein, M., Tramontana, G., van Gorsel, E., Wohlfahrt, G., Ráduly, B., 2015. Effect of spatial sampling from European flux towers for estimating carbon and water fluxes with artificial neural networks. J. Geophys. Res. Biogeosci. 120, 1941–1957. https://doi.org/10.1002/2015JG002997.
Papalem, D., Valentini, R., 2003. A new assessment of European forests carbon exchanges by eddy fluxes and artificial neural network spatialization. Glob. Chang. Biol. 9, 525–535. https://doi.org/10.1046/j.1365-2486.2003.00609.x.
Park Williams, A., Allen, C.D., Macalady, A.K., Griffin, D., Woodhouse, C.A., Meko, D.M., Swetnam, T.W., Rauscher, S.A., Seager, R., Grissino-Mayer, H.D., Dean, J.S., Cook, E. R., Gangodagamage, C., Cai, M., McDowell, N.G., 2013. Temperature as a potent driver of regional forest drought stress and tree mortality. Nat. Clim. Chang. 3, 292–297. https://doi.org/10.1038/nclimate1693.
Pedregosa, F., Varoquaux, G., Gramfort, A., Michel, V., Thirion, B., Grisel, O., Blondel, M., Prettenhofer, P., Wies, R., Dubourg, V., Vanderplas, J.T., Passos, A., Cournapeau, D., Brucher, M., Perrot, M., Duchesnay, E., 2011. Scikit-learn: Machine Learning in Python. J. Mach. Learn. Res. 12, 2825–2830.
Périé, C., de Blois, S., 2016. Dominant forest tree species are potentially vulnerable to climate change over large portions of their range even at high latitudes. PeerJ 4, e2218. https://doi.org/10.7717/peerj.2218.
Pieruschka, R., Schurr, U., 2019. Plant Phenotyping: Past, Present, and Future. Plant Phenomics 2019, 1–6. https://doi.org/10.34133/2019/7507131.
Powell, T.L., Galbraith, D.R., Christoffersen, B.O., Harper, A., Imbuzeiro, H.M.A., Rowland, L., Almeida, S., Brando, P.M., da Costa, A.C.L., Costa, M.H., Levine, N.M., Malhi, Y., Saleska, S.R., Sotta, E., Williams, M., Meir, P., Moorcroft, P.R., 2013. Confronting model predictions of carbon fluxes with measurements of Amazon forests subjected to experimental drought. New Phytol. 200, 350–365. https://doi.org/10.1111/nph.12390.
Saadaoui, E., Ben Yahia, K., Dhahri, S., Ben Jamaa, M.L., Khouja, M.L., 2017. An overview of adaptative responses to drought stress in Eucalyptus spp. For. Stud. 67, 86–96. https://doi.org/10.1515/fsmu-2017-0014.
Sabot, M.E.B., De Kauwe, M.G., Pitman, A.J., Medlyn, B.E., Verhoef, A., Ukkola, A.M., Abramowitz, G., 2020. Plant profit maximization improves predictions of European forest responses to drought. New Phytol. 226 https://doi.org/10.1111/nph.16376.
Schulze, E.-D., Hall, A.E., 1982. Stomatal Responses, Water Loss and CO2 Assimilation Rates of Plants in Contrasting Environments. In: Lange, O.L., Nobel, P.S., Osmond, C. B., Ziegler, H. (Eds.), Physiological Plant Ecology II: Water Relations and Carbon Assimilation. Springer Berlin Heidelberg, Berlin, Heidelberg, pp. 181–230. https://doi.org/10.1007/978-3-642-68150-9_8.
Shoemaker, D.A., Cropper, W.P., 2010. Application of remote sensing, an artificial neural network leaf area model, and a process-based simulation model to estimate carbon storage in Florida slash pine plantations. J. For. Res. 21, 171–176. https://doi.org/10.1007/s11676-010-0027-x.
Silva, F.C.e, Shvaleva, A., Maroco, J.P., Almeida, M.H., Chaves, M.M., Pereira, J.S., 2004. Responses to water stress in two Eucalyptus globulus clones differing in drought tolerance. Tree Physiol. 24, 1165–1172. https://doi.org/10.1093/treephys/24.10.1165.
Silva, J.C.F., Teixeira, R.M., Silva, F.F., Brommonschenkel, S.H., Fontes, E.P.B., 2019. Machine learning approaches and their current application in plant molecular biology: A systematic review. Plant Sci. 284, 37–47. https://doi.org/10.1016/j.plantsci.2019.03.020.
Smith, N.G., Dukes, J.S., 2013. Plant respiration and photosynthesis in global-scale models: Incorporating acclimation to temperature and CO2. Glob. Chang. Biol. https://doi.org/10.1111/j.1365-2486.2012.02797.x.
Sperry, J.S., Hacke, U.G., Oren, R., Comstock, J.P., 2002. Water deficits and hydraulic limits to leaf water supply. Plant. Cell Environ. 25, 251–263. https://doi.org/10.1046/j.0016-8025.2001.00799.x.
Sperry, J.S., Venturas, M.D., Anderegg, W.R.L., Mencuccini, M., Mackay, D.S., Wang, Y., Love, D.M., 2017. Predicting stomatal responses to the environment from the optimization of photosynthetic gain and hydraulic cost. Plant. Cell Environ. 40, 816–830. https://doi.org/10.1111/pce.12852.
Stewart, J.B., 1988. Modelling surface conductance of Pine forest. Agric. For. Meteorol. 43, 19–35.
Tramontana, G., Ichii, K., Camps-Valls, G., Tomelleri, E., Papale, D., 2015. Uncertainty analysis of gross primary production upscaling using Random Forests, remote sensing and eddy covariance data. Remote Sens. Environ. 168, 360–373. https://doi.org/10.1016/j.rse.2015.07.015.
Tramontana, G., Jung, M., Schwalm, C.R., Ichii, K., Camps-Valls, G., Ráduly, B., Reichstein, M., Arain, M.A., Cescatti, A., Kiely, G., Merbold, L., Serrano-Ortiz, P., Sickert, S., Wolf, S., Papale, D., 2016. Predicting carbon dioxide and energy fluxes across global FLUXNET sites with regression algorithms. Biogeosciences 13, 4291–4313. https://doi.org/10.5194/bg-13-4291-2016.
Trugman, A.T., Medvigy, D., Mankin, J.S., Anderegg, W.R.L., 2018. Soil Moisture Stress as a Major Driver of Carbon Cycle Uncertainty. Geophys. Res. Lett. 45, 6495–6503. https://doi.org/10.1029/2018GL078131.

Urban, J., Ingwers, M., McGuire, M.A., Teskey, R.O., 2017. Stomatal conductance increases with rising temperature. Plant Signal. Behav. 12 https://doi.org/10.1080/15592324.2017.1356534.

Vaca, R.A., Golicher, D.J., Cayuela, L., 2011. Using climatically based random forests to downscale coarse-grained potential natural vegetation maps in tropical Mexico. Appl. Veg. Sci. 14, 388–401. https://doi.org/10.1111/j.1654-109X.2011.01132.x.

van Dijk, A.D.J., Kootstra, G., Kruijer, W., de Ridder, D., 2021. Machine learning in plant science and plant breeding. iScience 24, 101890. https://doi.org/10.1016/j.isci.2020.101890.

van Genuchten, M.T., 1980. A Closed-form Equation for Predicting the Hydraulic Conductivity of Unsaturated Soils. Soil Sci. Soc. Am. J. 44, 892–898. https://doi.org/10.2136/sssaj1980.03615995004400050002x.

van Klompenburg, T., Kassahun, A., Catal, C., 2020. Crop yield prediction using machine learning: A systematic literature review. Comput. Electron. Agric. 177, 105709 https://doi.org/10.1016/j.compag.2020.105709.

Vitrack-Tamam, S., Holtzman, L., Dagan, R., Levi, S., Tadmor, Y., Azizi, T., Rabinovitz, O., Naor, A., Liran, O., 2020. Random Forest Algorithm Improves Detection of Physiological Activity Embedded within Reflectance Spectra Using Stomatal Conductance as a Test Case. Remote Sens 12, 2213. https://doi.org/10.3390/rs12142213.

Wang, Y., Sperry, J.S., Venturas, M.D., Trugman, A.T., Love, D.M., Anderegg, W.R.L., 2019. The stomatal response to rising CO2 concentration and drought is predicted by a hydraulic trait-based optimization model. Tree Physiol. 39, 1416–1427. https://doi.org/10.1093/treephys/tpz038.

Whitehead, D., Beadle, C.L., 2004. Physiological regulation of productivity and water use in Eucalyptus: A review. For. Ecol. Manage. 193, 113–140. https://doi.org/10.1016/j.foreco.2004.01.026.

Xiong, D., Nadal, M., 2020. Linking water relations and hydraulics with photosynthesis. Plant J. 101, 800–815. https://doi.org/10.1111/tpj.14595.

Xu, L., Baldocchi, D.D., 2003. Seasonal trends in photosynthetic parameters and stomatal conductance of blue oak (Quercus douglasii) under prolonged summer drought and high temperature. Tree Physiol. 23, 865–877.

Zhao, X., Zhao, P., Zhu, L., Wang, Q., Hu, Y., Cranston, B.M., Kaplick, J., Lei, O., Chen, X., Ni, G., Ye, Q., Macinnis-Ng, C., 2021. Exploring the influence of biological traits and environmental drivers on water use variations across contrasting forests. Forests 12, 1–18. https://doi.org/10.3390/f12020161.

Chapter 7

General conclusion

Chapter 7: General conclusion

Plants are constantly balancing a trade-off between water loss and carbon gain, a situation in which stomatal regulation constantly plays an important role (Xiong and Nadal 2020). There is increasing evidence that stomatal morphology and behaviour have evolved to optimise this trade-off (Sperry et al. 2017). Plant water supply, a major factor in understanding plant-level carbon sequestration, is, however, not only regulated by stomatal conductance, but also limited by a decrease in hydraulic conductance due to embolism formation (Tyree and Sperry 1988, Sperry et al. 1993). The reduction of xylem conductance due to embolism formation during drought cannot be directly regulated by the plant, although stomatal regulation can help prevent runaway cavitation (Sperry et al. 1993).

This thesis explored the important question of how plants constantly balance the trade-off between water loss and carbon gain. Two major aspects were considered. First to understand the stomatal behaviour, which play a critical role in controlling the rate of water loss and carbon gain through CO_2 uptake (Xiong and Nadal 2020), during drought and drought recovery. Second, the extent to which supply of water, a major factor in understanding plant-level carbon sequestration, is regulated by stomatal conductance as well as limited by a decrease in hydraulic conductance due to embolism formation (Tyree and Sperry 1988, Sperry et al. 1993). The research considered the drought strategies and drought recovery responses seen in two contrasting *Eucalyptus* hybrids, the role that stomatal and hydraulic characteristics played and finally on approaches to modelling the interaction. To that end, the research also compared widely used empirical approaches with machine learning models.

Recovery of lost hydraulic capacity in eucalypt hybrids

A wide range of drought strategies have been observed within *Eucalyptus* to help mitigate or reduce drought induced hydraulic failure (Saadaoui et al. 2017). Recovery of lost hydraulic conductance can also be an important mechanism used to avoid drought induced mortality, however many previous studies focussed on how plants avoid hydraulic failure (Pittermann et al. 2006, Gleason et al. 2016, Venturas et al. 2017, Barotto et al. 2018), with focus not always given to recovery strategies deployed by plants (Klein et al. 2018). Evidence of hydraulic recovery through refilling has been observed in *E. Saligna* (Choat et al. 2018), *E. camaldulensis* and *E. tereticornis* (Zeppel et al. 2019), however a more detailed analysis is still needed to determine if this phenomenon is observed throughout the *Eucalyptus* genus and how this is related to species-level drought strategies.

During this study both traditional hydraulic measurements and CT-scans were used to investigate the phenomenon of hydraulic recovery with in two *Eucalyptus* hybrids. Not withstanding the complexities inherent in interpreting the data, our results suggest that hydraulic recovery should be an important component to consider when assessing plant hydraulic strategies. Accordingly, it would be important to understand which taxonomic groups utilise refilling as a hydraulic strategy, in order to improve vegetation models. The effect of drought stress on production is highly linked to changes in hydraulic conductance and understanding the hydraulic recovery response of plants, will give further insight into the impact of drought on trees.

Modelling the balance between risk and gain

During drought conditions plants experience an increased loss of hydraulic conductance (Xiong and Nadal 2019), however plants can recover hydraulic conductance through refilling after drought. The timing and rate of embolism recovery should therefore be included when modelling plant responses. If embolism recovery takes place immediately after embolism formation at low water potentials, then embolism will recur immediately after recovery. It would therefore be more economical if embolism is only recovered when there is an increase in soil water potential. During this study, the use of a simplified gain-risk model was used to model stomatal responses at plant scale for two *Eucalyptus* hybrids. This is, to our knowledge, the first time this has been done on *Eucalyptus*. Our study also tested whether the inclusion of a partial/delayed recovery response would improve model predictions.

This simplified gain-risk model performed well at predicting stomatal responses in both *E. grandis X camaldulensis* (*GC*) and *E. urophylla X grandis* (*UG).* Our inclusion of a delayed/partial hydraulic recovery component only slightly improved model predictions, however, and more focus should be given to understanding hydraulic recovery after drought. The gain-risk model has the benefit of being to a great extent process-based, with model parameters based on measurable plant characteristics (Venturas et al. 2018). This reduces the assumptions regarding parameterisation, giving it an advantage over more empirical models where model parameters are often difficult to quantify (Damour et al. 2010). Furthermore, the gain-risk model has only been tested on a limited amount of species (Venturas et al. 2018, Wang et al. 2019), and focus should be given to test the model on plants with various hydraulic traits and water-use strategies (Ciemer et al. 2019). More research is also needed to determine how photosynthetic and hydraulic traits might change over time and affect long-term predictions (Anderegg 2018a).

Machine learning methods for predicting stomatal conductance

The increasing use of machine learning (ML) as an approach to modelling is rapidly gaining traction in a variety of fields (including plant physiology approaches) with shifts away from the use of more traditional empirical and process-based models, even for stomatal conductance (Papalem and Valentini 2003, Kurz et al. 2009, Johnson et al. 2016, Périé and de Blois 2016, Liu et al. 2018, Pan et al. 2020, Chen et al. 2020, van Klompenburg et al. 2020). ML models have been widely shown to improve predictions, especially when multiple environmental factors are included (Liu et al. 2018, Silva et al. 2019, Elavarasan and Vincent 2020, Vitrack-Tamam et al. 2020, van Klompenburg et al. 2020, Ellsäßer et al. 2020, Houshmandfar et al. 2021), and can also help make predictions of stomatal response without understanding the underlying physiology. They are however still not widely adapted to model fine-scale physiological processes like transpiration rates and stomatal response to environmental shifts, with one of the main limitations being the availability of suitable datasets. The ML models for stomatal conductance developed by other studies also only focused on modelling the response of one or two species in single study areas, limiting the versatility of these models (Vitrack-Tamam et al. 2020, Ellsäßer et al. 2020). In this thesis an important step was, therefore, to train a ML model to predict plant response on a global scale, across different forest biomes and for multiple tree species. The ML model outperformed the traditional Ball-Berry stomatal conductance model and was also able to capture species specific stomatal responses parsimoniously, without prior knowledge of the underlying physiology of each tree species.

It is clear that ML can be a useful tool for predicting stomatal response based on climate variables and species traits, highlighting the potential of ML for ecological modelling. To increase the strength of ML models focus should however be given to collect long-term data using standardised measuring protocols (Pieruschka and Schurr 2019). Data taken across different vegetation types and climatic regions can also help improve the adaptability of ML models (Papale et al. 2015, Tramontana et al. 2015, 2016).

Modelling plant responses in a changing climate

The modelling of hydraulic and stomatal responses of plants during drought and drought recovery can help improve predictions of plant productivity (Menezes-Silva et al. 2019). Although developments such as ML can help improve predictions and model plant response in a changing climate, traditional empirical models and process-based models still have the advantage that they give better insight into the underlying mechanisms and drivers of plant responses (Houshmandfar et al. 2021). These models are, however, still dependent on our understanding of the underlying

physiology and prior experimental work. But the discussion around modelling approaches needn't be an "either-or" paradigm. Different approaches will inherently bring different strengths and there is, perhaps, a better way forward to use a combined approach in which ML models are used in conjunction with more traditional models and sophisticated process-based frameworks.

An increase in drought-induced tree mortality which can be expected to have a significant impact on plant survival in a changing climate, has been found in several studies in the last few years (Anderegg, Plavcová, et al. 2013, Allen et al. 2015, McDowell et al. 2018, Hammond et al. 2019). Major increases in tree mortality are likely to have an impact on global carbon and hydrological cycles (Bonan 2008). Greater evaporative demand due to increasing temperature, in concert with decreased soil water availability during more frequent or intensive droughts (Pachauri et al. 2014), will increase tree stress and can ultimately be expected to reduce forest productivity (Park Williams et al. 2013, Anderegg, Anderegg, et al. 2013). In order to properly predict these changes, accurate models of plant responses to water limitations and other environmental changes are therefore becoming increasingly important for effective and sustainable forest management (Chen et al. 2020). Understanding how hydraulic traits and stomatal regulation covary, can help model drought-induced tree mortality in a changing climate (Mcdowell et al. 2013).

References

Abrams MD (1990) Adaptations and responses to drought in Quercus species of North America. Tree Physiol 7:227–238. http://treephys.oxfordjournals.org/

Allen CD, Breshears DD, McDowell NG (2015) On underestimation of global vulnerability to tree mortality and forest die-off from hotter drought in the Anthropocene. Ecosphere 6:art129. http://doi.wiley.com/10.1890/ES15-00203.1

Allen CD, Macalady AK, Chenchouni H, Bachelet D, McDowell N, Vennetier M, Kitzberger T, Rigling A, Breshears DD, Hogg EH (Ted., Gonzalez P, Fensham R, Zhang Z, Castro J, Demidova N, Lim JH, Allard G, Running SW, Semerci A, Cobb N (2010) A global overview of drought and heat-induced tree mortality reveals emerging climate change risks for forests. For Ecol Manage 259:660–684.

Almeida-Rodriguez AM, Cooke JEK, Yeh F, Zwiazek JJ (2010) Functional characterization of drought-responsive aquaporins in Populus balsamifera and Populus simonii×balsamifera clones with different drought resistance strategies. Physiol Plant 140:321–333.

Aloni R (2015) Ecophysiological implications of vascular differentiation and plant evolution. Trees - Struct Funct 29

Alvarez R (2009) Predicting average regional yield and production of wheat in the Argentine Pampas by an artificial neural network approach. Eur J Agron 30:70–77. https://linkinghub.elsevier.com/retrieve/pii/S1161030108000865

Anderegg WRL (2018a) Quantifying seasonal and diurnal variation of stomatal behavior in a hydraulic-based stomatal optimization model.

Anderegg W (2018b) AllData_EcologyLetters_Figshare_v1_3-18.csv. figshare. Dataset. https://doi.org/10.6084/m9.figshare.6066449.v1

Anderegg LDL, Anderegg WRL, Berry JA (2013) Not all droughts are created equal: translating meteorological drought into woody plant mortality. Tree Physiol 33:672–683. https://academic.oup.com/treephys/article-lookup/doi/10.1093/treephys/tpt044

Anderegg WRL, Berry JA, Smith DD, Sperry JS, Anderegg LDL, Field CB (2012) The roles of hydraulic and carbon stress in a widespread climate-induced forest die-off. Proc Natl Acad Sci U S A 109:233–237.

Anderegg WRL, Hicke JA, Fisher RA, Allen CD, Aukema J, Bentz B, Hood S, Lichstein JW, Macalady AK, McDowell N, Pan Y, Raffa K, Sala A, Shaw JD, Stephenson NL, Tague C, Zeppel M (2015) Tree mortality from drought, insects, and their interactions in a changing climate. New Phytol 208:674–683. http://doi.wiley.com/10.1111/nph.13477

Anderegg WRL, Klein T, Bartlett M, Sack L, Pellegrini AFA, Choat B, Jansen S (2016) Meta-analysis reveals that hydraulic traits explain cross-species patterns of drought-induced tree mortality across the globe. Proc Natl Acad Sci 113:5024–5029.

Anderegg WRL, Plavcová L, Anderegg LDL, Hacke UG, Berry JA, Field CB (2013) Drought's legacy: Multiyear hydraulic deterioration underlies widespread aspen forest die-off and portends increased future risk. Glob Chang Biol 19:1188–1196.

Anderegg WRL, Wolf A, Arango-Velez A, Choat B, Chmura DJ, Jansen S, Kolb T, Li S, Meinzer FC, Pita P, Resco de Dios V, Sperry JS, Wolfe BT, Pacala S (2018) Woody plants optimise stomatal behaviour relative to hydraulic risk Cameron D (ed). Ecol Lett 21:968–977. http://doi.wiley.com/10.1111/ele.12962

Aubry-Kientz M, Rossi V, Cornu G, Wagner F, Hérault B (2019) Temperature rising would slow down tropical forest dynamic in the Guiana Shield. Sci Rep 9

Azodi CB, Tang J, Shiu S-H (2020) Opening the Black Box: Interpretable Machine Learning for Geneticists. Trends Genet 36:442–455. https://linkinghub.elsevier.com/retrieve/pii/S016895252030069X

Ball JT, Wood IE, Berry JA (1987) A Model Predicting Stomatal Conductance and its Contribution to the Control of Photosynthesis Under Different Environmental Conditions. J. In: Progress in Photosynthesis Research.pp 221–224.

Barotto AJ, Fernandez ME, Gyenge J, Meyra A, Martinez-Meier A, Monteoliva S (2016) First insights into the functional role of vasicentric tracheids and parenchyma in eucalyptus species with solitary vessels: Do they contribute to xylem efficiency or safety? Tree Physiol 36:1485–1497.

Barotto AJ, Monteoliva S, Gyenge J, Martinez-Meier A, Fernandez ME (2018) Functional relationships between wood structure and vulnerability to xylem cavitation in races of Eucalyptus globulus differing in wood density. Tree Physiol 38:243–251.

Bartlett MK, Klein T, Jansen S, Choat B, Sack L (2016) The correlations and sequence of plant stomatal, hydraulic, and wilting responses to drought. Proc Natl Acad Sci 113:13098–13103. http://www.pnas.org/lookup/doi/10.1073/pnas.1604088113

Becker P, Gribben RJ, Lim C (2000) Tapered conduits can buffer hydraulic conductance from path-lenght effects. Tree Physiol 20:965–967.

Benito Garzón M, Sánchez de Dios R, Sainz Ollero H (2008) Effects of climate change on the distribution of Iberian tree species. Appl Veg Sci 11:169–178. https://onlinelibrary.wiley.com/doi/abs/10.3170/2008-7-18348

Bernacchi CJ, Bagley JE, Serbin SP, Ruiz-vera UM, Rosenthal DM, Vanloocke A (2013) Modelling C 3 photosynthesis from the chloroplast to the ecosystem. :1641–1657.

Bernacchi CJ, Portis AR, Nakano H, Caemmerer S Von, Long SP (2002) Temperature Response of Mesophyll Conductance . Implications for the Determination of Rubisco Enzyme Kinetics and for Limitations to Photosynthesis in Vivo. 130:1992–1998.

Binkley D, Campoe OC, Alvares CA, Carneiro RL, Stape JL (2020) Variation in whole-rotation yield among Eucalyptus genotypes in response to water and heat stresses: The TECHS project. For Ecol Manage 462

Blonquist JM, Norman JM, Bugbee B (2009) Automated measurement of canopy stomatal conductance based on infrared temperature. Agric For Meteorol 149:2183–2197. https://linkinghub.elsevier.com/retrieve/pii/S0168192309002329

Bonan GB (2008) Forests and Climate Change: Forcings, Feedbacks, and the Climate Benefits of Forests. Science (80-) 320:1444–1449.

Bonan GB, Williams M, Fisher RA, Oleson KW (2014) Modeling stomatal conductance in the Earth system: linking leaf water-use efficiency and water transport along the soil-plant-atmosphere continuum. Geosci Model Dev Discuss 7:3085–3159.

Boreham GR, Pallett RN (2009) The influence of tree improvement and cultural practices on the productivity of Eucalyptusplantations in temperate South Africa. South For 71:85–93.

Bourne AE, Creek D, Peters JMR, Ellsworth DS, Choat B (2017) Species climate range influences hydraulic and stomatal traits in Eucalyptus species. Ann Bot 120:123–133.

Breiman L (2001) Random Forests. Mach Learn 45:5–32. https://doi.org/10.1023/A:1010933404324

Brodersen CR, Knipfer T, McElrone AJ (2018) In vivo visualization of the final stages of xylem vessel refilling in grapevine (Vitis vinifera) stems. New Phytol 217:117–126.

Brodersen CR, McElrone AJ (2013) Maintenance of xylem Network Transport Capacity: A Review of Embolism Repair in Vascular Plants. Front Plant Sci 4. http://journal.frontiersin.org/article/10.3389/fpls.2013.00108/abstract

Brodersen CR, McElrone AJ, Choat B, Matthews MA, Shackel KA (2010) The dynamics of embolism repair in xylem: In vivo visualizations using high-resolution computed tomography. Plant Physiol 154:1088–1095.

Brodribb TJ (2009) Xylem hydraulic physiology: The functional backbone of terrestrial plant productivity. Plant Sci 177:245–251.

Brodribb TJ, Feild TS (2000) Stem hydraulic supply is linked to leaf photosynthetic capacity: Evidence from New Caledonian and Tasmanian rainforests. Plant, Cell Environ 23:1381–1388.

Brodribb TJ, Holbrook NM (2003) Stomatal Closure during Leaf Dehydration, Correlation with Other Leaf Physiological Traits. Plant Physiol 132:2166–2173. https://academic.oup.com/plphys/article/132/4/2166-2173/6111800

Brodribb TJ, Jordan GJ (2008) Internal coordination between hydraulics and stomatal control in leaves. Plant, Cell Environ 31:1557–1564.

Brodribb TJ, McAdam AM (2011) Passive Origins of Stomatal Control in Vascular Plants. Science (80-) 331:578–582. https://www.sciencemag.org/lookup/doi/10.1126/science.1197175

Buckley TN (2017) Modeling Stomatal Conductance. Plant Physiol 174:572–582. https://academic.oup.com/plphys/article/174/2/572-582/6117384

Buckley TN, Mott KA (2013) Modelling stomatal conductance in response to environmental factors. Plant, Cell Environ 36:1691–1699.

Buckley TN, Sack L, Farquhar GD (2017) Optimal plant water economy. Plant Cell Environ 40:881–896.

Bunce JA (2004) Carbon dioxide effects on stomatal responses to the environment and water use by crops under field conditions. Oecologia 140:1–10.

Cai Y, Guan K, Lobell D, Potgieter AB, Wang S, Peng J, Xu T, Asseng S, Zhang Y, You L, Peng B (2019) Integrating satellite and climate data to predict wheat yield in Australia using machine learning approaches. Agric For Meteorol 274:144–159. https://linkinghub.elsevier.com/retrieve/pii/S0168192319301224

Câmara AP, Vidaurre GB, Oliveira JCL, Teodoro PE, Almeida MNF, Toledo JV, Júnior AFD, Amorim GA, Pezzopane JEM, Campoe OC (2021) Changes in rainfall patterns enhance the interrelationships between climate and wood traits of eucalyptus. For Ecol Manage 485:118959. https://linkinghub.elsevier.com/retrieve/pii/S0378112721000487

Charrier G, Torres-Ruiz JM, Badel E, Burlett R, Choat B, Cochard H, Delmas CEL, Domec JC, Jansen S, King A, Lenoir N, Martin-StPaul N, Gambetta GA, Delzon S (2016) Evidence for hydraulic vulnerability segmentation and lack of xylem refilling under tension. Plant Physiol 172:1657–1668.

Chen J, Yang H, Man R, Wang W, Sharma M, Peng C, Parton J, Zhu H, Deng Z (2020) Using machine learning to synthesize spatiotemporal data for modelling DBH-height and DBH-height-age relationships in boreal forests. For Ecol Manage 466:118104. https://linkinghub.elsevier.com/retrieve/pii/S0378112720303194

Choat B, Badel E, Burlett R, Delzon S, Cochard H, Jansen S (2016) Noninvasive measurement of vulnerability to drought-induced embolism by X-Ray microtomography. Plant Physiol 170:273–282.

Choat B, Brodersen CR, Mcelrone AJ (2015) Synchrotron X-ray microtomography of xylem embolism in Sequoia sempervirens saplings during cycles of drought and recovery. New Phytol 205:1095–1105.

Choat B, Drayton WM, Brodersen C, Matthews MA, Shackel KA, Wada HIR, McElrone AJ (2010) Measurement of vulnerability to water stress-induced cavitation in grapevine: A comparison of four techniques applied to a long-vesseled species. Plant, Cell Environ 33:1502–1512.

Choat B, Jansen S, Brodribb TJ, Cochard H, Delzon S, Bhaskar R, Bucci SJ, Feild TS, Gleason SM, Hacke UG, Jacobsen AL, Lens F, Maherali H, Martínez-Vilalta J, Mayr S, Mencuccini M, Mitchell PJ, Nardini A, Pittermann J, Pratt RB, Sperry JS, Westoby M, Wright IJ, Zanne AE (2012) Global convergence in the vulnerability of forests to drought. Nature 491:752–755. http://www.nature.com/articles/nature11688

Choat B, Nolf M, Lopez R, Peters JMR, Carins-Murphy MR, Creek D, Brodribb TJ (2018) Non-invasive imaging shows no evidence of embolism repair after drought in tree species of two genera. Tree Physiol 39:113–121.

Ciemer C, Boers N, Hirota M, Kurths J, Müller-Hansen F, Oliveira RS, Winkelmann R (2019) Higher resilience to climatic disturbances in tropical vegetation exposed to more variable rainfall. Nat Geosci 12:174–179. http://www.nature.com/articles/s41561-019-0312-z

Cochard H, Bodet C, Améglio T, Cruiziat P (2000) Cryo-scanning Electron Microscopy Observations of Vessel Content during transpiration in Walnut Petioles. facts or Artifacts. Plant Physiol 124:1191–1202.

Cochard H, Delzon S, Badel E (2015) X-ray microtomography (micro-CT): A reference technology for high-resolution quantification of xylem embolism in trees. Plant, Cell Environ 38:201–206.

Cochard H, Lemoine D, Ameglio T, Granier A (2001) Mechanisms of xylem recovery from winter embolism in Fagus sylvatica. Tree Physiol 21:27–33. https://academic.oup.com/treephys/article-lookup/doi/10.1093/treephys/21.1.27

Coussement JR, De Swaef T, Lootens P, Roldán-Ruiz I, Steppe K (2018) Introducing turgor-driven growth dynamics into functional-structural plant models. Ann Bot 121:849–861.

Cowan IR, Farquhar GD (1977) Stomatal function in relation to leaf metabolism and environment Jennings DH (ed). Symp Soc Exp Biol:471–505.

Cruiziat P, Cochard H, Améglio T (2002) Hydraulic architecture of trees: Main concepts and results. Ann For Sci 59:723–752.

Dahmen T, Trampert P, Boughorbel F, Sprenger J, Klusch M, Fischer K, Kübel C, Slusallek P (2019) Digital reality: a model-based approach to supervised learning from synthetic data. AI Perspect 1:2. https://aiperspectives.springeropen.com/articles/10.1186/s42467-019-0002-0

Damour G, Simonneau T, Cochard H, Urban L (2010) An overview of models of stomatal conductance at the leaf level. Plant Cell Environ 33:no-no. http://doi.wiley.com/10.1111/j.1365-3040.2010.02181.x

DWAF (2005) Study of Supply and Demand of Industrial Roundwood. Pretoria.

Dewar RC (2002) The Ball-Berry-Leuning and Tardieu-Davies stomatal models: synthesis and extension within a spatially aggregated picture of guard cell function.

Dewar R, Mauranen A, Mäkelä A, Hölttä T, Medlyn B, Vesala T (2018) New insights into the covariation of stomatal, mesophyll and hydraulic conductances from optimization models incorporating nonstomatal limitations to photosynthesis. New Phytol 217:571–585.

van Dijk ADJ, Kootstra G, Kruijer W, de Ridder D (2021) Machine learning in plant science and plant breeding. iScience 24:101890. https://linkinghub.elsevier.com/retrieve/pii/S2589004220310877

Ding J, Johnson EA, Martin YE (2020) Optimization of leaf morphology in relation to leaf water status: A theory. Ecol Evol:ece3.6004. https://onlinelibrary.wiley.com/doi/abs/10.1002/ece3.6004

Drew DM, Downes GM (2009) The use of precision dendrometers in research on daily stem size and wood property variation: A review. Dendrochronologia 27:159–172.

Drew DM, Downes GM, Evans R (2011) Short-term growth responses and associated wood density fluctuations in variously irrigated Eucalyptus globulus. Trees - Struct Funct 25:153–161.

Drew DM, Downes GM, Grzeskowiak V, Naidoo T (2009) Differences in daily stem size variation and growth in two hybrid eucalypt clones. Trees - Struct Funct 23:585–595.

Duursma RA, Blackman CJ, Lopéz R, Martin-StPaul NK, Cochard H, Medlyn BE (2019) On the minimum leaf conductance: its role in models of plant water use, and ecological and environmental controls. New Phytol 221:693–705. https://onlinelibrary.wiley.com/doi/abs/10.1111/nph.15395

Dye PJ (1996) Response of Eucalyptus grandis trees to soil water deficits. Tree Physiol 16:233–238.

Dye PJ (2000) Water use efficiency in South African Eucalyptus plantations: A review. South African For J:17–26.

Elavarasan D, Vincent PMD (2020) Crop Yield Prediction Using Deep Reinforcement Learning Model for Sustainable Agrarian Applications. IEEE Access 8:86886–86901. https://ieeexplore.ieee.org/document/9086620/

Ellsäßer F, Röll A, Ahongshangbam J, Waite P-A, Hendrayanto, Schuldt B, Hölscher D (2020) Predicting Tree Sap Flux and Stomatal Conductance from Drone-Recorded Surface Temperatures in a Mixed Agroforestry System—A Machine Learning Approach. Remote Sens 12:4070. https://www.mdpi.com/2072-4292/12/24/4070

Farquhar GD, Von Caemmerer S, Berry JA (1980) A Biochemical Model of Photosynthetic CO 2 Assimilation in Leaves of C 3 Species.

Fatichi S, Pappas C, Zscheischler J, Leuzinger S (2019) Modelling carbon sources and sinks in terrestrial vegetation. New Phytol 221:652–668.

February EC, Stock WD, Bond WJ, Le Roux & DJ (1995) Relationships between water availability and selected vessel characteristics in Eucalyptus grandis and two hybrids. IAWA J 16:269–276.

Fernández ME, Barotto AJ, Martínez Meier A, Gyenge JE, Tesón N, Quiñones Martorello AS, Merlo E, Dalla Salda G, Rozenberg P, Monteoliva S (2019) New insights into wood anatomy and function relationships: How Eucalyptus challenges what we already know. For Ecol Manage 454

Flexas J, Medrano H (2002) Drought-inhibition of photosynthesis in C3 plants: Stomatal and non-stomatal limitations revisited. Ann Bot 89:183–189.

Franks PJ (2006) Higher rates of leaf gas exchange are associated with higher leaf hydrodynamic pressure gradients. Plant, Cell Environ 29:584–592.

Galar M, Fernandez A, Barrenechea E, Bustince H, Herrera F (2012) A review on ensembles for the class imbalance problem: Bagging-, boosting-, and hybrid-based approaches. IEEE Trans Syst Man Cybern Part C Appl Rev 42:463–484.

Galmés J, Medrano H, Flexas J (2007) Photosynthetic limitations in response to water stress and recovery in Mediterranean plants with different growth forms. New Phytol 175:81–93.

van Genuchten MT (1980) A Closed-form Equation for Predicting the Hydraulic Conductivity of Unsaturated Soils. Soil Sci Soc Am J 44:892–898. http://doi.wiley.com/10.2136/sssaj1980.03615995004400050002x

Gleason SM, Westoby M, Jansen S, Choat B, Hacke UG, Pratt RB, Bhaskar R, Brodribb TJ, Bucci SJ, Cao KF, Cochard H, Delzon S, Domec JC, Fan ZX, Feild TS, Jacobsen AL, Johnson DM, Lens F, Maherali H, Martínez-Vilalta J, Mayr S, Mcculloh KA, Mencuccini M, Mitchell PJ, Morris H, Nardini A, Pittermann J, Plavcová L, Schreiber SG, Sperry JS, Wright IJ, Zanne AE (2016) Weak tradeoff between xylem safety and xylem-specific hydraulic efficiency across the world's woody plant species. New Phytol 209:123–136.

Lo Gullo MA, Salleo S (1992) Water storage in the wood and xylem cavitation in 1-year-old twigs of Populus deltoides Bartr. Plant, Cell Environ 15:431–438.

Hacke UG, Sperry JS (2003) Limits to xylem refilling under negative pressure in Laurus nobilis and Acer negundo. Plant, Cell Environ 26:303–311.

Hacke UG, Sperry JS, Pockman WT, Davis SD, McCulloh KA (2001) Trends in wood density and structure are linked to prevention of xylem implosion by negative pressure. Oecologia 126:457–461.

Hacke UG, Sperry JS, Wheeler JK, Castro L (2006) Scaling of angiosperm xylem structure with safety and efficiency. Tree Physiol 26:689–701. https://academic.oup.com/treephys/article-lookup/doi/10.1093/treephys/26.6.689

Hammond WM, Yu K, Wilson LA, Will RE, Anderegg WRL, Adams HD (2019) Dead or dying? Quantifying the point of no return from hydraulic failure in drought-induced tree mortality. New Phytol 223:1834–1843.

Hartmann H, Schuldt B, Sanders TGM, Macinnis-Ng C, Boehmer HJ, Allen CD, Bolte A, Crowther TW, Hansen MC, Medlyn BE, Ruehr NK, Anderegg WRL (2018) Monitoring global tree mortality patterns and trends. Report from the VW symposium 'Crossing scales and disciplines to identify global trends of tree mortality as indicators of forest health'. New Phytol 217:984–987. http://doi.wiley.com/10.1111/nph.14988

Hastie T, Tibshirani R, Friedman J (2001) Springer Series in Statistics The Elements of Statistical Learning Data Mining, Inference, and Prediction. Springer, New York.

He H, Garcia EA (2009) Learning from imbalanced data. IEEE Trans Knowl Data Eng 21:1263–1284.

Houshmandfar A, O'Leary G, Fitzgerald GJ, Chen Y, Tausz-Posch S, Benke K, Uddin S, Tausz M (2021) Machine learning produces higher prediction accuracy than the Jarvis-type model of climatic control on stomatal conductance in a dryland wheat agro-ecosystem. Agric For Meteorol 304–305:108423. https://linkinghub.elsevier.com/retrieve/pii/S0168192321001064

Iglesias I, Wilstermann D (2009) Eucalypt Logics Information Resources on Eucalypt Cultivation Worldwide. http://git-forestry-blog.blogspot.com/ (3 March 2021, date last accessed).

Irvine J, Perks MP, Magnani F, Grace J (1998) The response of Pinus sylvestris to drought: stomatal control of transpiration and hydraulic conductance. Tree Physiol 18:393–402. http://www.heronpublishing.com

Jacobsen AL, Ewers FW, Pratt RB, Paddock WA, Davis SD (2005) Do xylem fibers affect vessel cavitation resistance? Plant Physiol 139:546–556.

Jarvis PG (1976) The Interpretation of the Variations in Leaf Water Potential and Stomatal Conductance Found in Canopies in the Field. Philos Trans R Soc London Ser B 273, 273:593–610. https://www.jstor.org/stable/2417554?seq=1&cid=pdf-

Johnson MD, Hsieh WW, Cannon AJ, Davidson A, Bédard F (2016) Crop yield forecasting on the Canadian Prairies by remotely sensed vegetation indices and machine learning methods. Agric For Meteorol 218–219:74–84. https://linkinghub.elsevier.com/retrieve/pii/S0168192315007546

Jung M, Reichstein M, Bondeau A (2001) Towards global empirical upscaling of FLUXNET eddy covariance observations: validation of a model tree ensemble approach using a biosphere model. www.biogeosciences.net/6/2001/2009/

Katul G, Manzoni S, Palmroth S, Oren R (2010) A stomatal optimization theory to describe the effects of atmospheric CO2 on leaf photosynthesis and transpiration. Ann Bot 105:431–442. https://academic.oup.com/aob/article-lookup/doi/10.1093/aob/mcp292

Kaul M, Hill RL, Walthall C (2005) Artificial neural networks for corn and soybean yield prediction. Agric Syst 85:1–18. https://linkinghub.elsevier.com/retrieve/pii/S0308521X04001398

Kim HK, Lee SJ (2010) Synchrotron X-ray imaging for nondestructive monitoring of sap flow dynamics through xylem vessel elements in rice leaves. New Phytol 188:1085–1098.

Kim SH, Lieth JH (2003) A coupled model of photosynthesis, stomatal conductance and transpiration for a rose leaf (Rosa hybrida L.). Ann Bot 91:771–781.

Kisi O, Cimen M (2009) Evapotranspiration modelling using support vector machines / Modélisation de l'évapotranspiration à l'aide de 'support vector machines'. Hydrol Sci J 54:918–928. https://www.tandfonline.com/doi/full/10.1623/hysj.54.5.918

Klein T (2014) The variability of stomatal sensitivity to leaf water potential across tree species indicates a continuum between isohydric and anisohydric behaviours. Funct Ecol 28:1313–1320.

Klein T, Cohen S, Yakir D (2011) Hydraulic adjustments underlying drought resistance of Pinus halepensis. Tree Physiol 31:637–648.

Klein T, Zeppel MJB, Anderegg WRL, Bloemen J, De Kauwe MG, Hudson P, Ruehr NK, Powell TL, von Arx G, Nardini A (2018) Xylem embolism refilling and resilience against drought-induced mortality in woody plants: processes and trade-offs. Ecol Res 33:839–855. http://doi.wiley.com/10.1007/s11284-018-1588-y

van Klompenburg T, Kassahun A, Catal C (2020) Crop yield prediction using machine learning: A systematic literature review. Comput Electron Agric 177:105709. https://linkinghub.elsevier.com/retrieve/pii/S0168169920302301

Knipfer T, Cuneo IF, Brodersen CR, McElrone AJ (2016) In situ visualization of the dynamics in xylem embolism formation and removal in the absence of root pressure: A study on excised grapevine stems. Plant Physiol 171:1024–1036.

Kramer PJ, Boyer JS (1995) Water relations of plants and soils. Academic Press Limited, San diago, California.

Kurz WA, Dymond CC, White TM, Stinson G, Shaw CH, Rampley GJ, Smyth C, Simpson BN, Neilson ET, Trofymow JA, Metsaranta J, Apps MJ (2009) CBM-CFS3: A model of carbon-dynamics in forestry and land-use change implementing IPCC standards. Ecol Modell 220:480–504. https://linkinghub.elsevier.com/retrieve/pii/S0304380008005012

Lamarque LJ, Corso D, Torres-Ruiz JM, Badel E, Brodribb TJ, Burlett R, Charrier G, Choat B, Cochard H, Gambetta GA, Jansen S, King A, Lenoir N, Martin-StPaul N, Steppe K, Van den Bulcke J, Zhang Y, Delzon S (2018) An inconvenient truth about xylem resistance to embolism in the model species for refilling Laurus nobilis L. Ann For Sci 75

Lambers H, Chapin III FS, Pons TL (1998) Plant physiological ecology. Springer, Berlin. https://onlinelibrary.wiley.com/doi/abs/10.1046/j.1439-037x.2000.00378-1.x

Leij FJ, Alves WJ, Van Genuchten MT, Williams JR (1996) The UNSODA Unsaturated Soil Hydraulic Database User's Manual Version 1.0 Project Officer.

Lens F, Sperry JS, Christman MA, Choat B, Rabaey D, Jansen S (2011) Testing hypotheses that link wood anatomy to cavitation resistance and hydraulic conductivity in the genus Acer. New Phytol 190:709–723.

Leuning R (1995) A critical appraisal of a combined stomatal-photosynthesis model for C3 plants. Plant Cell Environ 18:339–355. https://onlinelibrary.wiley.com/doi/abs/10.1111/j.1365-3040.1995.tb00370.x

Li Y, Cai W, Campbell EP (2005) Statistical modeling of extreme rainfall in southwest Western Australia. J Clim 18:852–863.

Li A, Liang S, Wang A, Qin J (2007) Estimating crop yield from multi-temporal satellite data using multivariate regression and neural network techniques. Photogramm Eng Remote Sens 73:1149–1157.

Lin Y-S, Medlyn BE, Duursma RA, Prentice IC, Wang H, Baig S, Eamus D, de Dios VR, Mitchell P, Ellsworth DS, de Beeck MO, Wallin G, Uddling J, Tarvainen L, Linderson M-L, Cernusak LA, Nippert JB, Ocheltree TW, Tissue DT, Martin-StPaul NK, Rogers A, Warren JM, De Angelis P, Hikosaka K, Han Q, Onoda Y, Gimeno TE, Barton CVM, Bennie J, Bonal D, Bosc A, Löw M, Macinins-Ng C, Rey A, Rowland L, Setterfield SA, Tausz-Posch S, Zaragoza-Castells J, Broadmeadow MSJ, Drake JE, Freeman M, Ghannoum O, Hutley LB, Kelly JW, Kikuzawa K, Kolari P, Koyama K, Limousin J-M, Meir P, Lola da Costa AC, Mikkelsen TN, Salinas N, Sun W, Wingate L (2015) Optimal stomatal behaviour around the world. Nat Clim Chang 5:459–464. http://www.nature.com/articles/nclimate2550

Liu J, Gu L, Yu Y, Huang P, Wu Z, Zhang Q, Qian Y, Wan X, Sun Z (2019) Corticular photosynthesis drives bark water uptake to refill embolized vessels in dehydrated branches of *Salix matsudana* Plant Cell Environ 42:2584–2596. https://onlinelibrary.wiley.com/doi/abs/10.1111/pce.13578

Liu Z, Peng C, Work T, Candau J-N, DesRochers A, Kneeshaw D (2018) Application of machine-learning methods in forest ecology: recent progress and future challenges. Environ Rev 26:339–350. http://www.nrcresearchpress.com/doi/10.1139/er-2018-0034

Lobo A, Torres-Ruiz JM, Burlett R, Lemaire C, Parise C, Francioni C, Truffaut L, Tomášková I, Hansen JK, Kjær ED, Kremer A, Delzon S (2018) Assessing inter- and intraspecific variability of xylem vulnerability to embolism in oaks. For Ecol Manage 424:53–61.

Loepfe L, Martinez-Vilalta J, Piñol J, Mencuccini M (2007) The relevance of xylem network structure for plant hydraulic efficiency and safety. J Theor Biol 247:788–803.

López R, Nolf M, Duursma RA, Badel E, Flavel RJ, Cochard H, Choat B (2018) Mitigating the open vessel artefact in centrifuge-based measurement of embolism resistance. Tree Physiol 39:143–155.

Lu Y, Duursma RA, Farrior CE, Medlyn BE, Feng X (2020) Optimal stomatal drought response shaped by competition for water and hydraulic risk can explain plant trait covariation. New Phytol 225:1206–1217.

Macfarlane C, White DA, Adams MA (2004) The apparent feed-forward response to vapour pressure deficit of stomata in droughted, field-grown Eucalyptus globulus Labill. Plant, Cell Environ 27:1268–1280. http://doi.wiley.com/10.1111/j.1365-3040.2004.01234.x

Maherali H, Moura CF, Caldeira MC, Willson CJ, Jackson RB (2006) Functional coordination between leaf gas exchange and vulnerability to xylem cavitation in temperate forest trees. Plant, Cell Environ 29:571–583.

Maherali H, Pockman WT, Jackson RB (2004) Adaptive Variation in the Vulnerability of Woody Plants to Xylem Cavitation. Ecology 85:2184–2199.

Manzoni S, Vico G, Katul G, Fay PA, Polley W, Palmroth S, Porporato A (2011) Optimizing stomatal conductance for maximum carbon gain under water stress: a meta-analysis across plant functional types and climates. Funct Ecol 25:456–467. http://doi.wiley.com/10.1111/j.1365-2435.2010.01822.x

Manzoni S, Vico G, Thompson S, Beyer F, Weih M (2015) Contrasting leaf phenological strategies optimize carbon gain under droughts of different duration. Adv Water Resour 84:37–51.

Martin-StPaul N, Delzon S, Cochard H (2017) Plant resistance to drought depends on timely stomatal closure Maherali H (ed). Ecol Lett 20:1437–1447. http://doi.wiley.com/10.1111/ele.12851

Martínez-Vilalta J, Garcia-Forner N (2017) Water potential regulation, stomatal behaviour and hydraulic transport under drought: deconstructing the iso/anisohydric concept. Plant Cell Environ 40:962–976.

Maseyk K, Hemming D, Angert A, Leavitt SW, Yakir D (2011) Increase in water-use efficiency and underlying processes in pine forests across a precipitation gradient in the dry Mediterranean region over the past 30 years. Oecologia 167:573–585.

Maurel C, Chrispeels MJ (2001) Aquaporins. A Molecular Entry into Plant Water Relations. Plant Physiol 125. www.plantphysiol.org

McDowell N, Allen CD, Anderson-Teixeira K, Brando P, Brienen R, Chambers J, Christoffersen B, Davies S, Doughty C, Duque A, Espirito-Santo F, Fisher R, Fontes CG, Galbraith D, Goodsman D, Grossiord C, Hartmann H, Holm J, Johnson DJ, Kassim AR, Keller M, Koven C, Kueppers L, Kumagai T, Malhi Y, McMahon SM, Mencuccini M, Meir P, Moorcroft P, Muller-Landau HC, Phillips OL, Powell T, Sierra CA, Sperry J, Warren J, Xu C, Xu X (2018) Drivers and mechanisms of tree mortality in moist tropical forests. New Phytol 219:851–869. http://doi.wiley.com/10.1111/nph.15027

Mcdowell NG, Fisher RA, Xu C, Domec JC, Hölttä T, Mackay DS, Sperry JS, Boutz A, Dickman L, Gehres N, Limousin JM, Macalady A, Martínez-Vilalta J, Mencuccini M, Plaut JA, Ogée J, Pangle RE, Rasse DP, Ryan MG, Sevanto S, Waring RH, Williams AP, Yepez EA, Pockman WT (2013) Evaluating theories of drought-induced vegetation mortality using a multimodel-experiment framework. New Phytol 200:304–321.

McDowell N, Pockman WT, Allen CD, Breshears DD, Cobb N, Kolb T, Plaut J, Sperry J, West A, Williams DG, Yepez EA (2008) Mechanisms of plant survival and mortality during drought: why do some plants survive while others succumb to drought? New Phytol 178:719–739. http://doi.wiley.com/10.1111/j.1469-8137.2008.02436.x

Medlyn BE, Duursma RA, Eamus D, Ellsworth DS, Prentice IC, Barton CVM, Crous KY, De Angekus P, Freeman M, Wingate L (2011) Reconciling the optimal and empirical approaches to modelling stomatal conductance. Glob Chang Biol 17:2134–2144. http://doi.wiley.com/10.1111/j.1365-2486.2010.02375.x

Meinzer FC, McCulloh KA (2013) Xylem recovery from drought-induced embolism: Where is the hydraulic point of no return? Tree Physiol 33:331–334.

Mencuccini M, Minunno F, Salmon Y, Martínez-Vilalta J, Hölttä T (2015) Coordination of physiological traits involved in drought-induced mortality of woody plants. New Phytol 208:396–409.

Menezes-Silva PE, Loram-Lourenço L, Alves RDFB, Sousa LF, Almeida SE da S, Farnese FS (2019) Different ways to die in a changing world: Consequences of climate change for tree species performance and survival through an ecophysiological perspective. Ecol Evol 9:11979–11999. https://onlinelibrary.wiley.com/doi/abs/10.1002/ece3.5663

Miner GL, Bauerle WL, Baldocchi DD (2017) Estimating the sensitivity of stomatal conductance to photosynthesis: a review. Plant Cell Environ 40:1214–1238.

Misson L, Panek JA, Goldstein AH (2004) A comparison of three approaches to modeling leaf gas exchange in annually drought-stressed ponderosa pine forests. Tree Physiol 24:529–541. https://academic.oup.com/treephys/article-lookup/doi/10.1093/treephys/24.5.529

Mitchell PJ, O'Grady AP, Tissue DT, White DA, Ottenschlaeger ML, Pinkard EA (2013) Drought response strategies define the relative contributions of hydraulic dysfunction and carbohydrate depletion during tree mortality. New Phytol 197:862–872.

Mokany K, McMurtrie RE, Atwell BJ, Keith H (2003) Interaction between sapwood and foliage area in alpine ash (Eucalyptus delegatensis) trees of different heights. Thee Physiol 23:949–958.

Monteith JL (1995) A reinterpretation of stomatal responses to humidity. Plant, Cell Envirotimerit 18:357–364.

Morris AR (2008) Realising the benefit of research in eucalypt plantation management. In: Southern Forests.pp 119–129.

Morrison JIL (1987) Intercellular CO2 concentration and stomatal response to CO2. Stomatal Funct:229–251.

Myburg AA, Grattapaglia D, Tuskan GA, Hellsten U, Hayes RD, Grimwood J, Jenkins J, Lindquist E, Tice H, Bauer D, Goodstein DM, Dubchak I, Poliakov A, Mizrachi E, Kullan ARK, Hussey SG, Pinard D, van der Merwe K, Singh P, van Jaarsveld I, Silva-Junior OB, Togawa RC, Pappas MR, Faria DA, Sansaloni CP, Petroli CD, Yang X, Ranjan P, Tschaplinski TJ, Ye C-Y, Li T, Sterck L, Vanneste K, Murat F, Soler M, Clemente HS, Saidi N, Cassan-Wang H, Dunand C, Hefer CA, Bornberg-Bauer E, Kersting AR, Vining K, Amarasinghe V, Ranik M, Naithani S, Elser J, Boyd AE, Liston A, Spatafora JW, Dharmwardhana P, Raja R, Sullivan C, Romanel E, Alves-Ferreira M, Külheim C, Foley W, Carocha V, Paiva J, Kudrna D, Brommonschenkel SH, Pasquali G, Byrne M, Rigault P, Tibbits J, Spokevicius A, Jones RC, Steane DA, Vaillancourt RE, Potts BM, Joubert F, Barry K, Pappas GJ, Strauss SH, Jaiswal P, Grima-Pettenati J, Salse J, Van de Peer Y, Rokhsar DS, Schmutz J (2014) The genome of Eucalyptus grandis. Nature 510:356–362. http://www.nature.com/articles/nature13308

Nardini A, Lo Gullo MA, Salleo S (2011) Refilling embolized xylem conduits: Is it a matter of phloem unloading? Plant Sci 180:604–611. https://linkinghub.elsevier.com/retrieve/pii/S0168945211000045

Nardini A, Lo Gullo MA, Trifilò P, Salleo S (2014) The challenge of the Mediterranean climate to plant hydraulics: Responses and adaptations. Environ Exp Bot 103:68–79.

Nardini A, Savi T, Losso A, Petit G, Pacilè S, Tromba G, Mayr S, Trifilò P, Lo Gullo MA, Salleo S (2017) X-ray microtomography observations of xylem embolism in stems of Laurus nobilis are consistent with hydraulic measurements of percentage loss of conductance. New Phytol 213:1068–1075.

Nikinmaa E, Sievänen R, Hölttä T (2014) Dynamics of leaf gas exchange, xylem and phloem transport, water potential and carbohydrate concentration in a realistic 3-D model tree crown. Ann Bot 114:653–666.

Niu CY, Meinzer FC, Hao GY (2017) Divergence in strategies for coping with winter embolism among co-occurring temperate tree species: the role of positive xylem pressure, wood type and tree stature. Funct Ecol 31:1550–1560.

Nolan RH, Tarin T, Santini NS, McAdam SAM, Ruman R, Eamus D (2017) Differences in osmotic adjustment, foliar abscisic acid dynamics, and stomatal regulation between an isohydric and anisohydric woody angiosperm during drought. Plant Cell Environ 40:3122–3134.

Nolf M, Lopez R, Peters JMR, Flavel RJ, Koloadin LS, Young IM, Choat B (2017) Visualization of xylem embolism by X-ray microtomography: a direct test against hydraulic measurements. New Phytol 214:890–898.

Ogasa M, Miki NH, Murakami Y, Yoshikawa K (2013) Recovery performance in xylem hydraulic conductivity is correlated with cavitation resistance for temperate deciduous tree species. Tree Physiol 33:335–344. https://academic.oup.com/treephys/article-lookup/doi/10.1093/treephys/tpt010

Ogasa MY, Utsumi Y, Miki NH, Yazaki K, Fukuda K (2016) Cutting stems before relaxing xylem tension induces artefacts in Vitis coignetiae, as evidenced by magnetic resonance imaging. Plant Cell Environ 39:329–337.

Otto MSG, Hubbard RM, Binkley D, Stape JL (2014) Dominant clonal Eucalyptus grandis×urophylla trees use water more efficiently. For Ecol Manage 328:117–121.

Pachauri RK, Mayer L, Intergovernmental Panel on Climate Change (2014) Climate change 2014 : synthesis report. Geneva, Switzerland.

Pan S, Pan N, Tian H, Friedlingstein P, Sitch S, Shi H, Arora VK, Haverd V, Jain AK, Kato E, Lienert S, Lombardozzi D, Nabel JEMS, Ottlé C, Poulter B, Zaehle S, Running SW (2020) Evaluation of global terrestrial evapotranspiration using state-of-the-art approaches in remote sensing, machine learning and land surface modeling. Hydrol Earth Syst Sci 24:1485–1509. https://hess.copernicus.org/articles/24/1485/2020/

Panda S, Amatya DM, Hoogenboom G (2014) Stomatal Conductance, Canopy Temperature, and Leaf Area Index Estimation Using Remote Sensing and OBIA techniques.

Papale D, Black TA, Carvalhais N, Cescatti A, Chen J, Jung M, Kiely G, Lasslop G, Mahecha MD, Margolis H, Merbold L, Montagnani L, Moors E, Olesen JE, Reichstein M, Tramontana G, van Gorsel E, Wohlfahrt G, Ráduly B (2015) Effect of spatial sampling from European flux towers for estimating carbon and water fluxes with artificial neural networks. J Geophys Res Biogeosciences 120:1941–1957. http://doi.wiley.com/10.1002/2015JG002997

Papalem D, Valentini R (2003) A new assessment of European forests carbon exchanges by eddy fluxes and artificial neural network spatialization. Glob Chang Biol 9:525–535. http://doi.wiley.com/10.1046/j.1365-2486.2003.00609.x

Park Williams A, Allen CD, Macalady AK, Griffin D, Woodhouse CA, Meko DM, Swetnam TW, Rauscher SA, Seager R, Grissino-Mayer HD, Dean JS, Cook ER, Gangodagamage C, Cai M, McDowell NG (2013) Temperature as a potent driver of regional forest drought stress and tree mortality. Nat Clim Chang 3:292–297. http://www.nature.com/articles/nclimate1693

Pedregosa F, Varoquaux G, Gramfort A, Michel V, Thirion B, Grisel O, Blondel M, Prettenhofer P, Wies R, Dubourg V, Vanderplas JT, Passos A, Cournapeau D, Brucher M, Perrot M, Duchesnay E (2011) Scikit-learn: Machine Learning in Python. J Mach Learn Res 12:2825–2830. http://scikit-learn.sourceforge.net.

Périé C, de Blois S (2016) Dominant forest tree species are potentially vulnerable to climate change over large portions of their range even at high latitudes. PeerJ 4:e2218. https://peerj.com/articles/2218

Petruzzellis F, Pagliarani C, Savi T, Losso A, Cavalletto S, Tromba G, Dullin C, Bär A, Ganthaler A, Miotto A, Mayr S, Zwieniecki MA, Nardini A, Secchi F (2018) The pitfalls of in vivo imaging techniques: evidence for cellular damage caused by synchrotron X-ray computed micro-tomography. New Phytol 220:104–110.

Pieruschka R, Schurr U (2019) Plant Phenotyping: Past, Present, and Future. Plant Phenomics 2019:1–6. https://spj.sciencemag.org/journals/plantphenomics/2019/7507131/

Pittermann J, Sperry JS, Hacke UG, Wheeler JK, Sikkema EH (2006) Inter-tracheid pitting and the hydraulic efficiency of conifer wood: The role of tracheid allometry and cavitation protection. Am J Bot 93:1265–1273.

du Plessis A, le Roux SG, Guelpa A (2016) The CT Scanner Facility at Stellenbosch University: An open access X-ray computed tomography laboratory. Nucl Instruments Methods Phys Res 384:42–49.

Poorter H, Niklas KJ, Reich PB, Oleksyn J, Poot P, Mommer L (2012) Biomass allocation to leaves, stems and roots: Meta-analyses of interspecific variation and environmental control. New Phytol 193:30–50.

Powell TL, Galbraith DR, Christoffersen BO, Harper A, Imbuzeiro HMA, Rowland L, Almeida S, Brando PM, da Costa ACL, Costa MH, Levine NM, Malhi Y, Saleska SR, Sotta E, Williams M, Meir P, Moorcroft PR (2013) Confronting model predictions of carbon fluxes with measurements of Amazon forests subjected to experimental drought. New Phytol 200:350–365. http://doi.wiley.com/10.1111/nph.12390

Prentice IC, Dong N, Gleason SM, Maire V, Wright IJ (2014) Balancing the costs of carbon gain and water transport: testing a new theoretical framework for plant functional ecology Penuelas J (ed). Ecol Lett 17:82–91. http://doi.wiley.com/10.1111/ele.12211

Ramanjulu S, Sreenivasulu N, Sudhakar C (1998) Effect of water stress on photosynthesis in two mulberry genotypes with different drought tolerance. Photosynthetica 35:279–283.

Ratliff LF, Ritchie JT, Cassel DK (1983) Field-Measured Limits of Soil Water Availability as Related to Laboratory-Measured Properties. Soil Sci Soc Am J 47:770–775. http://doi.wiley.com/10.2136/sssaj1983.03615995004700040032x

Rockwell FE, Wheeler JK, Holbrook NM (2014) Cavitation and its discontents: Opportunities for resolving current controversies. Plant Physiol 164:1649–1660.

Roman DT, Novick KA, Brzostek ER, Dragoni D, Rahman F, Phillips RP (2015) The role of isohydric and anisohydric species in determining ecosystem-scale response to severe drought. Oecologia 179:641–654.

Rouhi V, Samson R, Lemeur R, Damme P Van (2007) Photosynthetic gas exchange characteristics in three different almond species during drought stress and subsequent recovery. Environ Exp Bot 59:117–129.

Saadaoui E, Ben Yahia K, Dhahri S, Ben Jamaa ML, Khouja ML (2017) An overview of adaptative responses to drought stress in Eucalyptus spp. For Stud 67:86–96. http://content.sciendo.com/view/journals/fsmu/67/1/article-p86.xml

Sabot MEB, De Kauwe MG, Pitman AJ, Medlyn BE, Verhoef A, Ukkola AM, Abramowitz G (2020) Plant profit maximization improves predictions of European forest responses to drought. New Phytol 226:1638–1655. https://onlinelibrary.wiley.com/doi/10.1111/nph.16376

Sala A, Woodruff DR, Meinzer FC (2012) Carbon dynamics in trees: Feast or famine? Tree Physiol 32:764–775.

Salleo S, Lo Gullo MA, Trifilò P, Nardini & A (2004) New evidence for a role of vessel-associated cells and phloem in the rapid xylem refilling of cavitated stems of Laurus nobilis L. Plant, Cell Environ 27:1065–1076.

Sano Y, Morris H, Shimada H, Ronse De Craene LP, Jansen S (2011) Anatomical features associated with water transport in imperforate tracheary elements of vessel-bearing angiosperms. Ann Bot 107:953–964.

Saunders A, Drew DM (2021) Measurements done on excised stems indicate that hydraulic recovery can be an important strategy used by Eucalyptus hybrids in response to drought. Trees. https://link.springer.com/10.1007/s00468-021-02188-7

Savi T, Casolo V, Luglio J, Bertuzzi S, Trifilo' P, Lo Gullo MA, Nardini A (2016) Species-specific reversal of stem xylem embolism after a prolonged drought correlates to endpoint concentration of soluble sugars. Plant Physiol Biochem 106:198–207.

Schneider CA, Rasband WS, Eliceiri KW (2012) NIH Image to ImageJ: 25 years of Image Analysis HHS Public Access.

Schulze E-D, Hall AE (1982) Stomatal Responses, Water Loss and CO2 Assimilation Rates of Plants in Contrasting Environments. In: Lange OL, Nobel PS, Osmond CB, Ziegler H (eds) Physiological Plant Ecology II: Water Relations and Carbon Assimilation. Springer Berlin Heidelberg, Berlin, Heidelberg, pp 181–230. https://doi.org/10.1007/978-3-642-68150-9_8

Secchi F, Pagliarani C, Cavalletto S, Petruzzellis F, Tonel G, Savi T, Tromba G, Obertino MM, Lovisolo C, Nardini A, Zwieniecki MA (2021) Chemical inhibition of xylem cellular activity impedes the removal of drought-induced embolisms in poplar stems – new insights from micro-CT analysis. New Phytol 229:820–830.

Secchi F, Zwieniecki MA (2010) Patterns of PIP gene expression in Populus trichocarpa during recovery from xylem embolism suggest a major role for the PIP1 aquaporin subfamily as moderators of refilling process. Plant Cell Environ 33:1285–1297. http://doi.wiley.com/10.1111/j.1365-3040.2010.02147.x

Sevanto S, Mcdowell NG, Dickman LT, Pangle R, Pockman WT (2014) How do trees die? A test of the hydraulic failure and carbon starvation hypotheses. Plant, Cell Environ 37:153–161.

Shoemaker DA, Cropper WP (2010) Application of remote sensing, an artificial neural network leaf area model, and a process-based simulation model to estimate carbon storage in Florida slash pine plantations. J For Res 21:171–176. http://link.springer.com/10.1007/s11676-010-0027-x

Silva FC e, Shvaleva A, Maroco JP, Almeida MH, Chaves MM, Pereira JS (2004) Responses to water stress in two Eucalyptus globulus clones differing in drought tolerance. Tree Physiol 24:1165–1172. https://academic.oup.com/treephys/article-lookup/doi/10.1093/treephys/24.10.1165

Silva JCF, Teixeira RM, Silva FF, Brommonschenkel SH, Fontes EPB (2019) Machine learning approaches and their current application in plant molecular biology: A systematic review. Plant Sci 284:37–47. https://linkinghub.elsevier.com/retrieve/pii/S0168945218315802

Smith NG, Dukes JS (2013) Plant respiration and photosynthesis in global-scale models: Incorporating acclimation to temperature and CO2. Glob Chang Biol 19:45–63.

Sober A (1998) Hydraulic conductance, stomatal conductance, and maximal photosynthetic rate in bean leaves. Photosynthetica 34:599–603.

Souden S, Ennajeh M, Ouledali S, Massoudi N, Cochard H, Khemira H (2020) Water relations, photosynthesis, xylem embolism and accumulation of carbohydrates and cyclitols in two Eucalyptus species (E. camaldulensis and E. torquata) subjected to dehydration–rehydration cycle. Trees - Struct Funct 34:1439–1452.

Sperry JS (2003) Evolution of water transport and xylem structure. Int J Plant Sci 164:115–127.

Sperry JS (2004) Coordinating stomatal and xylem functioning - an evolutionary perspective. New Phytol 162:568–570.

Sperry JS, Alder NN, Eastlack SE (1993) The effect of reduced hydraulic conductance on stomatal conductance and Xylem Cavitation. 44:1075–1082.

Sperry JS, Hacke UG, Oren R, Comstock JP (2002) Water deficits and hydraulic limits to leaf water supply. Plant Cell Environ 25:251–263. http://doi.wiley.com/10.1046/j.0016-8025.2001.00799.x

Sperry JS, Love DM (2015) What plant hydraulics can tell us about responses to climate-change droughts. New Phytol 207:14–27. http://doi.wiley.com/10.1111/nph.13354

Sperry JS, Pockman W (1993) Limitation of transpiration by hydraulic conductance and xyiem cavitation in Betula occidental is.

Sperry JS, Venturas MD, Anderegg WRL, Mencuccini M, Mackay DS, Wang Y, Love DM (2017) Predicting stomatal responses to the environment from the optimization of photosynthetic gain and hydraulic cost. Plant Cell Environ 40:816–830. http://doi.wiley.com/10.1111/pce.12852

Stewart JB (1988) Modelling surface conductance of Pine forest. Agric For Meteorol 43:19–35.

Tardieu F, Davies WJ (1993) Integration of hydraulic and chemical signalling in the control of stomatal conductance and water status of droughted plants. Plant, Cell Environ 16:341–349. https://onlinelibrary.wiley.com/doi/abs/10.1111/j.1365-3040.1993.tb00880.x

Tenhunen JD, Weber JA, Filipek LH, Gates DM (1977) Development of a Photosynthesis Model with an Emphasis on Ecological Applications III. Carbon Dioxide and Oxygen Dependencies. Oecologia (Berl) 30:189–207.

Tng DYP, Apgaua DMG, Ishida YF, Mencuccini M, Lloyd J, Laurance WF, Laurance SGW (2018) Rainforest trees respond to drought by modifying their hydraulic architecture. Ecol Evol 8:12479–12491.

Tomasella M, Casolo V, Aichner N, Petruzzellis F, Savi T, Trifilò P, Nardini A (2019) Non-structural carbohydrate and hydraulic dynamics during drought and recovery in Fraxinus ornus and Ostrya carpinifolia saplings. Plant Physiol Biochem 145:1–9.

Tomasella M, Petrussa E, Petruzzellis F, Nardini A, Casolo V (2019) The Possible Role of Non-Structural Carbohydrates in the Regulation of Tree Hydraulics. Int J Mol Sci 21:144. https://www.mdpi.com/1422-0067/21/1/144

Tombesi S, Johnson RS, Day KR, Dejong TM (2010) Relationships between xylem vessel characteristics, calculated axial hydraulic conductance and size-controlling capacity of peach rootstocks. Ann Bot 105:327–331.

Torres-Ruiz JM, Jansen S, Choat B, McElrone AJ, Cochard H, Brodribb TJ, Badel E, Burlett R, Bouche PS, Brodersen CR, Li S, Morris H, Delzon S (2015) Direct X-Ray Microtomography Observation Confirms the Induction of Embolism upon Xylem Cutting under Tension. Plant Physiol 167:40–43. http://www.plantphysiol.org/lookup/doi/10.1104/pp.114.249706

Torres-Ruiz JM, Sperry JS, Fernández JE (2012) Improving xylem hydraulic conductivity measurements by correcting the error caused by passive water uptake. Physiol Plant 146:129–135.

Tramontana G, Ichii K, Camps-Valls G, Tomelleri E, Papale D (2015) Uncertainty analysis of gross primary production upscaling using Random Forests, remote sensing and eddy covariance data. Remote Sens Environ 168:360–373. https://linkinghub.elsevier.com/retrieve/pii/S0034425715300699

Tramontana G, Jung M, Schwalm CR, Ichii K, Camps-Valls G, Ráduly B, Reichstein M, Arain MA, Cescatti A, Kiely G, Merbold L, Serrano-Ortiz P, Sickert S, Wolf S, Papale D (2016) Predicting carbon dioxide and energy fluxes across global FLUXNET sites with regression algorithms. Biogeosciences 13:4291–4313. https://bg.copernicus.org/articles/13/4291/2016/

Trifilò P, Nardini A, Gullo MAL, Barbera PM, Savi T, Raimondo F (2015) Diurnal changes in embolism rate in nine dry forest trees: Relationships with species-specific xylem vulnerability, hydraulic strategy and wood traits. Tree Physiol 35:694–705.

Trifilò P, Raimondo F, Lo Gullo MA, Barbera PM, Salleo S, Nardini A (2014) Relax and refill: Xylem rehydration prior to hydraulic measurements favours embolism repair in stems and generates artificially low PLC values. Plant Cell Environ 37:2491–2499.

Trugman AT, Detto M, Bartlett MK, Medvigy D, Anderegg WRL, Schwalm C, Schaffer B, Pacala SW (2018) Tree carbon allocation explains forest drought-kill and recovery patterns Cameron D (ed). Ecol Lett 21:1552–1560. http://doi.wiley.com/10.1111/ele.13136

Trugman AT, Medvigy D, Mankin JS, Anderegg WRL (2018) Soil Moisture Stress as a Major Driver of Carbon Cycle Uncertainty. Geophys Res Lett 45:6495–6503. http://doi.wiley.com/10.1029/2018GL078131

Turnbull JW (2000) Economic and social importance of eucalypts. Keane PJ, Kile GA, Podger FD, Brown BN (eds).

Tuzet A, Perrier A, Leuning & R (2003) A coupled model of stomatal conductance, photosynthesis and transpiration.

Tyree MT, Ewers FW (1991) The hydraulic architecture of trees and other woody plants. New Phytol 119:345–360.

Tyree MT, Patino S, Bennink J, Alexander J (1995) Dynamic measurements of root hydraulic conductance using a high-pressure flowmeter in the laboratory and field. J Exp Bot 46:83–94.

Tyree MT, Salleo S, Nardini A, Assunta M, Gullo L, Mosca R (1999) Refilling of Embolized Vessels in Young Stems of Laurel. Do We Need a New Paradigm? Plant Physiol 120:11–21.

Tyree MT, Sperry JS (1988) Do Woody Plants Operate Near the Point of Catastrophic Xylem Dysfunction Caused by Dynamic Water Stress? Plant Physiol 88:574–0580.

Urban J, Ingwers M, McGuire MA, Teskey RO (2017) Stomatal conductance increases with rising temperature. Plant Signal Behav 12

Vaca RA, Golicher DJ, Cayuela L (2011) Using climatically based random forests to downscale coarse-grained potential natural vegetation maps in tropical Mexico. Appl Veg Sci 14:388–401. http://doi.wiley.com/10.1111/j.1654-109X.2011.01132.x

Vazquez-Cooz I, Meyer RW (2002) A differential staining method to identify lignii ed and unlignii ed tissues. Biotechinic Histochem 77:277–282.

Venturas MD, Sperry JS, Hacke UG (2017) Plant xylem hydraulics: What we understand, current research, and future challenges. J Integr Plant Biol 59:356–389. http://doi.wiley.com/10.1111/jipb.12534

Venturas MD, Sperry JS, Love DM, Frehner EH, Allred MG, Wang Y, Anderegg WRL (2018) A stomatal control model based on optimization of carbon gain versus hydraulic risk predicts aspen sapling responses to drought. New Phytol 220:836–850. https://nph.onlinelibrary.wiley.com/doi/abs/10.1111/nph.15333

Vesala T, Hölttä T, Perämäki M, Nikinmaa E (2003) Refilling of a hydraulically isolated embolized xylem vessel: Model calculations. Ann Bot 91:419–428.

Vialet-Chabrand SRM, Matthews JSA, McAusland L, Blatt MR, Griffiths H, Lawson T (2017) Temporal dynamics of stomatal behavior: Modeling and implications for photosynthesis and water use. Plant Physiol 174:603–613.

Vitrack-Tamam S, Holtzman L, Dagan R, Levi S, Tadmor Y, Azizi T, Rabinovitz O, Naor A, Liran O (2020) Random Forest Algorithm Improves Detection of Physiological Activity Embedded within Reflectance Spectra Using Stomatal Conductance as a Test Case. Remote Sens 12:2213. https://www.mdpi.com/2072-4292/12/14/2213

Wang Y-P, Leuning R (1998) A two-leaf model for canopy conductance, photosynthesis and partitioning of available energy I: Model description and comparison with a multi-layered model. Agric For Meterology 91:89–111.

Wang Y, Sperry JS, Anderegg WRL, Venturas MD, Trugman AT (2020) A theoretical and empirical assessment of stomatal optimization modeling. New Phytol 227:311–325. https://onlinelibrary.wiley.com/doi/abs/10.1111/nph.16572

Wang Y, Sperry JS, Venturas MD, Trugman AT, Love DM, Anderegg WRL (2019) The stomatal response to rising CO2 concentration and drought is predicted by a hydraulic trait-based optimization model Mäkelä A (ed). Tree Physiol 39:1416–1427. https://academic.oup.com/treephys/article/39/8/1416/5427464

Warburton M, Schulze R (2008) Potential impacts of climate change on the climatically suitable growth areas of Pinus and Eucalyptus : results from a sensitivity study in South Africa. South For a J For Sci 70:27–36. http://www.tandfonline.com/doi/abs/10.2989/SOUTH.FOR.2008.70.1.5.515

Wheeler JK, Huggett BA, Tofte AN, Rockwell FE, Holbrook NM (2013) Cutting xylem under tension or supersaturated with gas can generate PLC and the appearance of rapid recovery from embolism. Plant, Cell Environ 36:1938–1949.

Wheeler JK, Wheeler JK, Sperry JS, Hacke UG, Hoang N (2005) Safety versus efficiency trade-off in xylem transport Inter-vessel pitting and cavitation in woody Rosaceae and other vesselled plants: a basis for a safety versus efficiency trade-off in xylem transport. Plant, Cell Environ 28:800–812. http://rsb.info.nih.gov/ij/

Whitehead D, Beadle CL (2004) Physiological regulation of productivity and water use in Eucalyptus: A review. For Ecol Manage 193:113–140.

Whitehead D, Livingston NJ, Kelliher FM, Hogan KP, Pepin S, Mcseveny TM, Byers JN (1996) Response of transpiration and photosynthesis to a transient change in illuminated foliage area for a Pinus radiata D. Don tree. Plant, Cell Environ 19:949–957.

Van der Willigen C, Pammenter NW (1998) Relationship between growth and xylem hydraulic characteristics of clones of Eucalyptus spp. at contrasting sites. Tree Physiol 18:595–600. https://academic.oup.com/treephys/article-lookup/doi/10.1093/treephys/18.8-9.595

Wolf A, Anderegg WRL, Pacala SW (2016) Optimal stomatal behavior with competition for water and risk of hydraulic impairment. Proc Natl Acad Sci 113:E7222–E7230. http://www.pnas.org/lookup/doi/10.1073/pnas.1615144113

Wolfe BT, Sperry JS, Kursar TA (2016) Does leaf shedding protect stems from cavitation during seasonal droughts? A test of the hydraulic fuse hypothesis. New Phytol 212:1007–1018.

Xiong D, Nadal M (2020) Linking water relations and hydraulics with photosynthesis. Plant J 101:800–815. https://onlinelibrary.wiley.com/doi/abs/10.1111/tpj.14595

Xu L, Baldocchi DD (2003) Seasonal trends in photosynthetic parameters and stomatal conductance of blue oak (Quercus douglasii) under prolonged summer drought and high temperature. Tree Physiol 23:865–877.

Ye ZP, Yu Q (2008) A coupled model of stomatal conductance and photosynthesis for winter wheat. Photosynthetica 46:637–640. http://ps.ueb.cas.cz/doi/10.1007/s11099-008-0110-0.html

Yin X, Struik PC (2009) C3 and C4 photosynthesis models: An overview from the perspective of crop modelling. NJAS - Wageningen J Life Sci 57:27–38.

Zeppel MJB, Anderegg WRL, Adams HD, Hudson P, Cook A, Rumman R, Eamus D, Tissue DT, Pacala SW (2019) Embolism recovery strategies and nocturnal water loss across species influenced by biogeographic origin. Ecol Evol 9:5348–5361. https://onlinelibrary.wiley.com/doi/abs/10.1002/ece3.5126

Zhang Z, Zhao P, McCarthy HR, Ouyang L, Niu J, Zhu L, Ni G, Huang Y (2016) Hydraulic balance of a Eucalyptus urophylla plantation in response to periodic drought in low subtropical China. Front Plant Sci 7

Zhao X, Zhao P, Zhu L, Wang Q, Hu Y, Cranston BM, Kaplick J, Lei O, Chen X, Ni G, Ye Q, Macinnis-Ng C (2021) Exploring the influence of biological traits and environmental drivers on water use variations across contrasting forests. Forests 12:1–18.

Zhou S, Medlyn B, Sabaté S, Sperlich D, Colin Prentice I (2014) Short-term water stress impacts on stomatal, mesophyll and biochemical limitations to photosynthesis differ consistently among tree species from contrasting climates. Tree Physiol 34:1035–1046.

Zimmerman MH (1983) Xylem Structure and the Ascent of Sap Timell TW (ed). Berlin, Heidelberg.

Zwieniecki MA, Holbrook NM (2009) Confronting Maxwell's demon: biophysics of xylem embolism repair. Trends Plant Sci 14:530–534.

Zwieniecki MA, Melcher PJ, Ahrens ET (2013) Analysis of spatial and temporal dynamics of xylem refilling in Acer rubrum L. using magnetic resonance imaging. Front Plant Sci 4